Elutriation Technology in Heavy Mineral Separations

Matthew Donnel Eisenmann

Thesis submitted to the faculty of the Virginia Polytechnic Institute and State University in fulfillment of the requirements for the degree of

MASTER OF SCIENCE

IN

MINING AND MINERALS ENGINEERING

Gerald H. Luttrell, Chair

R.H. Yoon

G.T. Adel

November 5, 2001

Blacksburg, Virginia

Keywords: Heavy Mineral, TiO_2, Elutriation, CrossFlow, Model

Elutriation Technology in Heavy Mineral Separations

Matthew Donnel Eisenmann

ABSTRACT

Hindered-bed separators have been used in several different mineral processing fields for many years. Recent improvements in designs have led to the development of the CrossFlow separator. This new design employs a tangential feed system that has shown promise in several applications. This paper investigates the use of this relatively new technology to upgrade heavy mineral concentrates using Florida type ores. The intended use of this separatory device in this particular application is the removal of gangue quartz from other valuable heavy minerals such as ilmenite, leucoxene, rutile, zircon, and staurolite. The results of two different pilot-scale in-plant testing investigations are discussed. In general, quartz rejections in excess of 80% were achieved while maintaining TiO_2 and heavy mineral recoveries above 98% and 99%, respectively.

In addition to field test work, two separate unit models have been developed. The first model is an empirical investigation into understanding unit operation and functionality. The second model is a statistical prediction of unit operation based on specific field test work. These models can be used to effectively scale-up a CrossFlow unit for full-scale installation at any Florida heavy mineral sands operation. Emphasis is placed on unit capacity and other operational parameters such as elutriation flowrate and bed level.

ACKNOWLEDGEMENTS

The author wishes to express his deepest appreciation to Dr. Gerald Luttrell. His support, guidance, and knowledge throughout this thesis work was invaluable. The author would also like to thank Dr. Greg Adel and Dr. Roe-Hoan Yoon for their advice throughout undergraduate and graduate studies.

The author would like to thank Dupont White Pigments and Mineral Products for their continued support. Special thanks to Vincente Stutts, Process Engineer, and Francisco Parisi, R&D Supervisor, for their understanding, guidance, and assistance.

Sincere appreciation is extended to all those graduate students who spent many late nights at the Plantation Road Laboratory including: Jaisen Kohmuench, Tim McKeon, Ian Sherrell, and even Brian Halford. Special thanks to the Department of Mining and Minerals Engineering Administrative and Secretarial Staff.

The author would also like to express his thanks to his parents, siblings, and God; for their constant influence on his continued education. They all provided love and support throughout this entire process, as well.

Lastly, the author would like to express his love and appreciation to his wife, Colleen, for her love, support, understanding, and caring attitude that made this entire thesis possible.

TABLE OF CONTENTS

ABSTRACT i
ACKNOWLEDGEMENTS ii
TABLE OF CONTENTS iii
LIST OF FIGURES v
LIST OF TABLES vii
CHAPTER 1 1
1.1 Introduction 1
1.2 Literature Review 3
1.3 Typical Heavy Mineral Operations 7
1.3.1 Processing Overview 7
1.3.2 Florida TiO_2 Mineralogy 10
1.4 Problem Statement 17
1.5 Heavy Mineral Upgrading – Initial Test Work 18
CHAPTER 2 23
2.1 CrossFlow Testing 23
2.1.1 Overview 23
2.1.2 Equipment Setup 23
2.1.3 Testing Program 27
2.2 Mass Balancing 31
2.2.1 Introduction 31
2.2.2 Mass Balance Program Design 34
2.3 Experimental Results 35
2.3.1 Unit Performance 35
CHAPTER 3 56
3.1 Model Development 56
3.1.1 Overview and Objectives 56
3.2 Empirical Modeling 56
3.2.1 Model Introduction 56

3.2.2 Microscopic Population Balance Model of the CrossFlow Separator 59
3.2.3 Model Conclusions 65
3.3 Statistical Unit Modeling 66
3.3.1 Response Surface Modeling 66
3.3.2 Response Surface Design Selection 67
3.3.3 Testing Program 70
CHAPTER 4 72
4.1 Pilot-Scale CrossFlow Test Work 72
4.1.1 Overview 72
4.1.2 Equipment Setup 73
..... 78
4.1.3 Test Program 78
4.2 Pilot-Scale Model Test Work Results 80
4.3 Statistical Model 87
4.3.1 Introduction 87
4.3.2 Linear Regression Analysis for TiO_2 and HM 88
4.3.3 Multiple Regression Analysis for TiO_2 90
4.3.4 Multiple Regression Analysis for HM 99
4.4 Full-Scale Installation 106
4.5 Economic Analysis 109
CHAPTER 5 111
Conclusions 111
CHAPTER 6 113
Recommendations for Future Work 113
REFERENCES 115
APPENDIX A 119
APPENDIX B 156
VITA 160

LIST OF FIGURES

FIGURE 1: SCHEMATIC OF CROSSFLOW SEPARATOR 6
FIGURE 2: TYPICAL HEAVY MINERAL RECOVERY FLOWSHEET 9
FIGURE 3: LEACHING OF AN ILMENITE GRAIN 13
FIGURE 4: LEUCOXENE/ANATASE SHOW THE COMMON "SNOW BALL" APPEARANCE UNDER CROSSED POLARS 14
FIGURE 5: LEUCOXENE/ANATASE UNDER CROSSED POLARS SHOWING VISIBLE IRON STAINING 14
FIGURE 6: ZIRCON GRAIN SHOWING CHARACTERISTIC WHITE INTERNAL REFLECTIONS 15
FIGURE 7: RUTILE GRAIN SHOWING BOTH REDDISH BROWN INTERNAL REFLECTIONS AND LAMELLAR TWINNING 16
FIGURE 8: INVESTIGATIVE CROSSFLOW TEST WORK USING HEAVY MINERAL CONCENTRATE 19
FIGURE 9: TiO_2 AND HEAVY MINERAL RECOVERIES VERSUS QUARTZ REJECTION FOR LAB SCALE TEST WORK 20
FIGURE 10: CONCENTRATE GRADE VERSUS UNDERFLOW PERCENTAGE FOR LAB SCALE TEST WORK 21
FIGURE 11: SCHEMATIC OF LAB-SCALE CROSSFLOW 24
FIGURE 12: LAB SCALE CIRCUIT DESIGN AT THE MAXVILLE WET MILL STACKER 29
FIGURE 13: DEPICTION OF THE XRF PROCESS 31
FIGURE 14: SIMPLE PROCESS DEFINITION FOR MASS BALANCING 34
FIGURE 15: RECOVERY OF TiO_2 AND ZrO_2 37
FIGURE 16: TiO_2 RECOVERY AND OVERFLOW YIELD VERSUS QUARTZ AND SiO_2 REJECTION. 39
FIGURE 17: TiO_2 RECOVERY, QUARTZ REJECTION, AND FEED HM GRADE VERSUS OVERFLOW MASS YIELD 41
FIGURE 18: CROSSFLOW TiO_2 RECOVERY TIME SERIES PLOT 42
FIGURE 19: CROSSFLOW FEED AND PRODUCT HEAVY MINERAL GRADE FOR ALL TESTS 44
FIGURE 20: HEAVY MINERAL RECOVERY AND WEIGHT REDUCTION FOR ALL TEST RUNS 45
FIGURE 21: TYPICAL SIZE DISTRIBUTION DATA FOR CROSSFLOW OPERATION 46
FIGURE 22:TYPICAL FEED MINERALOGY 47
FIGURE 23: TYPICAL UNDERFLOW MINERALOGY 47

FIGURE 24: TYPICAL OVERFLOW MINERALOGY 48
FIGURE 25: RECOVERY OF TiO_2 VERSUS UNIT FEED GRADE 50
FIGURE 26: FEED GRADE VERSUS OUTPUT GRADE 51
FIGURE 27: NORMAL PROBABILITY PLOT FOR TiO_2 RECOVERY 53
FIGURE 28: NORMAL PROBABILITY PLOT FOR HM RECOVERY 54
FIGURE 29: BASIC STATISTICS FOR TiO_2 RECOVERY 55
FIGURE 30: PROPOSED MODEL OF THE CROSSFLOW UNIT 58
FIGURE 31: 3 FACTOR BOX-BEHNKEN DESIGN 69
FIGURE 32: PILOT SCALE FLOWSHEET 73
FIGURE 33: PILOT SCALE TESTING FACILITIES 74
FIGURE 34: DEFLECTION PLATE LOCATION 78
FIGURE 35: TiO_2 RECOVERY VS. QUARTZ REJECTION FOR PILOT-SCALE AND LAB-SCALE UNITS 83
FIGURE 36: TiO_2 RECOVERY AS A FUNCTION OF QUARTZ REJECTION 85
FIGURE 37: HM RECOVERY AS A FUNCTION OF QUARTZ REJECTION 85
FIGURE 38: BASIC STATISTICS FOR UNIT FEED (%TiO_2) 86
FIGURE 39: DESCRIPTIVE STATISTICS FOR UNIT OUTPUT (%TiO_2) 87
FIGURE 40: LINEAR REGRESSION OF TiO_2 RECOVERY BASED ON FEED GRADE 89
FIGURE 41: LINEAR REGRESSION OF HM RECOVERY BASED ON FEED GRADE 90
FIGURE 42: MATRIX PLOT ANALYSIS OF X INTERACTIONS FOR TiO_2 91
FIGURE 43: WIRE FRAME PLOT OF TiO_2 RECOVERY 96
FIGURE 44: OVERLAID CONTOUR PLOT FOR TiO_2 RECOVERY AND OUTPUT TiO_2 98
FIGURE 45: MATRIX PLOT ANALYSIS OF X INTERACTIONS FOR HM 99
FIGURE 46: SURFACE PLOT FOR HM RECOVERY 104
FIGURE 48: FULL SCALE INSTALLATION OPTION AFTER CAUSTIC SCRUB SYSTEM 107
FIGURE 49: FULL SCALE INSTALLATION OPTION BEFORE CAUSTIC SCRUB SYSTEM 108

LIST OF TABLES

TABLE I: INVESTIGATIVE HINDERED-BED SEPARATION TEST WORK ON HEAVY MINERAL CONCENTRATE 4
TABLE II: SUMMARY OF MINERAL CHARACTERISTICS 11
TABLE III: DETAILED SPECIFICATIONS ON PRESSURE TRANSMITTER 26
TABLE IV: EXAMPLE SPREADSHEET OF THE MASS BALANCE PROGRAM 35
TABLE V: GENERAL BOX-BEHNKEN DESIGNS 70
TABLE VI: DESIGN OF EXPERIMENT TESTING SCHEDULE 71
TABLE VII: HIGH/LOW VALUES FOR PILOT OPERATION 79
TABLE VIII: TEST DESIGN RESULTS 81
TABLE IX: AVERAGE PILOT-SCALE MODEL TESTING RESULTS 84
TABLE X: BEST SUBSETS REGRESSION FOR TiO_2 RECOVERY 93
TABLE XI: ESTIMATED REGRESSION COEFFICIENTS FOR TiO_2 RECOVERY 94
TABLE XII: ESTIMATED REGRESSION COEFFICIENTS FOR TiO_2 OUTPUT 95
TABLE XIII: BEST SUBSETS REGRESSION FOR HM RECOVERY 101
TABLE XIV: ESTIMATED REGRESSION COEFFICIENTS FOR HM RECOVERY 102
TABLE XV: ESTIMATED REGRESSION COEFFICIENTS FOR OUTPUT HM GRADE 103
TABLE XVI: ECONOMIC ANALYSIS OF CROSSFLOW INSTALLATION 110

CHAPTER 1

1.1 Introduction

Titanium Dioxide (TiO_2) is a material used in a variety of commercial products. Relatively pure titanium dioxide is used extensively as a pigment in the food, ceramics, paper, and paint industries. Titanium is also used in metal production where its low weight and high strength are beneficial in many different applications. The primary source of TiO_2 is a mineral called ilmenite. In 1998 the world production of ilmenite was over 4 million metric tons. Along with the United States, other major producers include South Africa, Australia, and Canada.

In the United States, Florida and Virginia are the two key production areas for titanium bearing minerals. These sites occur primarily as placer type deposits and span several miles. The TiO_2 in these deposits is primarily contained within the heavy minerals ilmenite ($FeTiO_3$), rutile (TiO_2), and leucoxene ($FeTiO_3$). Also contained within these deposits are significant amounts of zircon ($ZrSiO_4$) and staurolite ($Fe^{+2}Al_4[SiO_4]_2O_2[OH]_2$). Zircon is used in zirconium metal and various abrasive and foundry applications; and staurolite is used primarily as an abrasive in the sand blasting industry. Due to their high specific gravities, the above listed specific minerals are termed heavy minerals throughout the industry.

The initial processing of these heavy mineral sands is done primarily by the use of spiral separators. This type of separatory equipment uses the differences in densities of the material to concentrate the heavy minerals through low gravity means. Characteristics such as low unit efficiency and low capacity have plagued this type of wet separation in the past.

Until recent years, heavy mineral concentration was performed solely by spiral separators. However, several different gravity based separation techniques have been developed and implemented in various mineral processing applications.

Of these techniques, hindered-bed classifiers have been used quite frequently in various sections of the heavy mineral industry. Their low capital cost, ease of operation, and high capacities has led to promising results in several different applications. These devices have also been used quite successfully in other industries such as coal, mica, sand and gravel, and phosphate. This type of density based separator relies on two key physical properties of the mineral being separated, size and density. In a mono-density application this device is quite efficient in performing a size separation of the feed material. In a mono-size application a hindered-bed classifier is extremely efficient in performing a density separation. However, when the feed material contains varying mixtures of both size and density, unit performance is significantly reduced.

Several investigations have been performed on the implementation of hindered-bed separators and their use within the heavy minerals industry. They have proven to be successful when used in combination with the spiral circuits. Recent work has shown promise in specifically using this device as a final stage in order to upgrade the concentrate generated by the spiral circuit. A novel device known as the CrossFlow has been examined for this particular application. The CrossFlow uses a new feed introduction system which has been proven effective in several heavy mineral applications. Both laboratory and pilot-scale test work in this application are discussed within this report.

1.2 Literature Review

Hindered-bed classifiers have been used extensively throughout the minerals industry for several years. These classifiers are typically used to categorize mineral particles according to both size and density. They have been proven useful in recent years for density based separations in fine coal applications (Mankosa et al., 1995; Reed et al., 1995; Honaker, 1996). Also, these devices have been of particular interest for carbon recovery from both active fine coal streams and refuse ponds. With low capital cost and high capacities, hindered-bed classifiers have found their way into many different sectors of the mining industry.

Most hindered-bed classifiers operate on the same basic principles. First, material is introduced into a tank in slurry form. Water, termed teeter water, is then injected into the tank bottom. This process generates a zone of fluidized particles above the teeter water injection point. This zone is where separation of the particles takes place based on both differences in gravity and particle size. Within the fluidized zone, particles with a low settling velocity report to the unit overflow. Under normal operation, both fine particles and lower density particles have low enough settling velocities to report to this location. During the same process, coarser particles and heavy material with much greater settling velocities work their way through the unit and are eventually ejected from the bottom outlet of the device. The quantity of teeter water added to the unit and height location of the fluidized bed are the two main factors that determine the separation process.

These separators typically work quite efficient in applications where the feed material is either mono-density or mono-size. However, when the feed presented to the unit is varied in both size and density, efficient separation becomes difficult. Under this application the

shortcoming of this particular unit is that coarse low-density particles tend to accumulate in the teeter bed region. As other particles begin to congregate in this same zone, these coarse low-density particles are ultimately forced through the bottom unit discharge by mass action. To compensate for this unit phenomenon, the teeter water rate is typically increased, but this causes fine, dense material to become misplaced to the overflow. Both of these processes adversely affect the unit's overall separation efficiency.

Recent test work with Australian based mineral sands concentration has shown several successful circuit combinations using both spiral and hindered-bed separation technology (Elder et al., 2001). This test work employed the use of a typical hindered-bed separator as a final upgrading step after spiral concentration of heavy minerals. Although the results were promising, high heavy mineral recovery was only successful for low levels of quartz rejection. Table I shows the data derived during this investigation. For higher rejection levels of 81.7%, heavy mineral recovery drops to 96.6%. It may be possible that Australian mineralogy adversely affects the performance of this particular setup. The specific unit design employed for this testing could also negatively impact performance.

Table I: Investigative Hindered-bed Separation Test Work on Heavy Mineral Concentrate (Elder et al.,2001)

	Teeter water 85 gpm		Teeter water 100 gpm	
	Grade % HM	Recovery % HM	Grade % HM	Recovery % HM
Floatex feed	93.5		93.5	
Floatex underflow (Product)	96.2	99.3	98.7	96.6
Floatex overflow	19.4	0.7	37.2	3.4

Pilot-scale testing of a conventional hindered-bed separator for heavy mineral separation, which later developed into full-scale installation, was performed by McKnight et al., 1995. This particular application was the removal of quartz gangue from zircon rich tailings. These tailings contained approximately 3-8% Zircon, 18-22% Al_2O_3, and 1% TiO_2. Quartz rejections above 80% were achieved with zircon recoveries higher than 90%. In this particular application the density difference between zircon, 4.7, and quartz, 2.7, was sufficient to allow proper separation despite the tremendous size discrepancies between the two minerals. However, in near-density applications this conventional hindered-bed approach would prove insufficient (Dunn et al, 2000).

To overcome the shortcomings with typical hindered-bed separators, a novel device known as the CrossFlow separator was developed. This unit relies on an alternate feed presentation system that reduces the amount of fine, dense particles that become misplaced to the overflow launder. The CrossFlow is comprised primarily of a rectangular tank, as seen in Figure 1, that is divided into two regions; an upper separation chamber and a lower dewatering cone. Within this novel device, feed is presented tangentially across the upper portion of the unit. This tangential feed entry system allows for a lower velocity introduction of feed across the top of the classifier. This feed presentation design allows the unit to operate more efficiently than other conventional apparatuses.

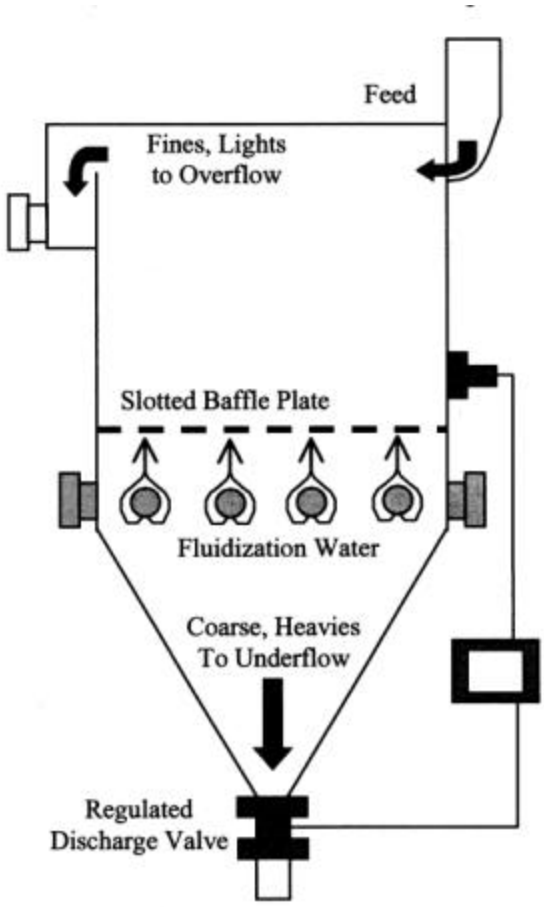

FIGURE 1: SCHEMATIC OF CROSSFLOW SEPARATOR

(Kohmuench et al., 2001)

Elutriation water is injected into the unit through a network of piping contained within the cell. This network is responsible for adequately distributing the load of water throughout the unit. It is above this pipe network where particle separation takes place. Below this region, the dense and coarse particles are drawn downward and compacted. This compaction allows for dewatering of the particle slurry to typical amounts of 60-75% solids. Even at this high content of solids, the product slurry is still very mobile and can be withdrawn from the bottom of the unit through a pneumatic control valve quite easily.

Given the advantages of the CrossFlow elutriator, testing began on various samples of heavy mineral concentrate from a typical Florida mineral sands operation (Dunn et al, 2000). The samples were comprised of several different minerals with differences in both size and density. The majority of the concentrate samples were comprised mostly of ilmenite, leucoxene, zircon, staurolite, and quartz. In this particular application, quartz represents the gangue/trash material that must be removed in order to produce pure heavy mineral products. Individual mineral characteristics are discussed later within this report.

1.3 Typical Heavy Mineral Operations

1.3.1 Processing Overview

Several heavy mineral operations are located in northern Florida. The deposits are relatively shallow and span many hundreds of acres stretching from south to north. The majority of heavy minerals contained within these deposits are present within the first 50 feet of ground depth. This thickness reduces to a mere 15 feet toward the outer edges of the deposit on both the west and east sides. The in-situ feed matrix is comprised mostly of sand, clay, and "hard pan". Hard pan is a composite material containing individual sand grains cemented together by humate, clay, and fine organics. This cemented material is located throughout the deposits in thin veinlets ranging from 1 to 4 feet thick.

The in-situ sand matrix is first excavated by means of a dredge. This dredging technique involves the use of a rotary cutter head to excavate and loosen the feed matrix. The dredge pivots around a spud system through use of several different swing lines. The dredging techniques developed by the mining industry are basically retrofitted canal dredging systems. The excavated material is then pumped directly to a rotating trommel, which

removes plus 1/4" material. The oversize material is primarily made up of roots, other organic material, and hard pan. Although hard pan contains economic levels of TiO_2 bearing minerals, it is extremely abrasive and difficult to process, and is thus rejected from the process immediately.

After the oversize has been removed, the feed material is sent through several stages of spiral classifiers. This spiral circuit is responsible for upgrading the feed from approximately 3-5% heavy mineral to a concentrate grade of 75-85%. The spiral circuit consists of four stages with numerous re-circulating loads. The four circuits used in this process are rougher, cleaner, finisher, and scavenger. Each of these stages consists of spirals specifically designed for certain separations. This circuit configuration is extremely effective in generating low grade, "throw away" tailings. These tailings are immediately pumped for re-contouring and subsequent reclamation activities at the mine site. However, this four stage configuration has proven inefficient in upgrading the concentrate above 85% heavy mineral without suffering high losses in both TiO_2 and heavy mineral recovery. Figure 2 shows the general flowsheet for this concentrate after gravity separation.

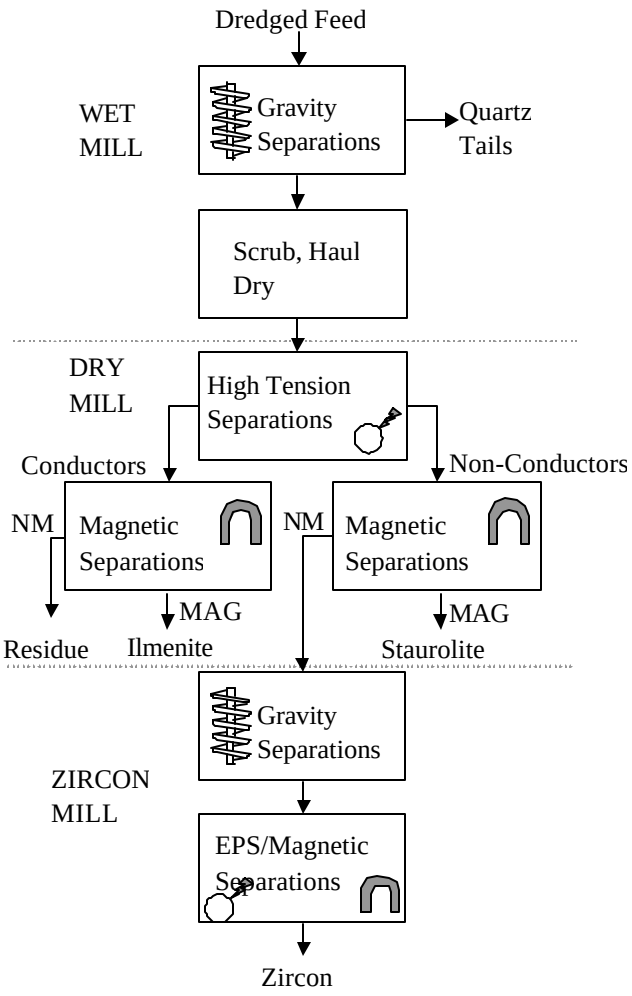

FIGURE 2: TYPICAL HEAVY MINERAL RECOVERY FLOWSHEET

(Dunn et al, 2000)

After gravity concentration, the wet mill concentrate undergoes attrition scrubbing to remove detrimental surface coatings on the sand grains. A solution of caustic, NaOH, is used during this particular process. These surface coatings consist primarily of humate and clay material generated by the mining and gravity separation processes. Without scrubbing, this coating would adversely affect subsequent dry mill separation and generate hazardous dust in the work environment. Proper rinse of the caustic solution from the sand grains is extremely

important, as it also adversely affects dry mill separation. The "clean" concentrate is then transported to several dry mill facilities, where electrostatic and magnetic separation techniques are used to segregate the various titanium bearing minerals and staurolite products.

Tailings generated from the dry mill consist mainly of quartz, zircon, and alumino-silicates. However, small amounts of TiO_2 bearing minerals and staurolite are still present from the previous imperfect separation. These dry mill tailings are further processed using spirals and additional dry milling equipment to produce a saleable zircon product. This zircon product must be extremely low in trash material such as alumina, iron, and titanium. The extremely high product quality required makes recovery of zircon a difficult process. Many stages of spirals and dry milling equipment are required to meet these specifications.

1.3.2 Florida TiO_2 Mineralogy

In the formation of these placer type deposits, the heavy mineral grains were selectively concentrated during various geologic transportational mechanisms. Evidence of these processes can be readily seen in "black sand" concentrations commonly found in most ocean beach environments. However, millions of tons of heavy mineral concentrate are required for deposits to be economically justifiable. Such deposits must have undergone lengthy geologic conditioning in order to reach concentrations of this magnitude. One example of this process is the Old Hickory Deposit owned and operated by Iluka Resources Limited, located in southeastern Virginia. Other deposits are located throughout northern Florida which are owned and operated by both Iluka Resources Limited and DuPont White Pigment and Mineral Products.

The heavy mineral assemblages contained within these deposits are comprised mostly of ilmenite, leucoxene, rutile, zircon, staurolite, and kyanite. Other minerals such as monazite, spinel, and garnet are also present, but in relatively low quantities. Table II gives general information on the density and composition of these minerals. The TiO_2 minerals which comprise the majority of production from these deposits are ilmenite, leucoxene, and rutile. Zircon and staurolite products are also produced in significant quantities from these deposits.

Table II: Summary of Mineral Characteristics

Mineral Type	Chemical Composition	Specific Gravity	% of HM Suite
Ilmenite	$FeTiO_3$	4.2 - 4.5	30
Leucoxene	TiO_2	3.6 - 4.3	10
Rutile	TiO_2	4.2 - 4.3	3
Zircon	$ZrSiO_4$	4.7	16
Staurolite	$Fe,AL(SiO_4)4(OH)$	3.7	18
Kyanite	$Al_2O_3(SiO_4)$	3.2 - 3.7	15

Of these minerals, the four that are of most economic interest are ilmenite, rutile, leucoxene, and zircon. Many other heavy minerals are present in this deposit, but are not of sufficient economic interest. The heavy mineral concentrate generated from the wet mill process also contains small amounts of clay and quartz, which were not properly separated. A set of four samples from this deposit where used for investigation using reflected light microscopy techniques. The textures and assemblages found within these samples are discussed.

For both primary products, ilmenite and zircon, chemical make-up as determined by x-ray fluorescence (XRF) is of much importance. The stoichiometric amount of iron (Fe), aluminum oxide (Al_2O_3), and zirconium oxide (ZrO_2) are also of importance. It is thus very important to determine what characteristics of the heavy mineral feed affect its chemical composition and separation efficiency.

Stoichiometric ilmenite contains 53% TiO_2, while, ilmenite in placer deposits varies widely in its actual titanium concentrations. This titanium concentration is dependent upon both the initial factors that occurred during deposition and those from subsequent weathering. Ilmenite is particularly resistant to weathering and displays a wide variety of textures in placer deposits. These textures can range from single crystals to polycrystalline aggregates. At very high temperatures ilmenite and hematite are in solid solution with one another. At lower temperatures the hematite will exsolve out of the solution and form lamellae structures within grains and at grain boundaries. These exsolution lamellae of hematite are often formed in crystallographic orientations.

During weathering and erosion, selective dissolution of the more soluble hematite proceeds from the margins of the grains and continues inward. This process leaves behind empty pits within the ilmenite grains. During this process of leaching, the ilmenite grain becomes increasingly enriched in its titanium concentration. The degree to which this leaching has occurred is important because iron is not a desired constituent of the ilmenite product. Figure 3 shows reflected light microscopy slides of an ilmenite grain that has not undergone complete leaching. The leaching and removal of iron occurs primarily at the grain boundaries and along internal discontinuities. Hematite is dissolved first from the ilmenite grains due to its greater solubility.

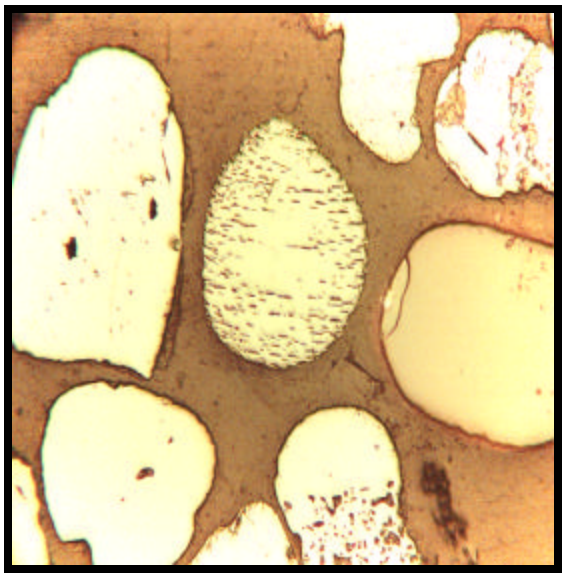

FIGURE 3: LEACHING OF AN ILMENITE GRAIN

Leucoxene and anatase form as alteration products of ilmenite. These alteration phases of ilmenite are subsequently higher in titanium and lower in iron content. These phases occur as a result of increased removal of iron and oxygen from the original structure. The resulting leucoxene and anatase become a finely crystalline aggregate which is seen as having a "snow ball" appearance under crossed polars, as seen in Figure 4. Although ilmenite and leucoxene/anatase are close in chemical composition, they look very different under reflected light microscopy. Various amounts of iron staining occurring during deposition can be frequently observed on both the leucoxene and anatase grains. Figure 5 shows leucoxene/anatase which has undergone various iron staining processes.

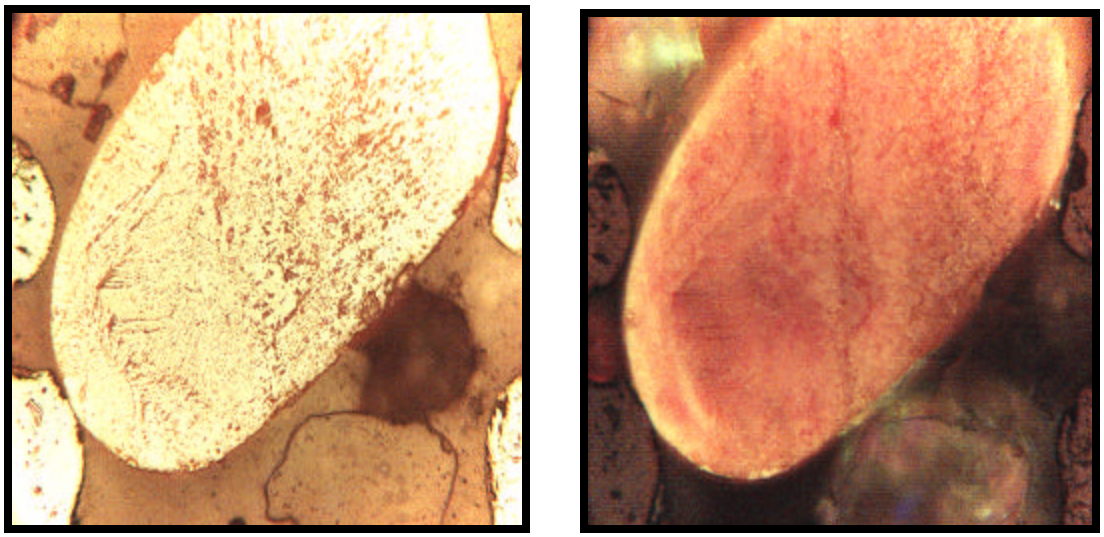

FIGURE 4: LEUCOXENE/ANATASE SHOW THE COMMON "SNOW BALL" APPEARANCE UNDER CROSSED POLARS

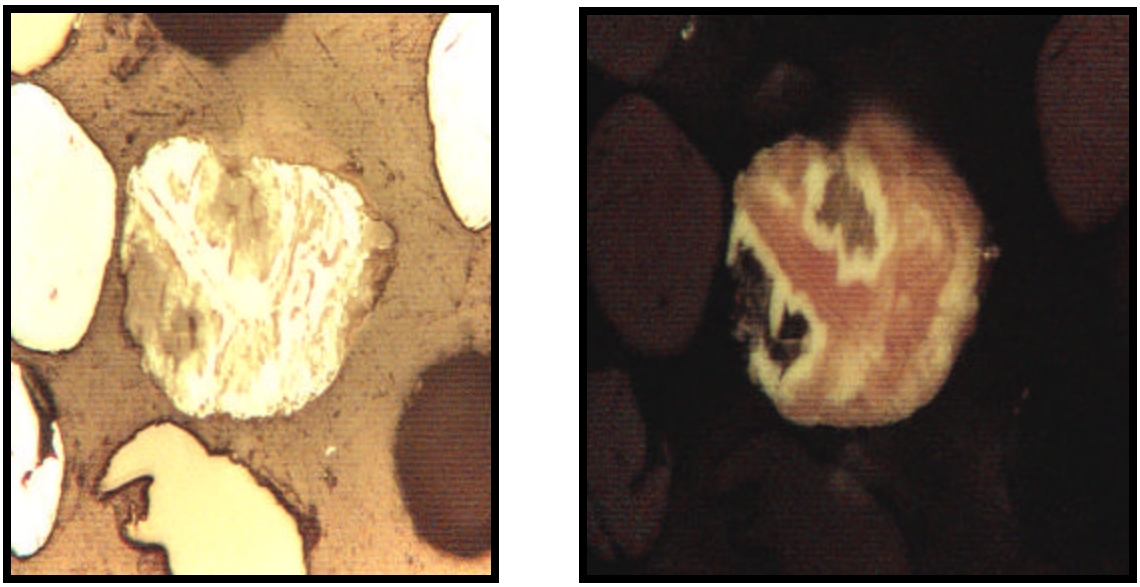

FIGURE 5: LEUCOXENE/ANATASE UNDER CROSSED POLARS SHOWING VISIBLE IRON STAINING

Zircon, another heavy mineral of economic interest, is also present in sufficient quantities to be of economic importance. Zircon grains exhibit a mild luster and appear as a

pale cream color under reflected light microscopy. Typical zircon grains are both nonmagnetic and nonconductive, although some grains exhibit para-magnetic properties due to small internal impurities in their grain structure. Zircon grains are often elongated and more angular than ilmenite due to breakage along cleavage planes during weathering. These grains show strong white internal reflection under crossed polars, as seen in Figure 6. Reflected light microscopy is a very important diagnostic tool in identifying various levels of internal impurities that may affect both separation and recovery.

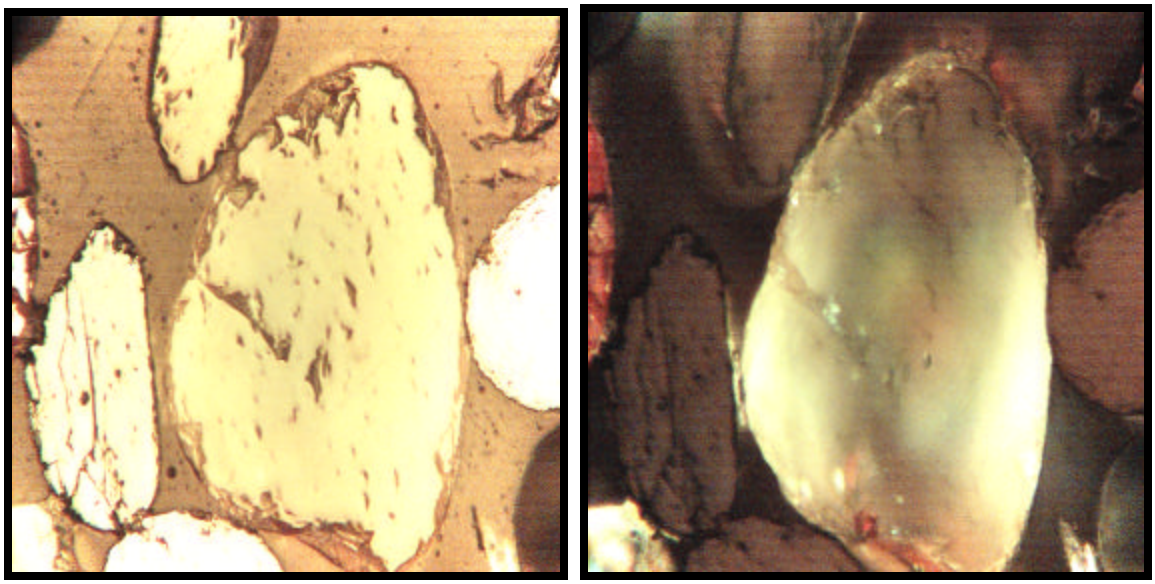

FIGURE 6: ZIRCON GRAIN SHOWING CHARACTERISTIC WHITE INTERNAL REFLECTIONS

Rutile is also present in the mineral samples, but in much lower concentrations. Rutile has almost a pure TiO_2 assemblage. It is a non-magnetic, conductor which often tends to be finer in nature than the other heavy minerals present. Under reflected light, rutile is most noticeable by its internal reflections that are reddish brown. The existence of twinning is also an important diagnostic tool when locating rutile under the microscope. Figure 7

shows common twinning within a rutile grain. Their strong anisotropism under crossed polars are usually masked by the strong internal reflections.

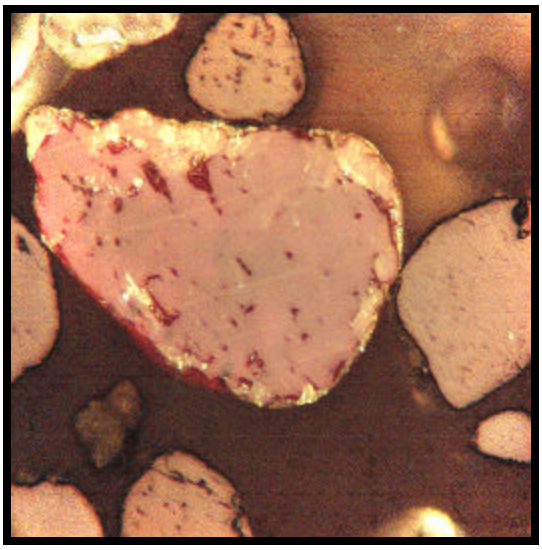

FIGURE 7: RUTILE GRAIN SHOWING BOTH REDDISH BROWN INTERNAL REFLECTIONS AND LAMELLAR TWINNING

During investigation of the samples, a few characteristics were observed that can be used for interpretation of the geologic conditions. The primary diagnostic tools for heavy mineral sands deposits are:

- Degree of leaching of hematite from ilmenite grains
- Degree of alteration of ilmenite into anatase and leucoxene
- Existence of quartz and clays showing separation efficiency

The void areas generated during the leaching process of ilmenite effectively lower the apparent specific gravity of the individual grain. For example, an ilmenite grain having undergone extensive hematite leaching may exhibit void areas totaling more than 25% of the

total grain structure. In this circumstance, the specific gravity of the grain becomes 2.8, instead of 3.7 for a uniform ilmenite grain. When submersed under water, these void spaces also generate buoyancy forces. The existence of buoyancy forces within dense minerals present in an elutriation device, cause significant reduction in unit separation efficiency. These grains are inherently more difficult to separate in a density based separatory device.

1.4 Problem Statement

Typical concentrate generated from the wet mill facilities is comprised of only 70-85% heavy mineral. This particular composition is the maximum concentration possible using the existing spiral circuits without suffering excessive recovery penalties. The excess quartz fraction present must be scrubbed, hauled, and dried along with the valuable heavy minerals prior to dry mill separation. This quartz fraction also reduces dry mill capacity and lowers the magnetic and electrostatic separation efficiencies. The potential benefits of installing an effective upgrading technology at the wet mill facilities are numerous and include:

- Reduced haulage costs
- Reduced chemical consumption during attrition scrubbing
- Reduced drying costs
- Increased dry mill TiO_2 recovery as a result of higher grade feed

Due to space restrictions at both wet mills, the addition of a fifth spiral circuit to achieve the required concentrate upgrade is not seen as a feasible solution. Another negative for spiral separation is the need for many secondary devices such as distributors, launders, piping, and additional pumps if gravity flow is not possible. The addition of another stage of

spirals would also complicate the existing circuit quite drastically making the selection of overall circuit optimum settings extremely difficult. The particular properties of the concentrate produced through the current circuit are such that an alternate separation device would be required to achieve the desired results.

Based on available data, an elutriator is one such device that employs different separation mechanisms to achieve mineral separation than the current spiral technology employed. Installation of an elutriation device would require less space and less ancillary equipment. The device would also be considerably less difficult to operate and maintain. The goal of this final elutriation stage would be to generate a "throw away" tailings stream with maximum recovery of the valuable TiO_2 bearing minerals present in the feed material.

1.5 Heavy Mineral Upgrading – Initial Test Work

Initial testing of the CrossFlow separator as an effective separation device for Florida heavy minerals began by using lab-scale equipment (Dunn et al, 2000). The goal of these initial tests was to evaluate the potential for effective heavy mineral upgrade by means of hydraulic classification. This test work used a 5 x 15 cm laboratory scale CrossFlow unit to simulate the process. The design of the unit was typical of the CrossFlow design principles, an upper tangential feed presentation system and a lower dewatering zone. Figure 8 shows a picture of the lab-scale CrossFlow used for testing. The disadvantage of this setup was the use of a manual control valve to regulate the underflow rate and fluidized bed level. The unit was initially fed at a target nominal feed rate of 1 tph/ft^2. Efforts were made by the operators to ensure the teeter water rate was minimized for the desired amount of quartz rejection required.

Given the assemblage of the concentrate samples being examined, quartz would need to be efficiently removed. To achieve this separation, a process that relies on the lower density of the quartz grains, 2.7, would need to be employed. To understand the ability of this system to separate the quartz efficiently, some preliminary investigations were performed and are discussed. Figure 8 shows investigative testing of the CrossFlow to achieve the previously stated goals. A relatively clean separation can be seen, with the light quartz grains teetering above the darker heavy mineral grains. This separation was relatively easy to achieve using a lab-scale CrossFlow unit.

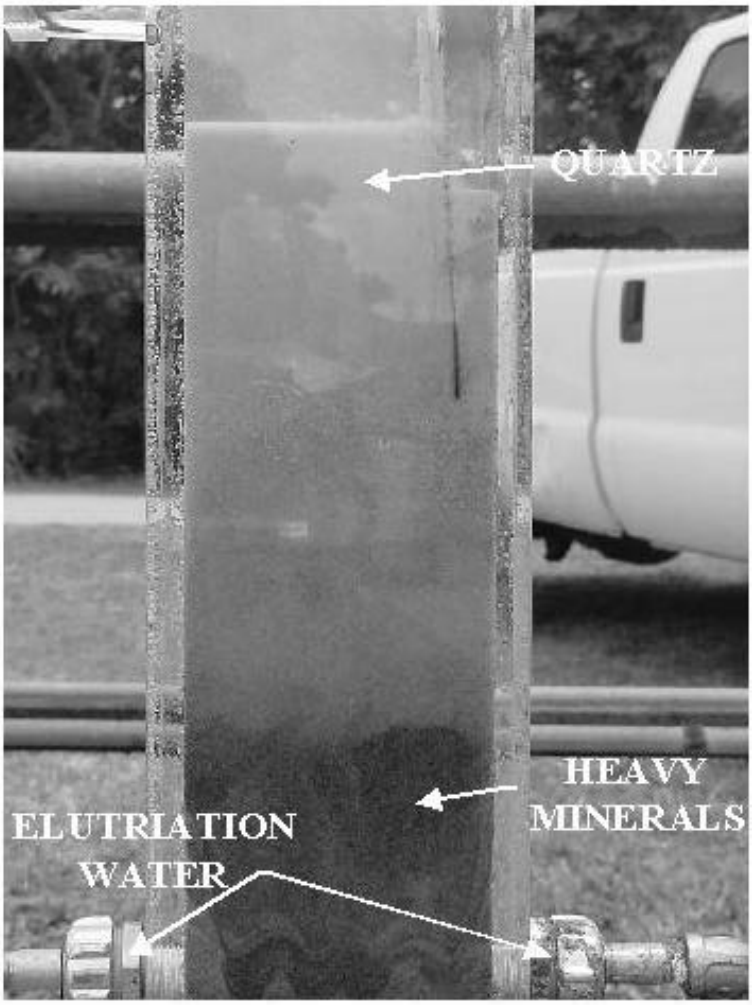

FIGURE 8: INVESTIGATIVE CROSSFLOW TEST WORK USING HEAVY MINERAL CONCENTRATE

The primary goal of this preliminary investigation was to reject as much quartz material as possible and yet recover most, if not all, of the heavy mineral assemblage. The results generated during this lab work were extremely promising. Quartz rejections greater than 90% were possible, while still maintaining recoveries of TiO_2 above 95%. Figure 9 shows a representation of the data collected during this preliminary work. The results exceeded both expectations and performance guidelines.

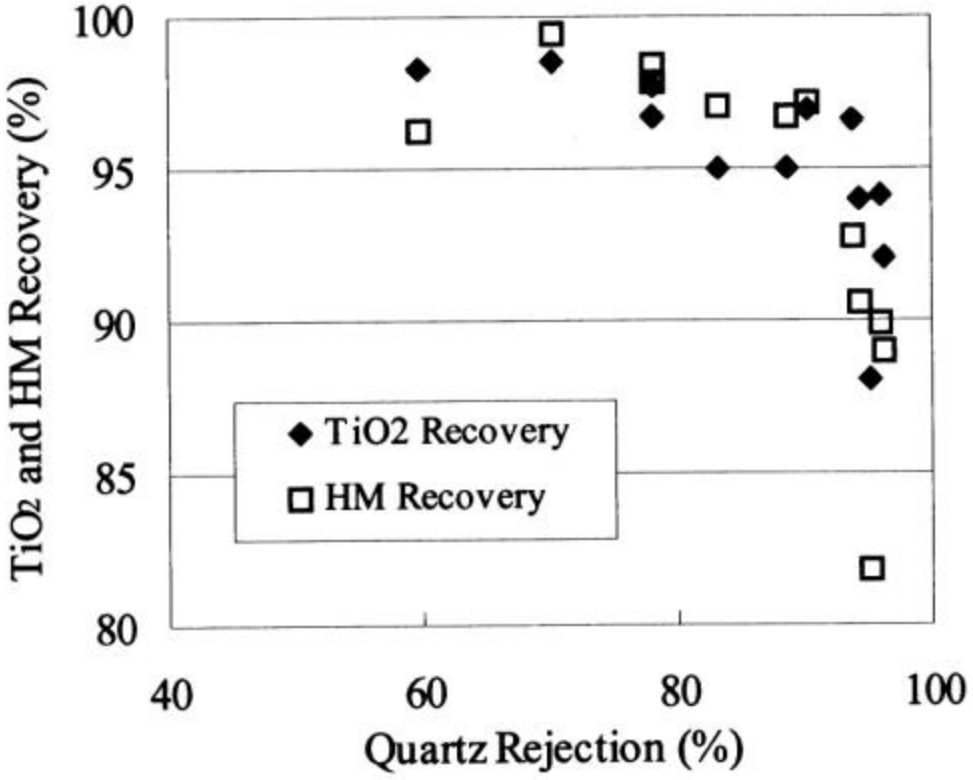

FIGURE 9: TiO_2 AND HEAVY MINERAL RECOVERIES VERSUS QUARTZ REJECTION FOR LAB SCALE TEST WORK

(Dunn et al, 2000)

The second goal of the test work performed was to generate an underflow material extremely high in both heavy mineral and TiO_2. To reach this goal, various tests were run by varying the percent of material reporting to the underflow. As seen in Figure 10, the 70-80% range of underflow resulted in concentrate grades of 95% heavy mineral and 33% TiO_2.

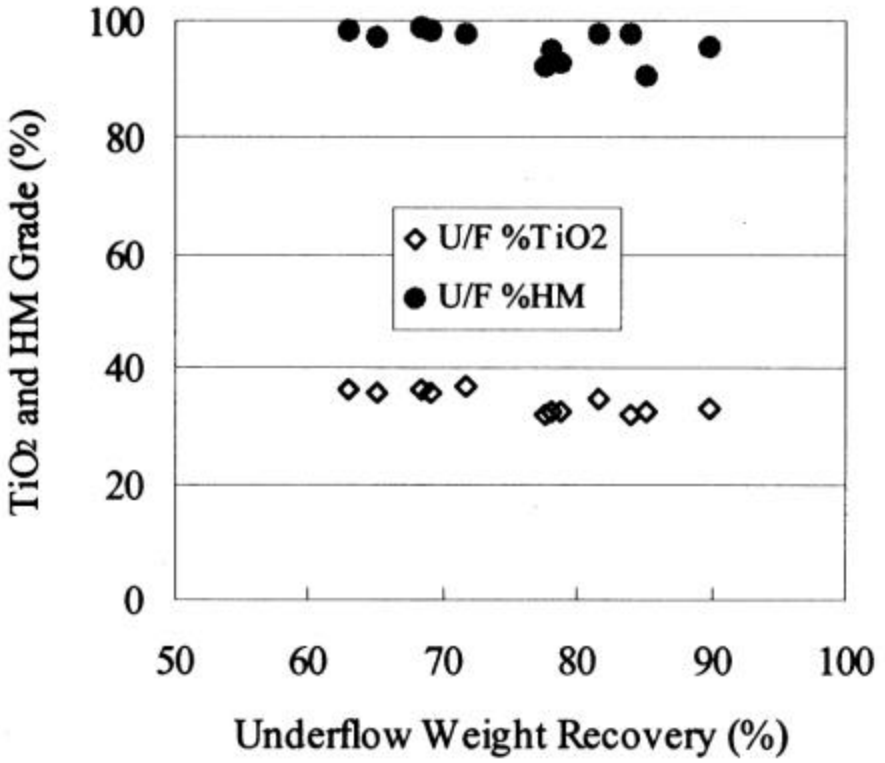

FIGURE 10: CONCENTRATE GRADE VERSUS UNDERFLOW PERCENTAGE FOR LAB SCALE TEST WORK

(Dunn et al, 2000)

The testing results carried out by Dunn et al. proved that hindered-bed classification can be used effectively to upgrade heavy mineral concentrate. These results showed significant promise and warranted further investigation. Preliminary economic analysis showed that a sustained recovery for this process averaging 98% would prove viable.

Associated quartz rejections above 60% would also be necessary for economic feasibility. Continuous pilot-scale test work would be needed in order to prove the proposed system. Successful pilot-scale testing would lead to full-scale installation of a CrossFlow elutriator at a mineral sands operation.

CHAPTER 2

2.1 CrossFlow Testing

2.1.1 Overview

The first stage in scale-up elutriation test work began with continuous open circuit testing on a small lab/pilot-scale device. The CrossFlow unit used during this period of testing was installed for continuous field operation. It was installed directly in line with the final wet mill concentrate. This particular location was placed directly after the attrition scrub system and prior to dewatering and stacking. This positioning allowed introduction of clean "scrubbed" concentrate into the test unit. Clean well water was used for the elutriation network in order to additionally scrub and rinse the individual concentrate grains, thus enhancing downstream dry processing.

2.1.2 Equipment Setup

The test unit was constructed by Eriez Magnetics and designed for continuous operation for approximately 0.5 to 1.0 tph of feed material. To accomplish this task, the unit was constructed with a cross-sectional area measuring 4" x 16", allowing for feed introduction of approximately 1.0 to 2.0 tph per ft^2 of cross-sectional area. The unit was constructed from stainless steel in order to prevent erosion and rust from any residual caustic (NaOH) still present in the feed stream due to attrition scrubbing. An engineering diagram of the unit constructed can be seen in Figure 11. To facilitate continuous operation, the unit was outfitted with a pneumatic underflow valve controlled through use of a microprocessor based controller system.

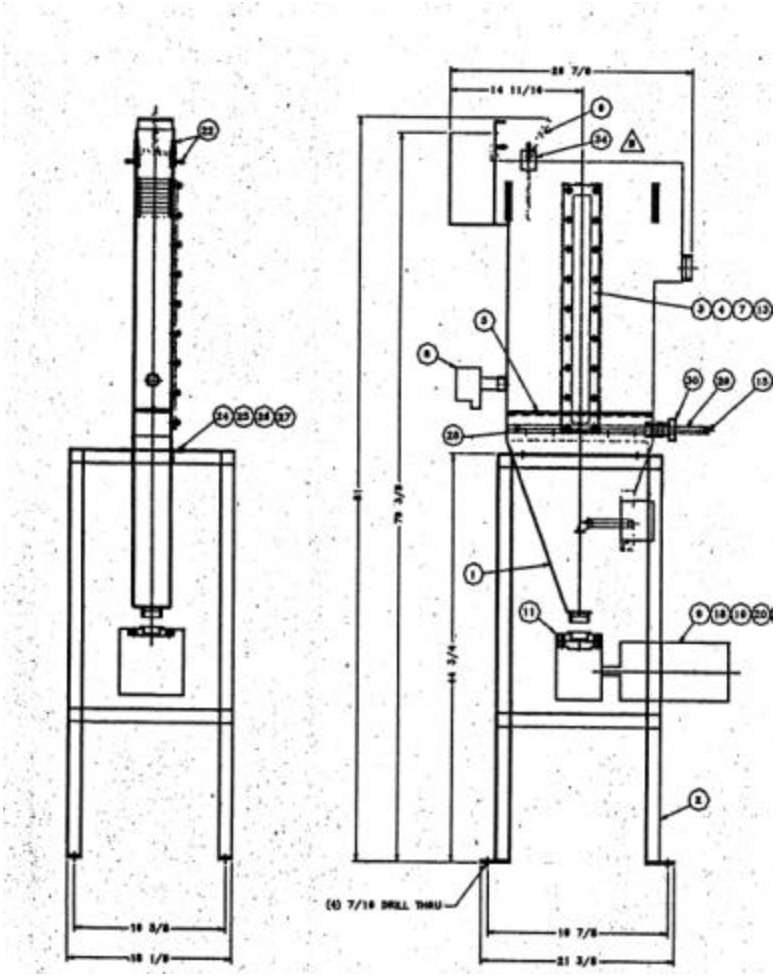

FIGURE 11: SCHEMATIC OF LAB-SCALE CROSSFLOW

Installation of the actual CrossFlow test unit was made possible by construction of a test stand capable of holding the unit along with several occupants. It measured roughly 10 feet in height, which allowed sufficient slope for the transport of unit underflow by means of a PVC pipe. This added height also allowed for proper material stacking from the underflow stream. The test stand was outfitted with the necessary electrical connections needed for unit control and operation. All required efforts were taken to ensure that the testing facilities were sound and met all applicable safety regulations.

The unit was fed directly from the final wet mill concentrate piping system. This particular point in the process circuit was located directly after the attrition scrub system and prior to dewatering and stacking. To accomplish installation at this particular location, a 2" bypass line was installed on the pipe feeding the stacker cyclone. This bypass feed contained significant amounts of pressure and was far lower in percent solids than desired. Because of these reasons, it was necessary to install an intermittent sump that could store material from the bypass and allow for greater control of the unit feed. This setup allowed the user to adjust feed rate with ease and also allowed the feed material to dewater to the necessary process percent solids.

Elutriation water was delivered to the process from a fresh water well located onsite by over 600 feet of high-pressure hose. Although the pressure and flowrate in this particular line fluctuated quite drastically, a 500-gallon intermittent storage tank was installed which could pump water directly to the elutriation network. This storage and pumping system allowed for a relatively constant volume and pressure to be delivered to the unit elutriation network. The water fed to the unit through this system was extremely clean, showing no signs of added viscosity affects from humate and clay loading. All other process water located onsite contained varying degrees of humate and clay, making use of well water most desirable. The well water used typically had a pH of 5.5 and a viscosity of 1.0 cp for the majority of test work. The acidic nature of the well water used for testing was expected from prior experience with typical Florida ground water. Elutriation flowrate was controlled by use of a Cole Parmer flow meter. This particular unit is a fixed orifice flow sensor, which allows greater ease of operation compared to mechanical or ultrasonic sensors.

This particular lab-scale CrossFlow was identical in design to the previous unit used, however, the underflow was controlled by a pneumatic actuator, which was regulated by a pressure sensor. The use of this particular valve control system allowed for continuous adjustment of the underflow rate in order to maintain a specified bed level and pressure within the unit. The pressure sensor used in this process correlates the pressure at a particular point within the tank to the underflow rate necessary to maintain this setting. This measurement is an indirect reading of the teeter bed interface location/height within the unit. Being able to control elutriation water rate and bed level/pressure independently is extremely important to achieve proper testing conditions.

The unit was fitted with an industrial pressure transmitter capable of monitoring the ranges of pressures expected during testing. As stated previously, these pressure readings are an indirect measure of the actual teeter bed level within the unit. The transmitter selected for this application was manufactured by Omega, model #PX726-300WCGI. This particular transmitter was fitted with a weatherproof enclosure and all wetted parts were compatible with corrosive media. The most important factor for selection of this model transmitter was its rated 0.15% accuracy while used in difficult and hazardous conditions. Installation of this instrument was made possible by use of the ½" npt adapter located on the test unit's exterior. More detailed information on this particular model can be seen in Table III.

Table III: Detailed Specifications on Pressure Transmitter

Output	Accuracy	Repeatability	Stability	Respons Time
4 - 20 mA	0.15%	0.05%	0.25% of URL	50 ms

Required adjustments to the process are based on the information available from the transmitter output. To accomplish this task, a 2600 series microprocessor based controller manufactured by Love Controls was selected. This particular controller was capable of both manual program functions and fuzzy logic control. It allowed for direct input of process rate functions, allowing for more user defined process control. The controller output was connected directly to the pneumatic pinch valve, allowing for teeter bed level control. Extensive work was required in order to calibrate the valve functions for use with the controller output.

Feed material provided by the intermittent sump was sent directly to a 2" Mosley Hydrocyclone. This device allowed significant increase in feed percent solids, which is known to be beneficial to unit operation. The underflow from this hydrocyclone was fed directly into the feed box on the CrossFlow unit. Overflow from this hydrocyclone was sent to a tank to be discarded later. Although very small portions of the feed material did report to this overflow stream, it was decided that this loss was inconsequential to the overall performance of this equipment setup. Pilot-scale and full-scale installations would require a properly sized hydrocyclone to ensure minimal loss of material during the dewatering process.

2.1.3 Testing Program

Initial unit application began with preliminary testing aimed at identifying relative high and low operational conditions. The conditions tested included feed rate, teeter water rate, and bed level. Although other variables existed, they were not directly controllable with

the current testing arrangement. Given this specific testing arrangement, examples of such uncontrolled variables are feed grade and feed percent solids.

The feed rate used during this test program varied from 1.0 to 1.5 tph/ft^2. This tonnage range appeared to offer the most quiescent flow in the separation tank. The target percent solids for this tonnage, given the cyclone feed system used, was approximately 50%. The elutriation flowrate necessary for separation given these conditions was 2.0 to 4.0 gpm/ft^2. Flowrates below 2.0 gpm/ft^2 caused the separation tank to clog and those above 4.0 gpm/ft^2 led to significant unit overflow of heavy mineral.

A total of 72 individual tests were conducted. Sampling was done approximately every four hours of unit operation. This practice allowed for the unit to experience a wide variety of feed conditions and operational fluctuations. However, this timed procedure generated occasional data points during both wet mill startup and shutdown. This led to drastic changes, beyond expectations, in unit feed heavy mineral grade. The feed rate, teeter water rate, and bed level previously used for normal process operations were incorrect for these particular periods. Inability to control these variations in unit feed grade led test operators to make small adjustments to teeter water rate and bed level. The majority of these changes were done by visual observation of the heavy mineral present in the unit overflow. Future test work will be focused around development of models capable of determining optimum operational settings for use during periods of such drastic changes in concentrate grade.

Samples were taken at three different locations around the CrossFlow separator. The first sample taken was located at the CrossFlow overflow stream. A bypass valve was installed in order to facilitate sample collection. The second sample, CrossFlow underflow,

was also taken at this time. The last sample point was unit feed located at the underflow of the hydrocyclone. This process stream was simply diverted for sample collection. This sample was taken last due to its drastic influence on the unit overflow. Collection of this stream prior to the overflow would have resulted in erroneous readings of the overflow stream if steady state had not resumed within the unit. The diamond symbols shown in Figure 12 represent the sample points used during this phase of test work.

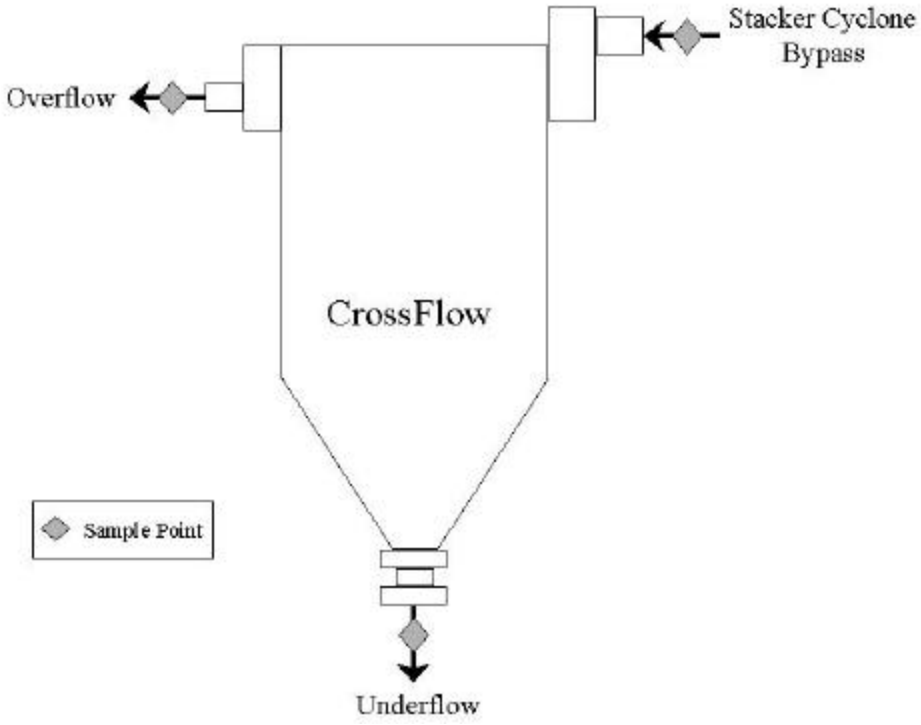

FIGURE 12: LAB SCALE CIRCUIT DESIGN AT THE MAXVILLE WET MILL STACKER

The samples taken from these locations were decanted and promptly sent for drying. Temperature during the drying process was not an important factor since no degradation of the material is experienced at high temperatures. Frequent stirring of the samples during the initial part of the drying process was necessary to prevent "popping" of the material. The samples were next weighed in order to obtain dry weight values, and then split into smaller

representative samples by use of a Jones Riffler. Approximately 100 grams of material was needed for the heavy mineral analysis for low grade samples, 0-15% HM, and about 50 grams for higher grades, 15-100% HM. Another 50 grams of sample was required for TiO_2 analysis by x-ray fluorescence techniques. Retains were also split out from the original sample and stored for various analysis which might become necessary at a later date.

Heavy Mineral analysis is accomplished by using a material of known specific gravity to separate the various minerals. Current industry standards are to use LMT, Lithium Metatungstate, as the separation media. This particular chemical can be heated in order to alter the specific gravity to the required value. Typically a value of 2.7 is used for this particular analysis. At this value, light material such as quartz and other gangue minerals are removed from the heavy mineral assemblage. Two separate fractions are retained from this process, a light mineral fraction and a heavy mineral fraction. These samples must be rinsed with warm water in order to remove the excess LMT left on individual mineral grains. The samples are then dried and weighed, in order to compare with each other, so that the percent heavy mineral of the original sample may be determined. This analysis procedure is used quite frequently for exploratory drilling programs as well as wet process analysis. This procedure is not typically used for material once it enters the dry mill processing facilities. During dry mill separation, other characteristics such as conductivity and magnetic susceptibly are more useful in understanding the individual sample characteristics.

TiO_2 analysis is accomplished by using x-ray fluorescence technology. Wavelength-dispersive x-ray fluorescence spectrometry, "XRF", is a non-destructive analytical technique used to identify and determine the concentrations of the elements present in solids, powders and liquids. XRF is capable of measuring all elements from beryllium (atomic number 4) to

uranium (atomic number 92) and beyond (at trace levels, often below one part per million, and up to 100%). Figure 13 depicts the equipment setup and process used for this measurement process.

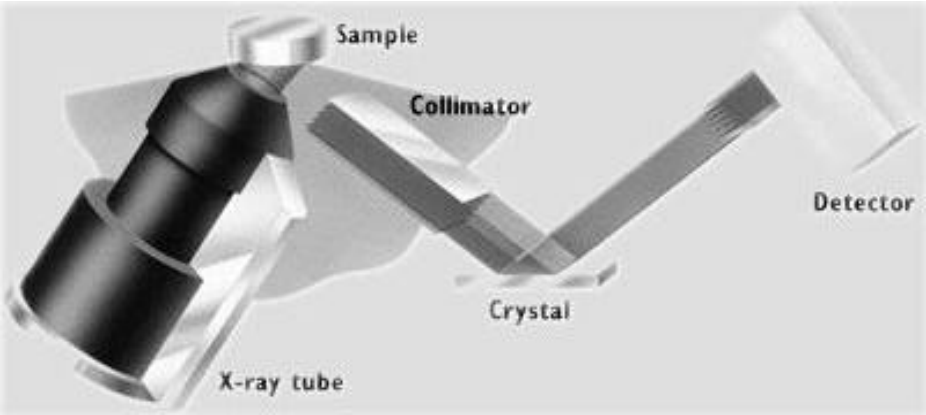

FIGURE 13: DEPICTION OF THE XRF PROCESS

2.2 Mass Balancing

2.2.1 Introduction

The primary focus of the sampling and laboratory work done during testing is to generate viable data in order to allow for interpretations and conclusions of the process under investigation. In order to achieve this, the data must fit some predetermined level of quality and accuracy. Test work designed to compare extremely small process variations must be handled in a more controlled fashion than those of a large process simulation. To this end, the level of accuracy needed to draw the desired conclusions from an experiment will dictate the procedures used during sampling and laboratory processing.

The usefulness of sampling data as a process-modeling tool is drastically dependent on the quality of the input data. The data used for modeling can come from a number of

different sources, such as human sampling, automated sampling, process outputs, and process inputs. Data collected from these various sampling and testing procedures is quite frequently susceptible to many different forms of errors. While some of these can be attributed solely to human error, others are more innate within the sampling and laboratory processes themselves. These errors have many different underlying causes, but the majority can be characterized as follows:

- Statistical Effects
- Sampling Procedures
- Assay Procedures
- Sizing Procedures
- Plant Process Fluctuations

Due to the innate nature of these errors, various mass balancing programs/models are used within the industry. The purpose of these mass balancing techniques is to generate statistically viable data which remains as close as possible to the actual measured data. The overall procedure for mass balancing is as follows:

- Data Collection
- Data Analysis
- Observation of Data Fit
- Statistically Refine Experimental Values

The basis for mass balancing algorithms used within industry are compositional differences of the various streams generated by the process equipment. A typical mass balancing routine takes all selected streams and calculates the smallest set of data adjustments required, which in turn make the total data set consistent. Consistency of the

sample data is based on a simple principle, input must equal output. An example of this principle would be that the TiO_2 content entering the CrossFlow must equal the unit's output of TiO_2. Information such as this is fundamental throughout the entire mass balancing routine.

Consider a process which contains three streams having assays of a, b, and c (where a, b and c may be assays of size, TiO_2, or any other conserved property specific to the process). A simple schematic of this situation is seen in Figure14. If we assume the flowrate in stream of assay a is 100 tph, then:

$$100a = x*b + (100 - x)*c$$

where x is the flowrate in stream of assay b, then:

$$x = 100(a-c)/(b-c)$$

The most important aspect of this equation is that there must be some differences between the assay values. If the process where simply a splitter device and the assays remained constant:

$$a = b = c$$

and therefore x = 0/0 which is undefined.

Expressed in a different way, values can only be estimated for mass balancing if a process imposes a difference on its product streams. If no difference is imposed, the information obtained by sampling cannot be used to calculate erroneous or missing data. It follows that the most useful properties used for mass balancing are those that generate the largest difference in the process streams sampled. This means that heavy mineral assays work well around a spiral circuit while size analysis works well around a hydrocyclone

circuit. The true ability of a mass balance program lies in its capacity to use a wide range of assays and flowrates over an entire process flowsheet.

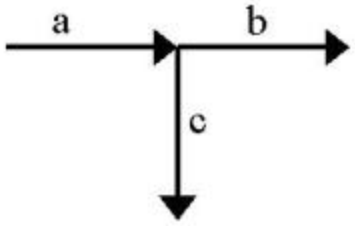

FIGURE 14: SIMPLE PROCESS DEFINITION FOR MASS BALANCING

2.2.2 Mass Balance Program Design

In an effort to better understand and draw statistically viable data from the samples taken during testing, a mass balance spreadsheet was constructed. The spreadsheet designed was written in Microsoft Excel format. It was designed to take user defined sample data and convert it to statistically viable data.

The developed mass balance spreadsheet first takes user entered experimental data into the Experimental Values section. This data is then duplicated into the Adjusted Values section. From these values, the relative change and weighted sum of squares are calculated. Several constraints have been entered into the spreadsheet. A total of four constraints dealing with mass, HM tonnage, TiO_2 tonnage, and ZrO_2 tonnage are used in this program. These constraints force the output of the system into equaling the input for both mass and assay values. Next, a "solver" routine is used which alters the data in the Adjusted Values section. The goal of this solver routine is to calculate the experimental values needed to meet

the constraints, while making the smallest changes possible to the original data set. Table IV shows an example sample set where feed, underflow, and overflow data has been entered.

Table IV: Example Spreadsheet of the Mass Balance Program

	Experimental Values				Adjusted Values			
	tph	% HM	% TiO_2	% ZrO_2	tph	% HM	% TiO_2	% ZrO_2
Feed	0.29	78.21	29.10	10.20	0.29	79.63	28.46	10.41
Underflow	0.24	91.35	32.30	12.40	0.25	89.69	32.98	12.14
Overflow	0.04	19.89	1.58	0.15	0.04	19.88	1.58	0.15

	Relative Change				Relative Error			
	tph	% HM	% TiO_2	% ZrO_2	tph	% HM	% TiO_2	% ZrO_2
Feed	0.18	1.82	-2.21	2.05	5.00	1.00	1.00	1.00
Underflow	0.29	-1.82	2.10	-2.14	5.00	1.00	1.00	1.00
Overflow	-0.48	-0.07	0.02	0.00	5.00	1.00	1.00	1.00

	Weighted Sum-of-Squares				Total
	tph	% HM	% TiO_2	% ZrO_2	WSSQ
Feed	0.00	0.00	0.00	0.00	0.00
Underflow	0.00	0.00	0.00	0.00	0.00
Overflow	0.00	0.00	0.00	0.00	0.00
					0.00

2.3 Experimental Results

2.3.1 Unit Performance

Experimental results were tracked for two basic types of assay information, heavy mineral recovery and TiO_2 recovery. Another important factor for the analysis of unit performance was the amount of overflow material generated during the various tests. This factor determines the amount of haulage and drying costs reduced by the proposed system. These aspects can then determine the economic viability of any future proposed system.

Complete mineral composition analysis using XRF analysis was run on each of the individual test runs. Figure 15 shows the various data for these runs. It can be seen that ZrO_2, zircon, generally maintained higher recoveries than TiO_2. This phenomenon was expected and can be attributed to the higher specific gravity of the zircon grains, 4.7. Rejection of the alumino-silicates, AL_2O_3, was typically less than 10%. Alumino-silicates are significantly less dense than other heavy minerals, 3.2 – 3.7 specific gravity, and would normally be expected to report to overflow in an elutriation system such as the one tested. These particular heavy minerals, specifically kyanite and sillmanite, have no significant value and must typically be removed during subsequent processing. Removal of this material is another beneficial feature of the proposed elutriation system.

The average TiO_2 recovery and ZrO_2 recovery experienced during the test work were 97.68% and 98.05%, respectively. At these levels of recovery, TiO_2 in the unit feed was upgraded from an average 26.01% to an underflow grade of 31.18%. The average overflow experienced during the testing program was only 2.95% TiO_2. Although these results are typically better than those achieved by Dunn et al, the same degree of upgrading needs to be achieved while generating an overflow stream less than 2% TiO_2 in order for this project to become industrially feasible.

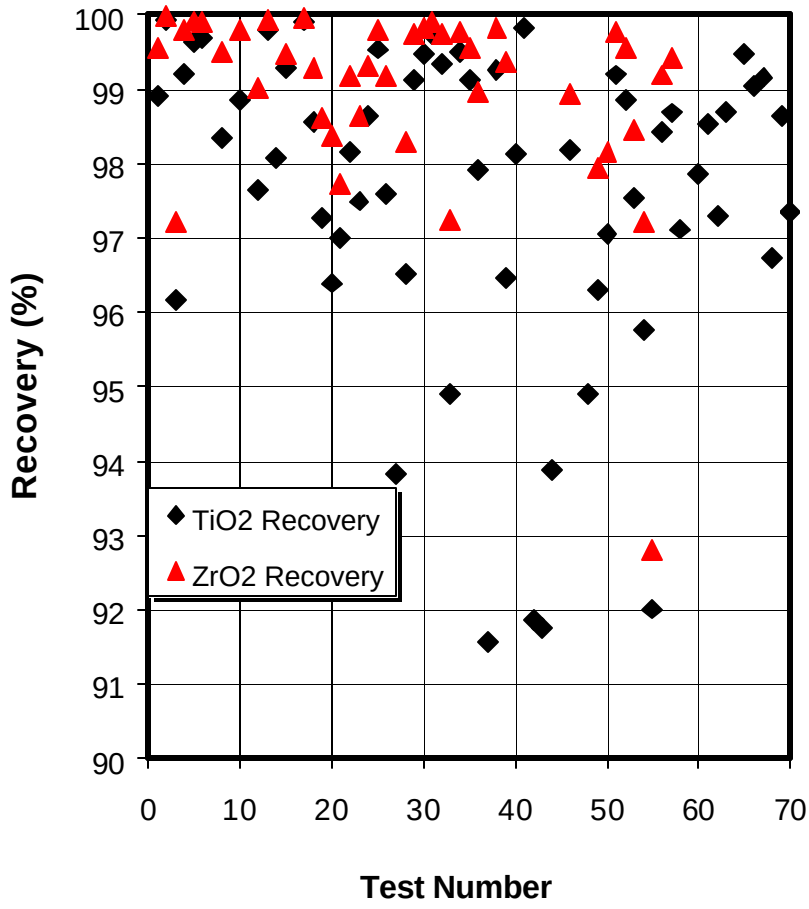

FIGURE 15: RECOVERY OF TiO_2 AND ZrO_2

Both heavy mineral separation and SiO_2 calculation using XRF were performed in order to assess the level of quartz rejection experienced. As previously stated, heavy mineral separation uses a dense media to remove quartz (all material <2.7 s.g.) from individual samples. This technique is the standard used throughout the mineral sands industry. Figure 16 (A) shows a plot of TiO_2 recovery versus the level of quartz rejection achieved. It can be seen that a 50% rejection of quartz was achievable with a TiO_2 recovery of approximately 98% and an overflow mass yield of 20%. Although the data correlates somewhat, it remains scattered in the upper levels of quartz rejection. The mass yield of the overflow stream is

also scattered in this testing range. It is believed that the +30 mesh quartz present in the feed and underflow causes this scatter of the data. This coarse quartz fraction, known as "rice rock", is extremely sporadic in quantity and thus difficult to accurately evaluate. Future testing will remove this material prior to laboratory analysis in order to achieve more accurate quartz rejection information.

Using the SiO_2 data obtained through XRF analysis, a less sporadic trend can be seen in Figure 16 (B). The only mineral present in the heavy mineral concentrate which contains specific levels of SiO_2 is quartz. However, the SiO_2 data and heavy mineral separation data show limited correlation to one another. It is believed that the particular SiO_2 analysis program used during the XRF analysis incorporates silicon readings from other minerals such as staurolite, kyanite, sillminite, and zircon. Therefore, the SiO_2 data obtained from XRF for this test program cannot be used as an accurate indication of quartz content. Although some correlation of SiO_2 to the content of quartz, staurolite, kyanite, sillminite, and zircon can be achieved, it is neither recommended nor needed for this test program.

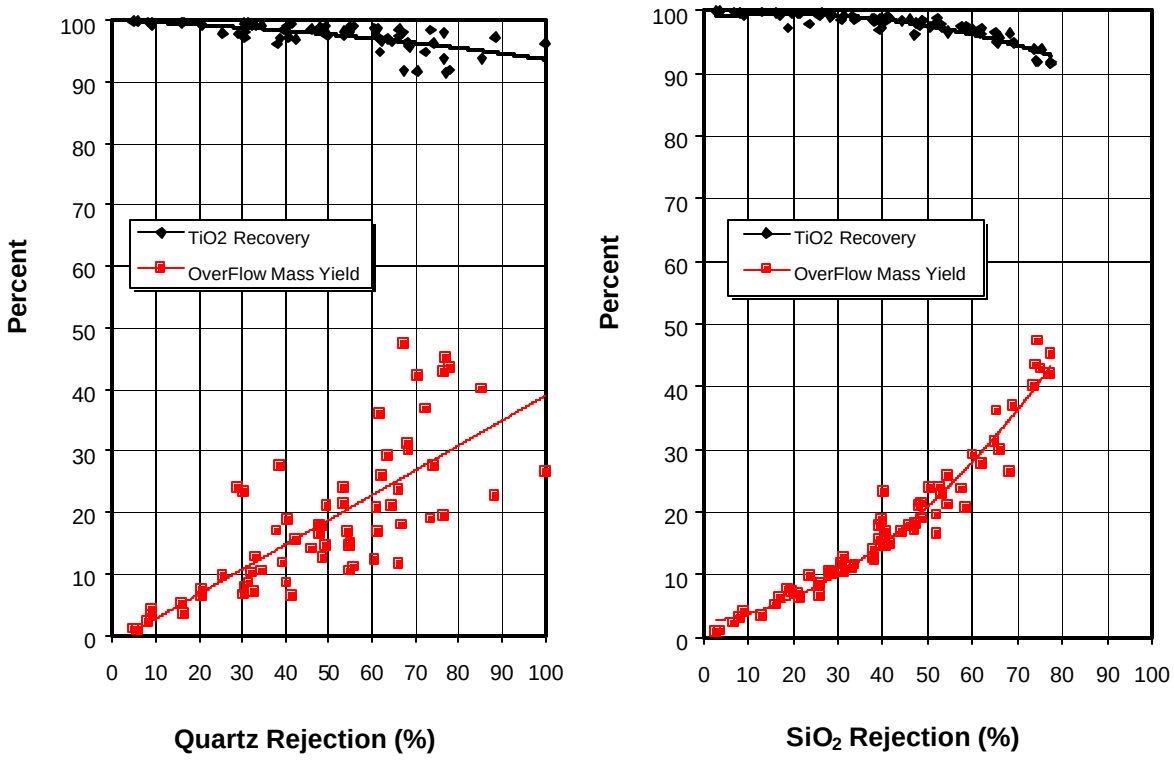

(A) (B)

FIGURE 16: TiO_2 RECOVERY AND OVERFLOW YIELD VERSUS QUARTZ AND SiO_2 REJECTION

Further examination of TiO_2 recovery shows a relatively strong trend when compared to overflow mass yield. Although test work was carried out at several different operational settings and feed grades, the data suggests that TiO_2 recovery is directly related to the quantity, or percentage, of material being forced into the unit overflow stream. In order to accomplish the different levels of mass rejection, an operator can manipulate both elutriation flowrate and bed level. Feed grade in terms of heavy mineral content, as seen in Figure 17, also exhibits drastic influence over the percentage of material in the unit overflow. It is plausible for high levels of quartz flowing upward in the test unit toward the overflow to trap

or entrain large amounts of fine heavy mineral. The majority of these lost heavy minerals, when introduced into an empty elutriation system under the same operational settings, typically would report to the underflow stream. Feed grade, however, is relatively uncontrollable using the testing setup developed for this stage of test work. In order to affect feed grade, drastic changes to the multi-stage wet mill spiral circuit supplying this test setup would be required.

Quartz rejection as a function of overflow mass yield gives insight into the size of quartz present in the concentrate. The largest portion of quartz rejection occurs in the initial, lower levels of mass rejection. This phenomenon would tend to describe the easy removal of fine/medium quartz grains. However, as mass rejection increases, the rate of quartz rejection decreases significantly. The medium/coarse quartz remaining in the concentrate becomes increasingly difficult to separate above mass rejections of 20%, resulting in the associated loss of fine heavy minerals such as leucoxene and rutile. It can be stated that the most efficient rejection of quartz occurs were less than 20% mass rejection is desired. Operation above these settings results in significant recovery penalties for both heavy mineral and TiO_2.

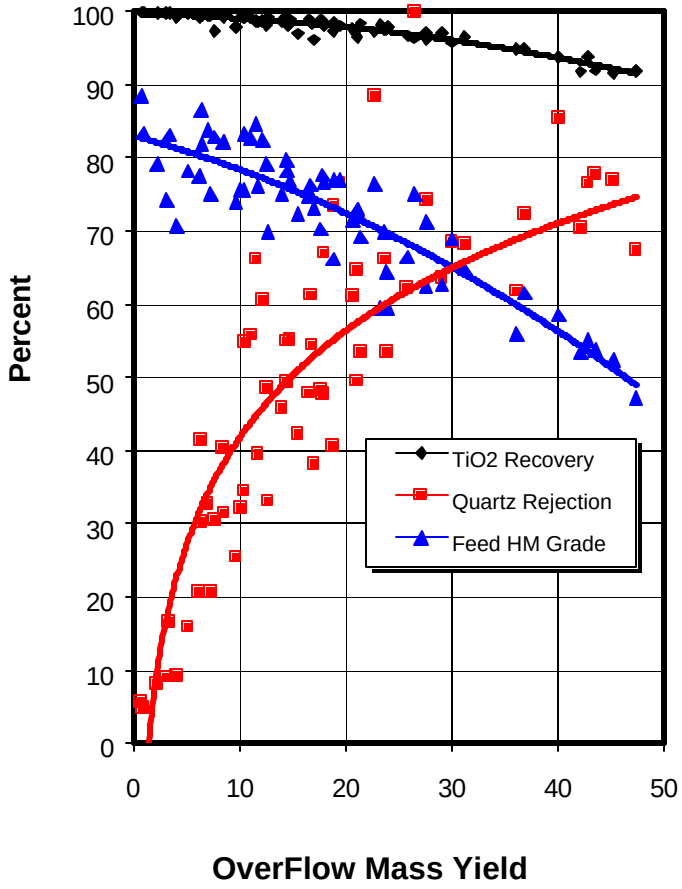

FIGURE 17: TiO_2 RECOVERY, QUARTZ REJECTION, AND FEED HM GRADE VERSUS OVERFLOW MASS YIELD

Further investigation of the TiO_2 recovery experienced under the testing program showed extreme fluctuations between successive samples. These fluctuations are most probably due to changes in feed grade, feed percent solids, and feed tonnage experienced using this particular testing setup. The time series plot in Figure 18 shows the variability of TiO_2 recovery experienced as a function of time for the entire testing period. For the CrossFlow to become a viable proposal in this particular field location, recovery variance as

a function of these dramatic fluctuations would need to be reduced. A constant recovery above 97% would be a successful achievement under these circumstances.

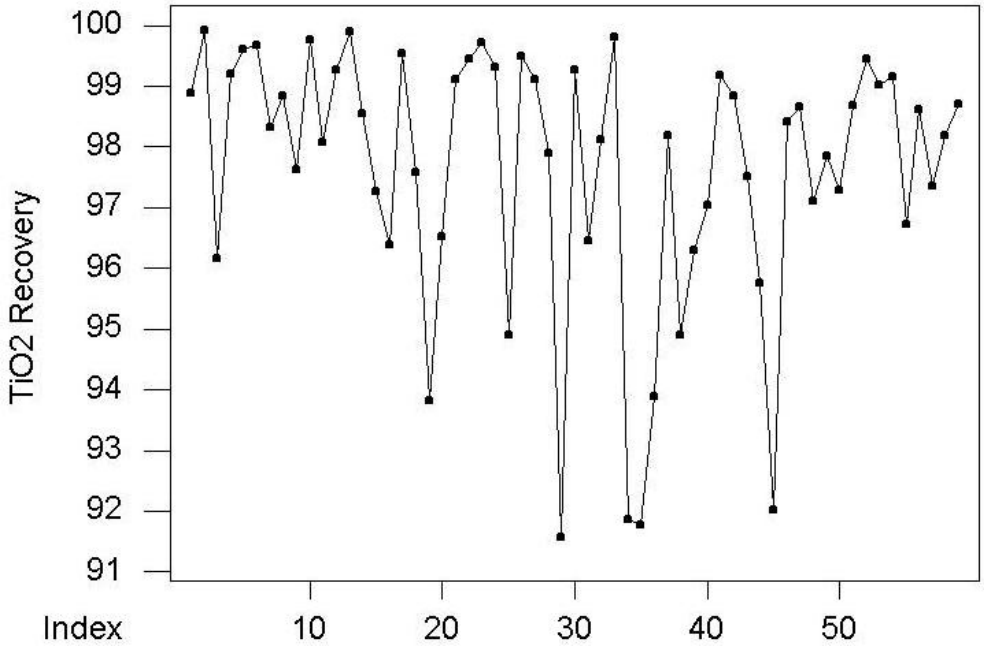

FIGURE 18: CROSSFLOW TiO_2 RECOVERY TIME SERIES PLOT

The average heavy mineral feed grade encountered during this stage of test work was 72.57%. This value was much lower than expected, when compared to the plant performance goal of 85%. While some of the lower grades experienced may be due to plant operational conditions, others may be associated with the location of the bypass line feeding the CrossFlow unit. One possibility is that heavy minerals in slurry tend to settle towards the bottom of the flow in a horizontal pipe, making collection of representative unit feed difficult. Another possibility for this lower than expected feed grade might be due to the presence of large amounts of coarse quartz. This coarse material is not considered part of the heavy mineral concentrate assemblage and is typically dry screened before any dry mill

separation occurs. For this reason, future test work will remove this material from heavy mineral determination.

Although the feed encountered during test work was lower than expected, the CrossFlow unit was successful in upgrading this material to an average grade of 86.84% heavy mineral. Figure 19 shows trend fit data for the CrossFlow feed and product streams encountered during testing. The average heavy mineral concentrate upgrade produced during the entire testing was 14.27%. The upgrade produced during periods of low feed grade was much more pronounced than during periods of high feed grade. However, during these periods of high upgrading, heavy mineral recovery decreased significantly. This can be attributed to an increase in retention time of the heavy mineral matrix within the unit. Operation under these particular conditions would require decreased unit bed pressure in order to reduce the amount of heavy mineral present in the upper separation zone. These lower grade periods operating at low pressure levels allow a thicker bed of light material to develop within the separation zone. It is also feasible that during periods of high overflow rates, fine heavy mineral particles tend to become trapped in the upward movement of light material being rejected to the overflow stream. It may prove beneficial to unit performance to lower teeter water rates and/or bed levels during these situations, reducing particles caught in carryover and those lost due to increased retention time.

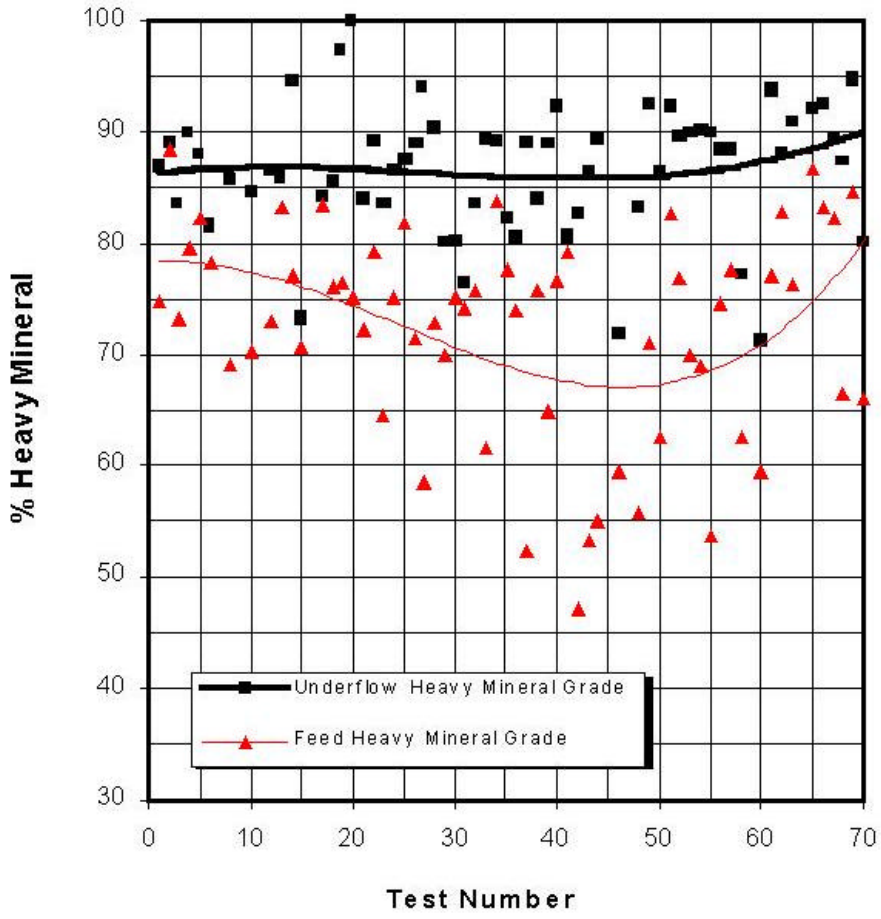

FIGURE 19: CROSSFLOW FEED AND PRODUCT HEAVY MINERAL GRADE FOR ALL TESTS

Although, slight variations in heavy mineral recoveries were experienced during tests, the majority of data was above 95%. On average, the heavy mineral recovery was 97.32%, above initial expectations for continuous unit operation. The majority of recoveries below 95% were attributed to overflow weight percentages above 25%. As previously stated, overflow levels of this magnitude can cause associated carry over of fine dense material. On average, the test work showed that an 18.34% reduction in mass was possible during continuous operation. Weight reduction of the feed introduced to the CrossFlow and the associated heavy mineral recoveries can be seen in Figure 20.

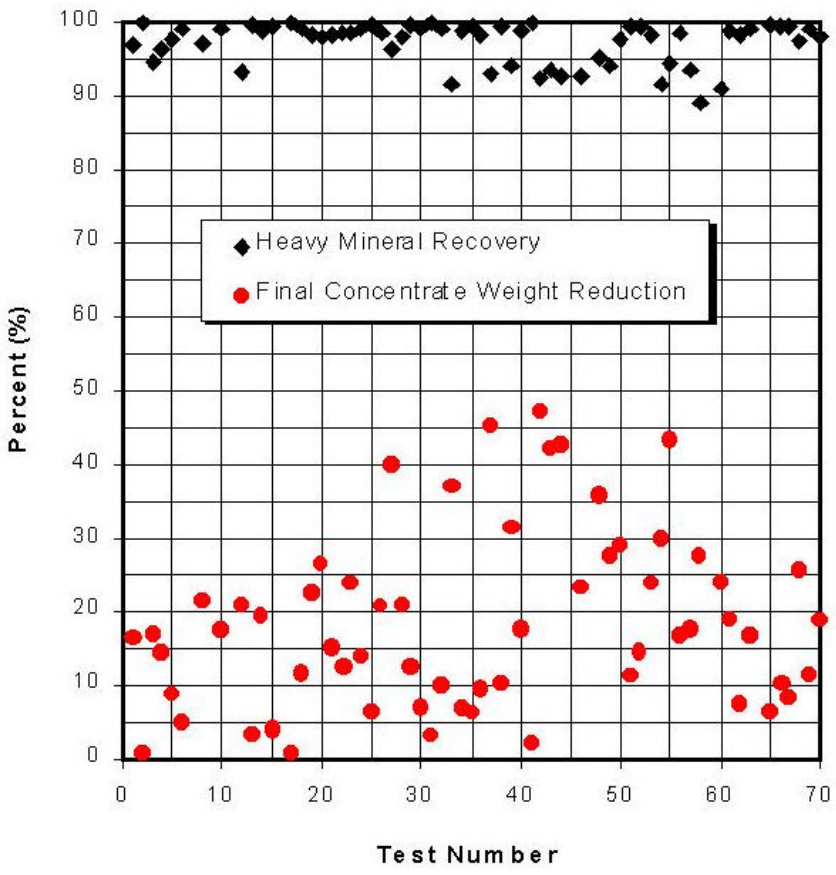

FIGURE 20: HEAVY MINERAL RECOVERY AND WEIGHT REDUCTION FOR ALL TEST RUNS

Sieve analysis was performed on each of the individual test runs. Averages of the individual tests can used in order to obtain typical size analysis for the feed, underflow, and overflow unit streams. In general, the 50% passing (d50) value for the unit feed was approximately 152 microns. Unit underflow tended to be slightly coarser with a d50 of 170 microns. Figure 21 displays the average size analysis for the various unit streams. The removal of fine/medium quartz and fine heavy mineral would explain this underflow coarsening affect. The overflow stream tended to be significantly finer in nature with a d50 of 127 microns. Removal of fine material and the associated increase in particle size would have significant impact on the downstream dry mill processes. Removal of this fine fraction

would not only increase dry mill recovery, but also reduce the significant amounts of dust present in the current work environment.

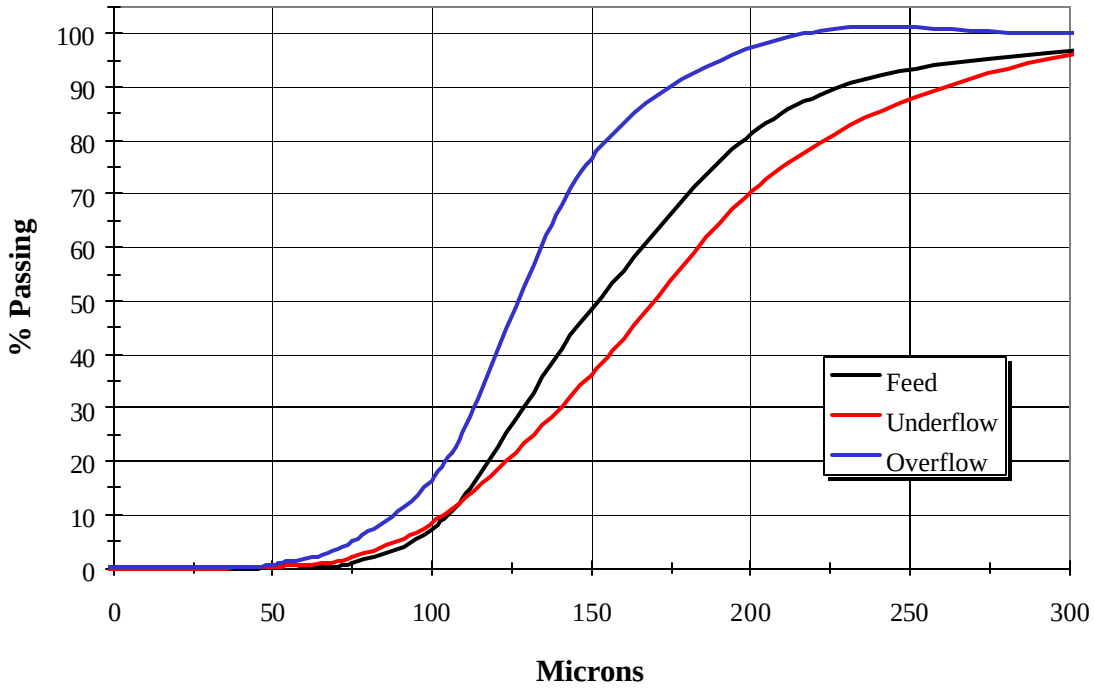

FIGURE 21: TYPICAL SIZE DISTRIBUTION DATA FOR CROSSFLOW OPERATION

Microscopic analysis of the unit streams aids in the understanding of mineralogical conditions experienced during the test work. Figures 22, 23 and 24 are mineral photos taken using a stereoscope. Large amounts of quartz, seen as almost transparent, can be seen in the feed sample along with the typical heavy mineral assemblage of ilmenite, leucoxene, zircon, and staurolite. The upgrade of material can be seen in the underflow photo where heavy minerals predominate the assemblage. It can easily be seen that TiO_2 bearing minerals are much more prominent in the unit underflow sample. Unit overflow consisted primarily of quartz, however, small amounts of ilmenite and leucoxene can be seen in Figure 24.

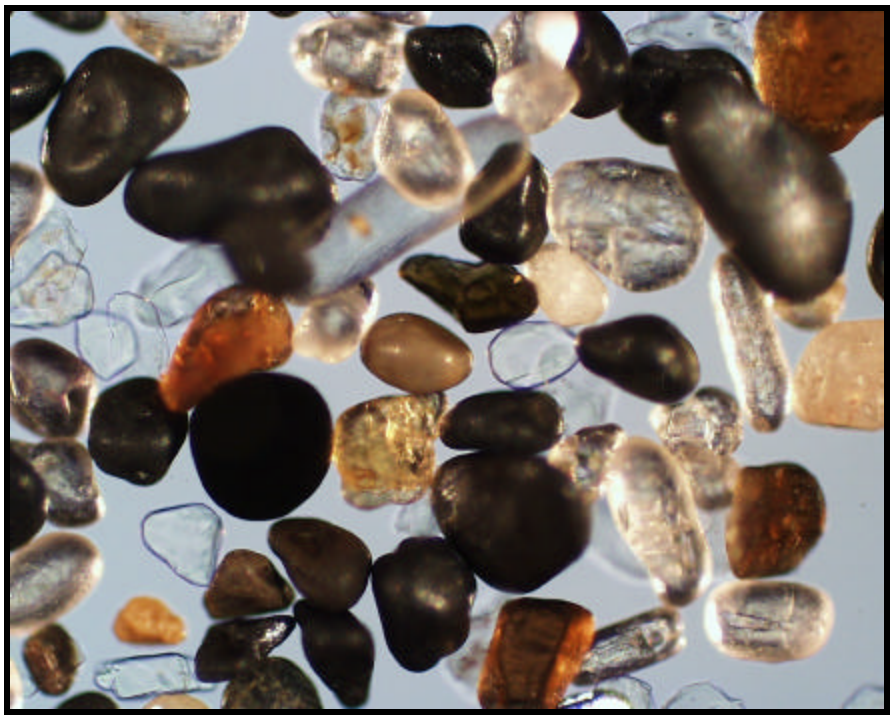

FIGURE 22: TYPICAL FEED MINERALOGY

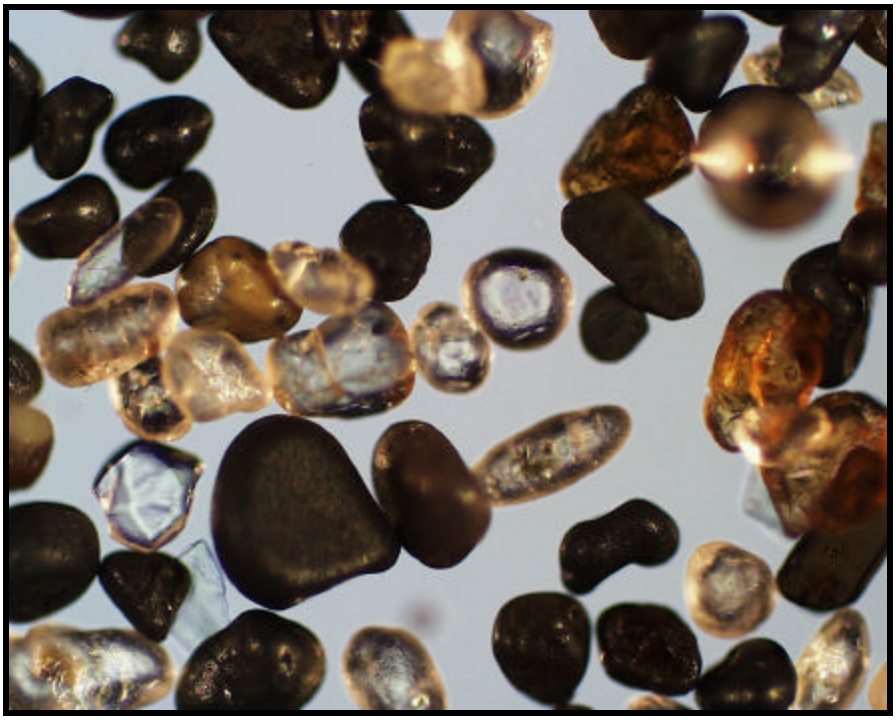

FIGURE 23: TYPICAL UNDERFLOW MINERALOGY

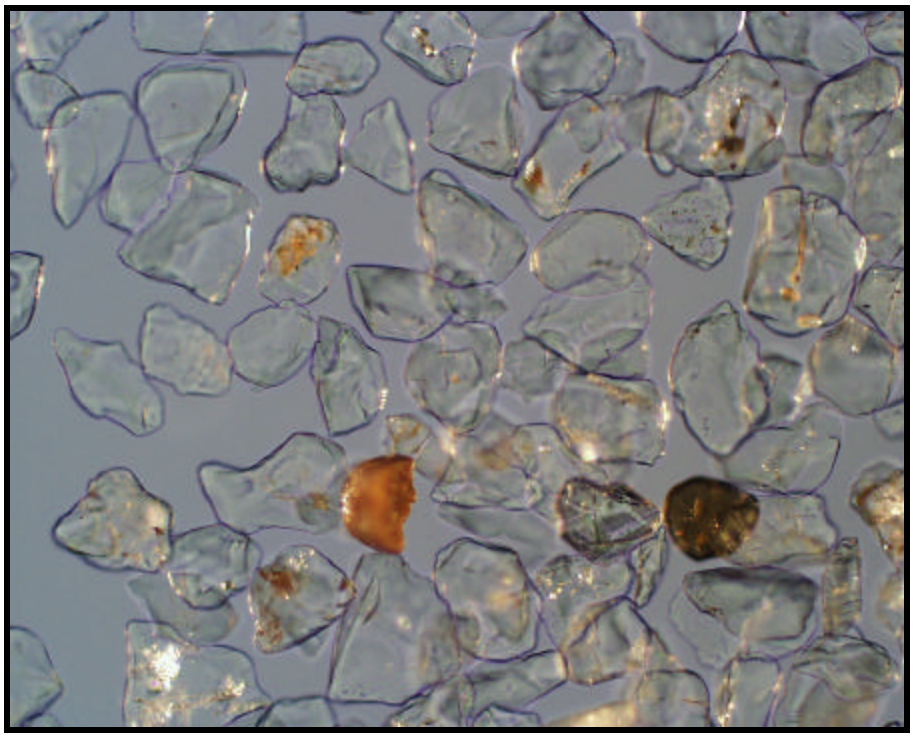

FIGURE 24: TYPICAL OVERFLOW MINERALOGY

Although operation of the unit was relatively sporadic, many different trends become visible in the data. Given uncontrollable fluctuations in operational conditions, tests run in series can usually be used to efficiently track and predict unit performance. Based on the laboratory data, both TiO_2 and HM recoveries can be fitted in order to reach several desired unit process outputs. These desired outputs are unit recovery and underflow grade. Both of these outputs are direct functions of the feed grade entering the CrossFlow. Figure 25 shows trend fit data for the testing series, correlating unit recovery based on incoming feed grade. In general, a tight correlation for recovery as a function of feed grade can be seen, with only a few data points lying outside of the predicted range. These outlier points are most likely

due to influences beyond feed grade such as percent solids, elutriation flowrate, or bed level. The derived equation for TiO_2 recovery as a function of unit feed grade is as follows:

$$TiO_2 \text{ Recovery} = -0.0275(\text{Feed Grade})^2 + 1.838(\text{Feed Grade}) + 68.829 \qquad [1]$$

Equation [1] is very useful in quickly determining the expected recoveries for the various wet mill concentrate grades. This data allows operators to determine the optimal feed grade to send the unit from the existing wet mill in order to optimize overall plant performance. Although gpm and bed level can be manipulated in order to achieve improved recoveries for the various feed grades, the overall trend is quite explicit from the data.

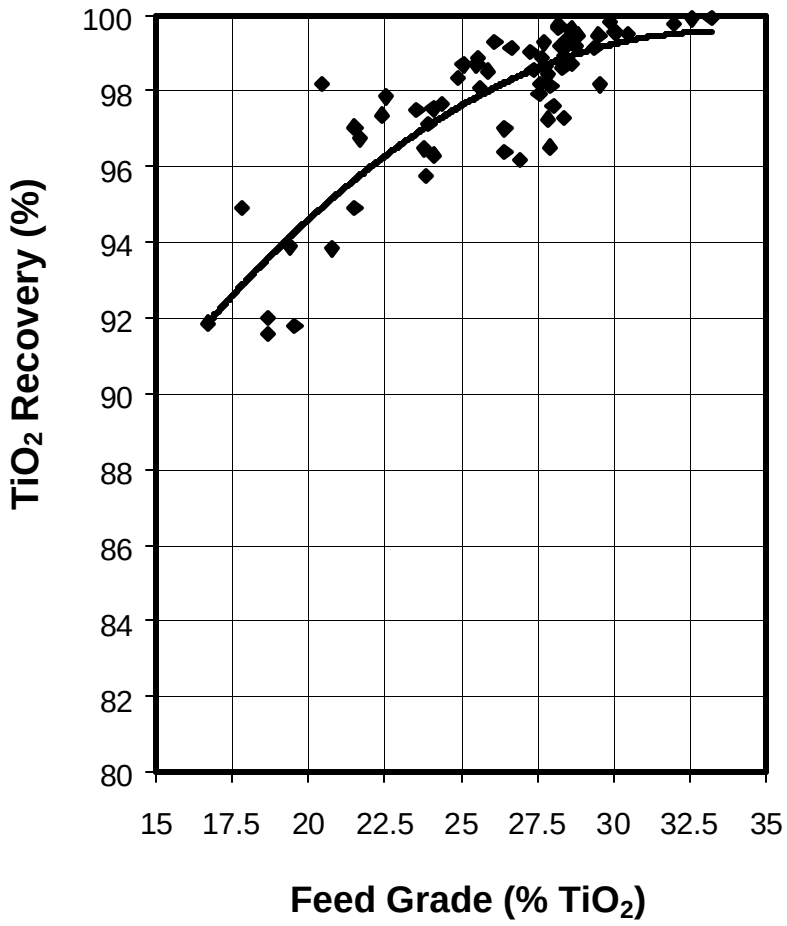

FIGURE 25: RECOVERY OF TiO_2 VERSUS UNIT FEED GRADE

Expected output grades from the unit is also of much importance. This data allows operators to understand the various output grades that would be sent to the existing dry mill for processing. Although more scattered than the recovery data, the output grades can be roughly estimated from the trend curve in Figure 26. This figure shows many more outlying values, which may be attributed to the various operational conditions under which the unit was operated. The simple model equation using only feed grade as a predictive variable is as follows:

$$\text{Underflow Grade} = 0.0035(\text{Feed Grade})^2 + 0.0583(\text{Feed Grade}) + 27.26 \quad [2]$$

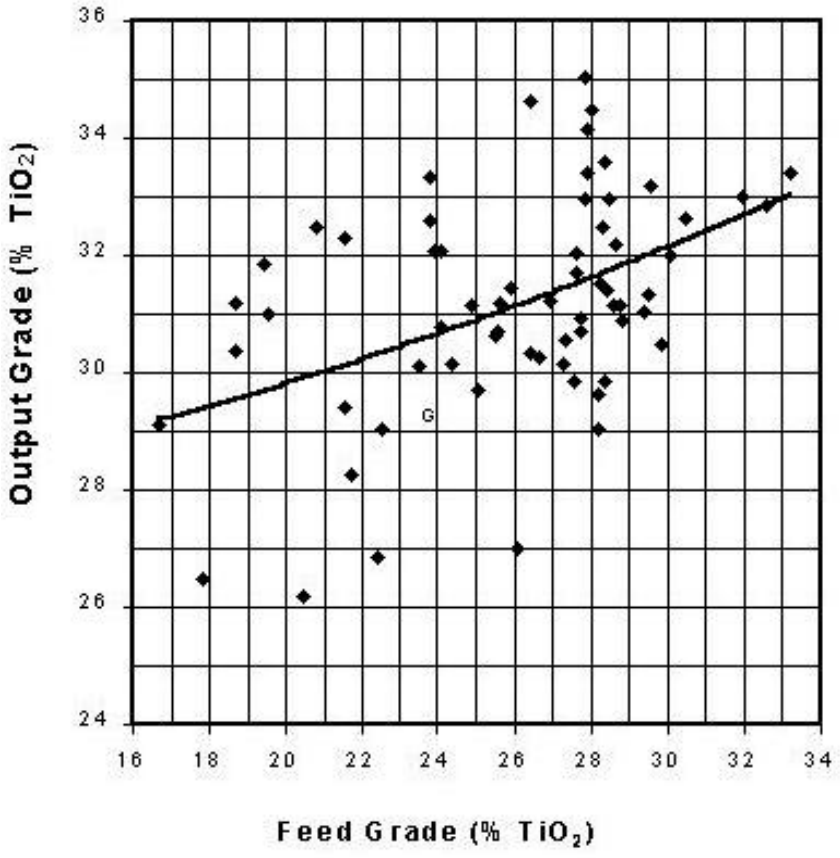

FIGURE 26: FEED GRADE VERSUS OUTPUT GRADE

It is the hope that later test work can develop a better model to more accurately predict the unit output. Equation [2] would need to incorporate feed grade, teeter water rate, bed level, feed percent solids, and feed tonnage. This data would become particularly important for operators wishing to achieve various level of unit operation.

Statistical evaluation of the various test runs was accomplished through the use of MiniTAB. Various interactions were examined in order to better understand this particular process. Even under the extreme process fluctuations experienced, unit TiO_2 recoveries

remained in a relatively narrow range. A normal probability plot of the experienced TiO_2 recoveries is shown in Figure 27. The standard deviation of 2.07% for this process was much higher than expected. The probability plot for TiO_2 recovery does not exhibit a typically normal pattern. Few points fall within the 95% confidence intervals predicted by a normal distribution function. There are too many points in the left tail (points above the limits) as well as too many points in the right tail (points above the limits) compared to that of the expected normal distribution function. The Anderson-Darling statistic for this situation is 3.304. This measurement is an interpretation of how far the plot points fall from the fitted line for the probability plot. The statistic is a weighted squared distance from the plot points to the fitted line with larger weights in the tails of the distribution. A smaller Anderson-Darling statistic indicates that the distribution fits the data better. For some limited purposes, assuming a normal distribution for this data would be acceptable. However, an attempt was made to find a better result using six other common distributions including: lognormal base 10, lognormal base e, Weibull, extreme value, exponential, logistic, and loglogistic distributions. Of these distributions, extreme value exhibits the best Anderson-Darling statistic, 1.16. Thus for determining maximum likelihood estimates of the population parameters and percentiles of the distribution for this data, an extreme value distribution should be used.

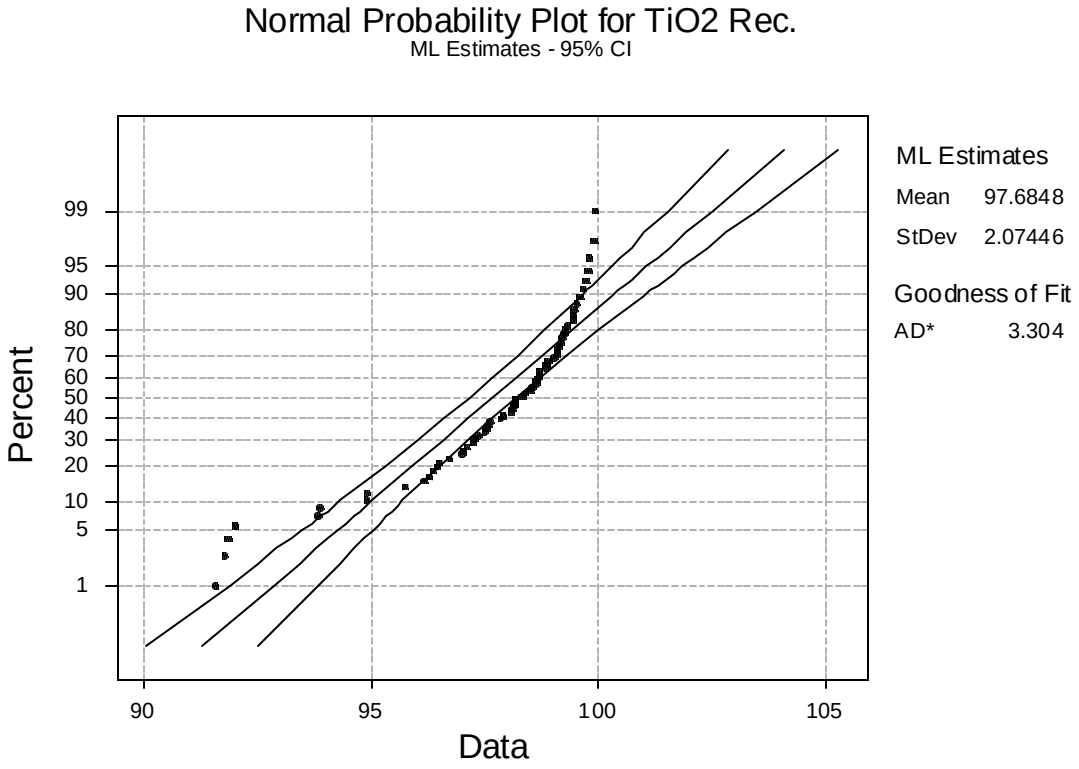

FIGURE 27: NORMAL PROBABILITY PLOT FOR TiO_2 RECOVERY

A normal probability plot of the experienced HM recoveries can be seen in Figure 28. Standard deviation for this process is slightly higher than the TiO_2 data, 2.72%. The probability plot for HM recovery also does not exhibit a typical normal distribution pattern. The majority of the points fall outside the 95% confidence intervals predicted by a normal distribution. There are too many points in the left tail (points above the limits) as well as too many points in the center (points below the limits) compared to what is expected in a normal distribution function. Assuming a normal distribution for these data would not be acceptable, given the AD value of 4.97. After examining all other typical distributions, it was found that an extreme value distribution gives a slightly better AD value of 3.54. Neither the normal or extreme value distributions appear to accurately predict HM recovery for this test work.

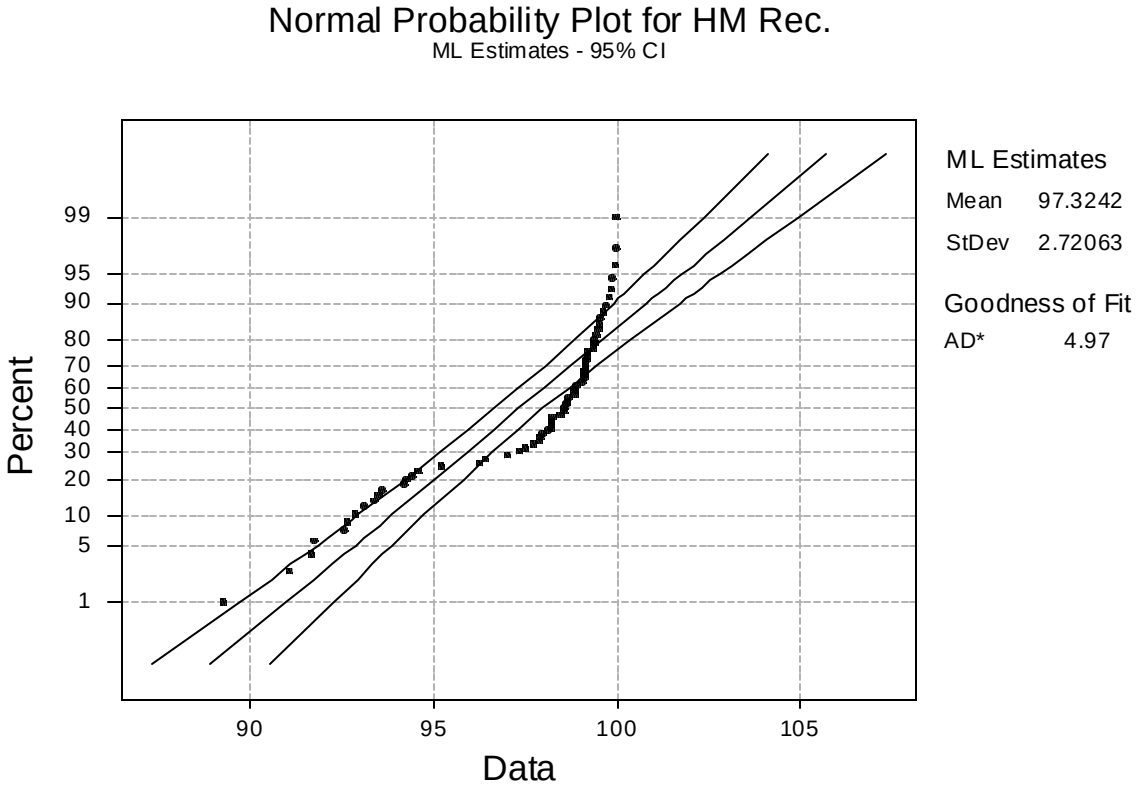

FIGURE 28: NORMAL PROBABILITY PLOT FOR HM RECOVERY

Another way of interpreting the data is by a histogram plot of the various TiO_2 recoveries expeienced during the test work. Figure 29 shows a histogram of this data set as well as other descriptive statistical information. It is immediately visible that the vast majority of recovery data lies between 97% and 99%, with only a few outlier points in the low 90's. Due to the influence of these outlier points, the mean TiO_2 recovery has been calculated as 97.7%. However, in these circumstances, utilizing the median value may prove more practical or fundamental in estimating the typical recovery possible when using the CrossFlow for this application. The 95% confidence interval for the median TiO_2 recovery is between 97.6% and 98.7%.

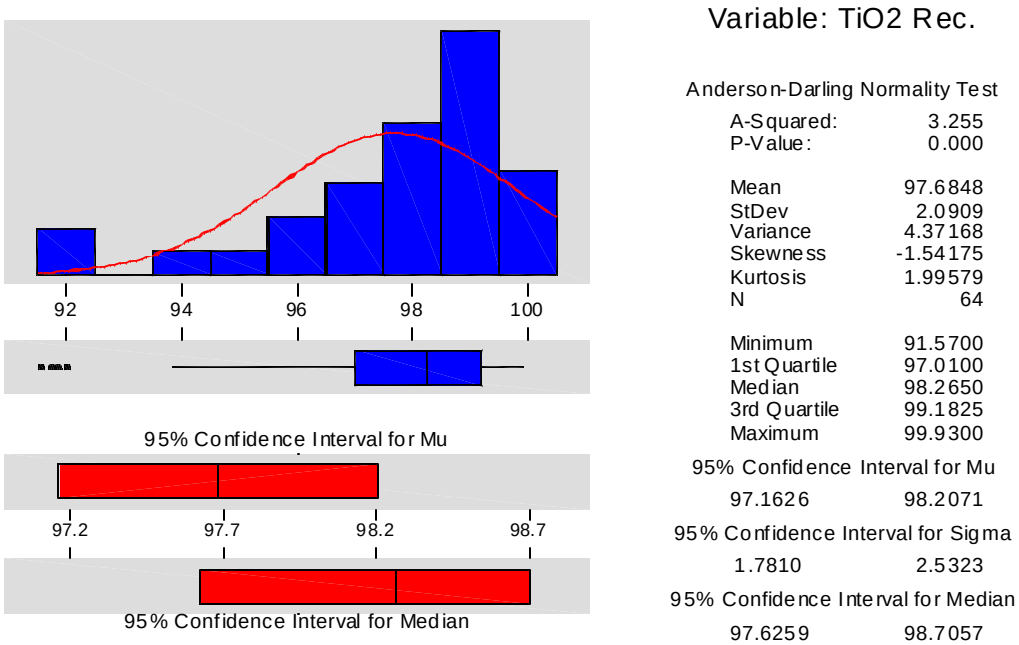

FIGURE 29: BASIC STATISTICS FOR TiO_2 RECOVERY

CHAPTER 3

3.1 Model Development

3.1.1 Overview and Objectives

For this particular set of test work, two individual unit models will be developed. The first model is based on numerous empirical equations that together represent the intricacies involved in a CrossFlow elutriation device. This model will allow the reader general understanding of unit operational functions, however, will not attempt to answer or predict exact unit operational outputs. The second model developed will be based entirely from field testing data obtained from a pilot-scale unit. This field data will be input into statistical software, MiniTAB, and used to model the particular pilot-scale unit given the same operational conditions. Data obtained from this model should be able to accurately predict unit operation and allow the reader to properly scale-up a production size unit. The testing program and developments will be discussed later.

3.2 Empirical Modeling

3.2.1 Model Introduction

The primary object of the proposed empirical model is to develop a mathematical description of the processes involved within the CrossFlow unit. The goal of the model is to represent the particle size and density within the cell as a function of height, z. This information can then be used to estimate the particle concentrations anywhere within the cell and also determine the concentrations within the overflow and underflow. The proposed model will assume that the unit has been operating at steady state, therefore, the teeter-bed has already been formed. In this case, the initial fluid flow conditions while the bed is

forming will not be required. The proposed model will encompass the entire unit above the elutriation network. Two sections in the model will separate this zone, the area above the teeter-bed and the area below the teeter-bed. A second model for the dewatering cone is not necessary since no settling occurs, velocity is constant, and the feed material entering equals the underflow material exiting.

The proposed setup of the model is quite similar to that of the actual CrossFlow unit, as seen in Figure 30. Feed enters through the center of the cell and discharges at the teeter-bed level. The feed material then flows in the positive and negative x directions as separation occurs. Both water and air addition to the cell occurs at the elutriation network level, z = 0. Material that rises, due to low density or attachment to bubbles, reports to the overflow product stream. Material that does not rise, eventually settles into the teeter-bed reports to the underflow via mass-action.

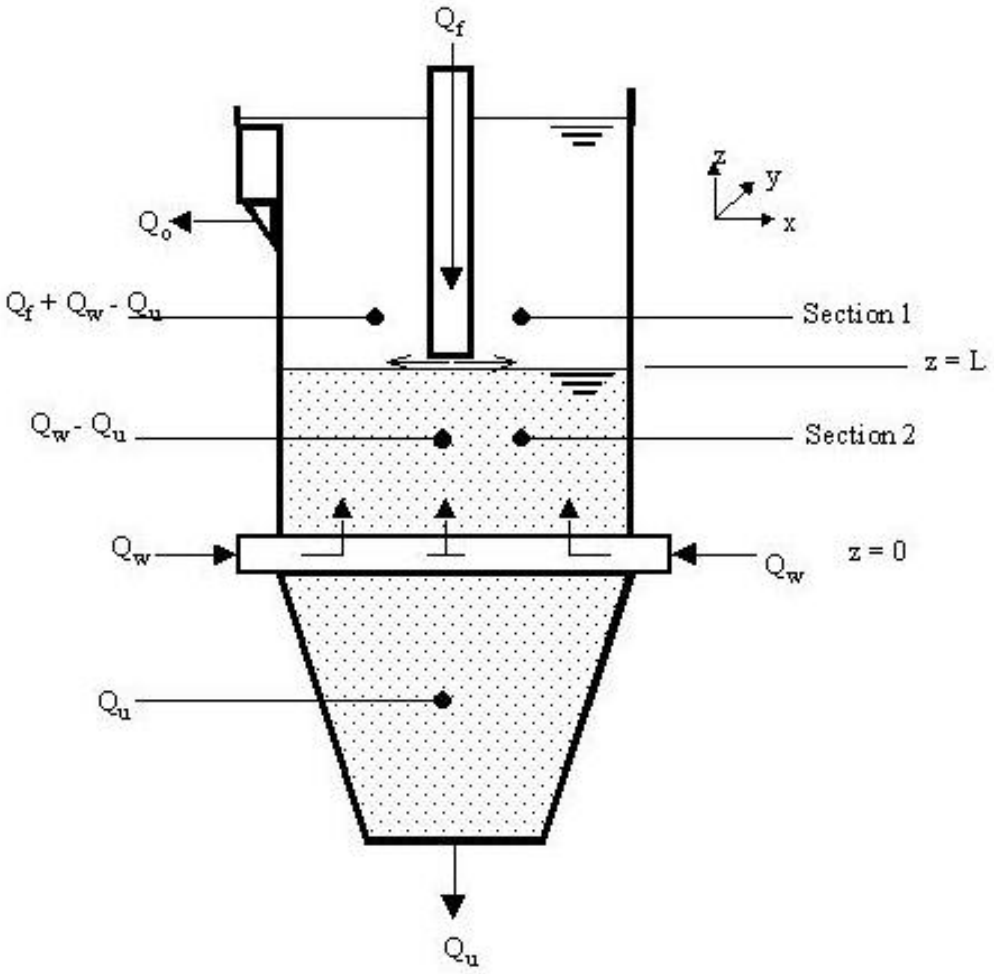

FIGURE 30: PROPOSED MODEL OF THE CROSSFLOW UNIT

Let:

Q_f = volume flow rate of feed

Q_o = volume flow rate of overflow

Q_u = volume flow rate of underflow

Q_w = volume flow rate of water addition

A = unit area, constant

L = height of teeter-bed, constant

3.2.2 Microscopic Population Balance Model of the CrossFlow Separator

Given a general microscopic population balance model as follows:

$$\underset{(i)}{\frac{dy}{dt}} + \underset{(ii)}{\frac{d}{dx}(v_x y)} + \underset{(iii)}{\frac{d}{dy}(v_y y)} + \underset{(iv)}{\frac{d}{dz}(v_z y)} + \sum_{j=1}^{J} \underset{(v)}{\frac{d}{dz_j}(v_j y)} + \underset{(vi)}{\dot{D}} - \underset{(vii)}{\dot{A}} = 0$$

where:

$\frac{dy}{dt}$ = Accumulation

$\frac{d}{dx}(v_x y), \frac{d}{dy}(v_y y), \frac{d}{dz}(v_z y)$ = Continuous changes due to particle motion

$\sum_{j=1}^{J} \frac{d}{dz_j}(v_j y)$ = Continuous changes in property space

$\dot{D}$ = Disappearance

$\dot{A}$ = Appearance

The assumptions which must be used in order to analyze the population balance are:

1. Two properties of interest; size, δ, and density, ρ.
2. The bank is completely mixed in the y direction.
3. The bank is completely mixed in the x direction. This assumption, although somewhat incorrect, simplifies the preliminary model development.
4. Particle size does not change continuously.
5. No disappearance of particles from one density class or size class to another exists
6. No appearance of particles from one density class or size class to another exists.
7. The cell is operating under steady state conditions.

8. Material in the dewatering cone moves only as a function of mass action, i.e. no settling occurs within this region.
9. Teeter-bed level/height remains constant

Using the information from the assumptions, several adjustments and updates can be made to the specific terms used in the balance.

Term		**Assumptions**
(i)	= 0	Assumption 7
(ii)	= 0	Assumption 3
(iii)	= 0	Assumption 2
(iv)	$= \frac{d}{dz}(v_z y)$	Assumption 2 + 3
(v)	= 0	Assumption 4
(vi)	= 0	Assumption 5
(vii)	= 0	Assumption 5

Therefore:

$$\frac{d}{dz}(v_z y) = 0$$

Boundary Condition:

$y(d, r, z)\big|_{z=L} = y(d, r, L)$ • Particle concentration in the cell at z = L = particle concentration in the feed

Expression for $v_z = f(y)$

1. Flow Component, v_f = constant above elutriation network, different for each section
2. Settling Component, $v_s = f(\psi) = f(z)$

Flow Component:

Section 1:

$$v_f = \frac{Q_f + Q_w - Q_u}{A}$$

Section 2:

$$v_f = \frac{Q_w - Q_u}{A}$$

Settling Component:

$$v_s = \frac{gd^2(1-f)^b\left(r_p - r_{slurry}\right)}{18m\ \left(1+0.15\mathrm{Re}^{0.687}\right)}$$

- Hindered settling velocity in a multiple species particle system, non-Stokes flow

where:

g = gravitational acceleration

ϕ = volume fraction solids

ρ_p = particle density

ρ_{slurry} = suspension density

Re = Reynolds Number

μ = fluid viscosity

β = constant, if Re<1, then $\beta = 4.36\mathrm{Re}^{-0.03}$

if Re>1, then $\beta = 4.4/\mathrm{Re}^{0.1}$

Finally:

$$v_z = v_f - v_s$$

$$v_z = \frac{Q_f + Q_w - Q_u}{A} - \frac{gd^2(1-f)^b\left(r_p - r_{slurry}\right)}{18m\left(1+0.15\,\mathrm{Re}^{0.687}\right)}$$ • Section 1

$$v_z = \frac{Q_w - Q_u}{A} - \frac{gd^2(1-f)^b\left(r_p - r_{slurry}\right)}{18m\left(1+0.15\,\mathrm{Re}^{0.687}\right)}$$ • Section 2

Also Note:

$$\overline{y} = \overline{n} f_{n,d,r}$$

Therefore, the CrossFlow model equation

$\frac{d}{dz}(v_z y) = 0$ *becomes:*

$$\frac{d}{dz}\left[\left(\frac{Q_f + Q_w + Q_a - Q_u}{A} - \frac{gd^2(1-f)^b\left(r_p - r_{slurry}\right)}{18m\left(1+0.15\,\mathrm{Re}^{0.687}\right)}\right)\overline{n} f_{n,d,r}\right] = 0$$ • Section 1

$$\frac{d}{dz}\left[\left(\frac{Q_w + Q_a - Q_u}{A} - \frac{gd^2(1-f)^b\left(r_p - r_{slurry}\right)}{18m\left(1+0.15\,\mathrm{Re}^{0.687}\right)}\right)\overline{n} f_{n,d,r}\right] = 0$$ • Section 2

Since:

$Mf_{m,\delta,\rho}d\delta d\rho$ = mass of particles in size range $d\delta$ and density range $d\rho$

$$Mf_{m,d,r}\,ddd r = V_s k_v d^3 r_p(r)\bar{n} f_{n,d,r}\,ddd r$$

where:

ρ_p = density of particles in density range $d\rho$

thus:

$$\frac{M}{V_s} f_{m,d,r} = k_v d^3 r_p(r)\bar{n} f_{n,d,r} \qquad [3]$$

next:

- Convert equation [1] and [2] from number-size-density to mass-size-density by multiplying both sides by $k_v d^3 r_p(r)$
- Then substitute equation [3] into equations [1] and [2]

Thus:

$$\frac{d}{dz}\left[\left(\frac{Q_f + Q_w - Q_u}{A} - \frac{gd^2(1-f)^b\left(r_p - r_{slurry}\right)}{18m\left(1+0.15\mathrm{Re}^{0.687}\right)}\right)\frac{M}{V_s} f_{m,d,r}\right] = 0 \qquad \bullet \text{ Section 1}$$

$$\frac{d}{dz}\left[\left(\frac{Q_w - Q_u}{A} - \frac{gd^2(1-f)^b\left(r_p - r_{slurry}\right)}{18m\left(1+0.15\,\mathrm{Re}^{0.687}\right)}\right)\frac{M}{V_s}\,f_{m,d,r}\right] = 0$$ • Section 2

Both M and V_s are constants

Therefore:

$$\frac{d}{dz}\left[\left(\frac{Q_f + Q_w - Q_u}{A} - \frac{gd^2(1-f)^b\left(r_p - r_{slurry}\right)}{18m\left(1+0.15\,\mathrm{Re}^{0.687}\right)}\right)f_{m,d,r}\right] = 0$$ • Section 1

$$\frac{d}{dz}\left[\left(\frac{Q_w - Q_u}{A} - \frac{gd^2(1-f)^b\left(r_p - r_{slurry}\right)}{18m\left(1+0.15\,\mathrm{Re}^{0.687}\right)}\right)f_{m,d,r}\right] = 0$$ • Section 2

Then by multiplying and pulling constants out,

the final Microscopic Population Balance Model for the CrossFlow Unit becomes:

$$\frac{Q_f + Q_w - Q_u}{A}\frac{d}{dz}\left[f_{m,d,r}\right] - \frac{g}{18m}\frac{d}{dz}\left[\frac{d^2(1-f)^b\left(r_p - r_{slurry}\right)}{\left(1+0.15\,\mathrm{Re}^{0.687}\right)}\left(f_{m,d,r}\right)\right] = 0$$ • Section 1

$$\frac{Q_w - Q_u}{A}\frac{d}{dz}\left[f_{m,d,r}\right] - \frac{g}{18m}\frac{d}{dz}\left[\frac{d^2(1-f)^b\left(r_p - r_{slurry}\right)}{\left(1+0.15\,\mathrm{Re}^{0.687}\right)}\left(f_{m,d,r}\right)\right] = 0$$ • Section 2

Conditions needed to solve model:

- $y(d,r,z)\big|_{z=L}$; feed concentration in terms of size, δ, and density, ρ, at the feed inlet, z = L
- Q_f : volume flow rate of feed at the inlet, z = L

- Q_w : volume flow rate of water addition at z = 0
- Q_u : volume flow rate of underflow at z = 0, same as flow rate through dewatering cone
- $\frac{d}{dz}(f)$; volume fraction solids as a function of height, z, within the cell; requires sampling at various heights throughout the cell at various flow and feed rates
- $\frac{d}{dz}\mathrm{Re}$; Reynolds Number as a function of height, z, within the cell; determination of $\frac{d}{dz}(f)$ and flow and feed rates will allow calculation of this term

3.2.3 Model Conclusions

The developed CrossFlow model contains many unknown quantities and functions. While some are relatively simple to calculate, although time consuming, others are much more involved. While the determination of the volume fraction solids and Reynolds numbers as a function of height z within the cell are beyond the scope of this project, it is hoped that an analytical solution to these terms can be achieved in the near future.

Use of this model should aid the reader in the general understanding of the CrossFlow unit. However, exact predictions of unit recovery performance and operational settings are outside the range of the particular model developed. Additionally, a unit model that determines conditions without the assumption of complete mixing in the x direction. This assumption makes computation much simpler, however, recent studies by Komuench et al. have shown this assumption to be incorrect. This model enhancement would allow for more realistic model calculations, but requires significantly more computations.

3.3 Statistical Unit Modeling

3.3.1 Response Surface Modeling

In order to accurately predict unit performance and determine scale-up information, a more elaborate model for unit operation was required. Statistical modeling of unit operation would allow the precise predictions of unit operational conditions needed for engineering analysis. Response surface modeling techniques were employed through use of statistical software, primarily MiniTAB. These techniques were used throughout the testing and analysis programs.

Response surface methods are used to examine the relationship between one or more response variables and a set of quantitative experimental variables or factors. These methods are often used after identification of specific controllable factors has taken place. They are then used to find the particular settings that optimize the response (recovery, rejection, etc.). Response surface designs are usually chosen when curvature, or nonlinear interaction, is suspected within the response surface. Response surface methods are typically employed in order to:

- find operating conditions that produce the desired response
- find operating conditions that satisfy operating or process specifications
- identify new operating conditions that produce demonstrated improvement of the response
- develop a model of the relationships between defined operational conditions and the response

Many response surface applications are sequential in nature in that they require more than one stage of experimentation and analysis. The steps shown below are typical of a response surface experiment.

- Choose a response surface design for the experiment.
- Create a response surface design, central composite or Box-Behnken.
- Modify the design by renaming the factors, changing the factor levels, replicating the design, and randomizing the design.
- Perform the experiment and collect the response data.
- Enter the data into MiniTAB.
- Analyze the response surface design in order to fit a model to the experimental data.
- Generate wireframe plots in order to visualize response surface patterns.
- Optimize the desired responses by using a response optimizer to obtain a numerical and graphical analysis.

Depending on the experiment, steps can be performed in different orders, a given step can be performed more than once, or a step can be entirely eliminated.

3.3.2 Response Surface Design Selection

Before the use of statistical software, determination of the most appropriate design for the particular experiment is required. Choosing the correct design for a given experiment ensures that the response surface is fit in the most efficient manner. MiniTAB's software package provides both central composites and Box-Behnken designs. When choosing a design it is most important to:

- Identify the number of factors that are of interest.
- Determine the number of test runs physically possible, given time and sampling requirements.
- Ensure adequate coverage of the region of interest on the response surface.
- Determine the impact that other considerations (such as cost, time, or the availability of facilities) have on your choice of a design.

Depending on the particular experiment, there are other considerations that make a particular design most desirable. It is important to use designs that show consistent performance in the criteria considered important, such as the ability to:

- Increase the order of the design sequentially.
- Perform the experiment in orthogonal blocks. Orthogonally blocked designs allow for model terms and block effects to be estimated independently and minimize the variation in the estimated coefficients.
- Rotate the design. Rotatable designs provide the desirable property of constant prediction variance at all points that are equidistant from the design center, thus improving the quality of the prediction.
- Detect model lack of fit.

Given the requirements of the experiments, a Box-Behnken design was chosen. This particular design can be created as a blocked or unblocked design. The illustration below, Figure 31, shows the general layout of a three-factor Box-Behnken design. The points on the diagram represent the experimental runs that are performed and used for response analysis. Box-Behnken designs are often used when performing non-sequential experiments. That is, planning to perform the experiment only once. These designs allow efficient estimation of

the first and second-order coefficients. Because Box-Behnken designs have fewer design points, they are less expensive to run than central composite designs with the same number of factors.

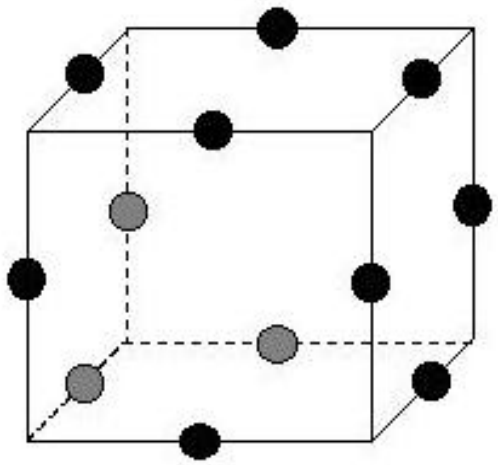

FIGURE 31: 3 FACTOR BOX-BEHNKEN DESIGN

Box-Behnken designs can also prove useful if the safe operating zone for the process is known. Central composite designs usually have axial points outside the "cube". These points may not be in the region of interest, or may be impossible to run because they are beyond safe operating limits. Box-Behnken designs do not have axial points, thus, you can be sure that all design points fall within your safe operating zone. Box-Behnken designs also ensure that all factors are never set at their high levels simultaneously. Table V displays a general summary of the Box-Behnken designs that are generated by MiniTABb for several factor levels.

Table V: General Box-Behnken Designs

# of factors	# of runs	# of blocks	# of center points
3	15	1	3
4	27	3	3
5	46	2	3
6	54	2	6
7	62	2	6

3.3.3 Testing Program

Using the Box-Behnken designs for a three factor testing program, a testing program for the pilot-scale CrossFlow was developed. This program used the relative high and low process values described in the next chapter in Table VII. This particular testing program required 15 individual test runs. Due to fluctuations in the system beyond the control of the author, a replicate of the required tests runs was also performed. This made the total number of tests runs 30. Table VI shows the various test runs and their associated testing parameters. It can also be seen from the table that the test runs were randomized in order to reduce the complications associated with changes in feed grade, percent solids, and feed tonnage.

Table VI: Design of Experiment Testing Schedule

RunOrder	Blocks	TPH	GPM	Bed Level
1	1	4	16	94
2	1	4	14	92
3	1	6	14	94
4	1	6	14	94
5	1	8	14	92
6	1	6	14	94
7	1	8	14	96
8	1	6	12	92
9	1	6	12	96
10	1	6	16	92
11	1	4	12	94
12	1	8	12	94
13	1	8	16	94
14	1	6	16	96
15	1	4	14	96
16	2	4	16	94
17	2	4	14	92
18	2	6	14	94
19	2	6	14	94
20	2	8	14	92
21	2	6	14	94
22	2	8	14	96
23	2	6	12	92
24	2	6	12	96
25	2	6	16	92
26	2	4	12	94
27	2	8	12	94
28	2	8	16	94
29	2	6	16	96
30	2	4	14	96

CHAPTER 4

4.1 Pilot-Scale CrossFlow Test Work

4.1.1 Overview

The next stage in elutriation testing as an effective heavy mineral upgrade tool began with continuous open circuit testing on a larger pilot-scale CrossFlow. The unit used during this period of testing was installed in the field and arranged for continuous field operation. The unit constructed for this test work had a cross-sectional area of 2' x 2'. This pilot unit was installed directly in line with the final wet mill concentrate at a Florida mineral sands operation. This particular unit was positioned in the exact feed location as the 4"x16" lab unit previously tested, immediately following the attrition scrub system and prior to dewatering and stacking. It was surmised that scale-up testing using a unit of this size and capacity would generate much more realistic data for any future full-scale installation plans.

Although significant modifications were required to functionally install the pilot scale unit, the basic flowsheet remained the same. Figure 32 shows the basic overview of the flowsheet used for pilot-scale operation. Feed material was taken directly from the wet mill final concentrate line and fed to the CrossFlow's tangential feed box. Two 4" hydrocyclones were used to dewater the feed slurry to the necessary 50-60% solids recommended by the manufacturer. Two additional 4" hydrocyclones and a 7.5 HP pump with a variable speed drive were required in order to transport and stack the underflow process stream. In addition to these ancillary equipment needs, additional steel work was required in order to sustain the weight of the larger unit.

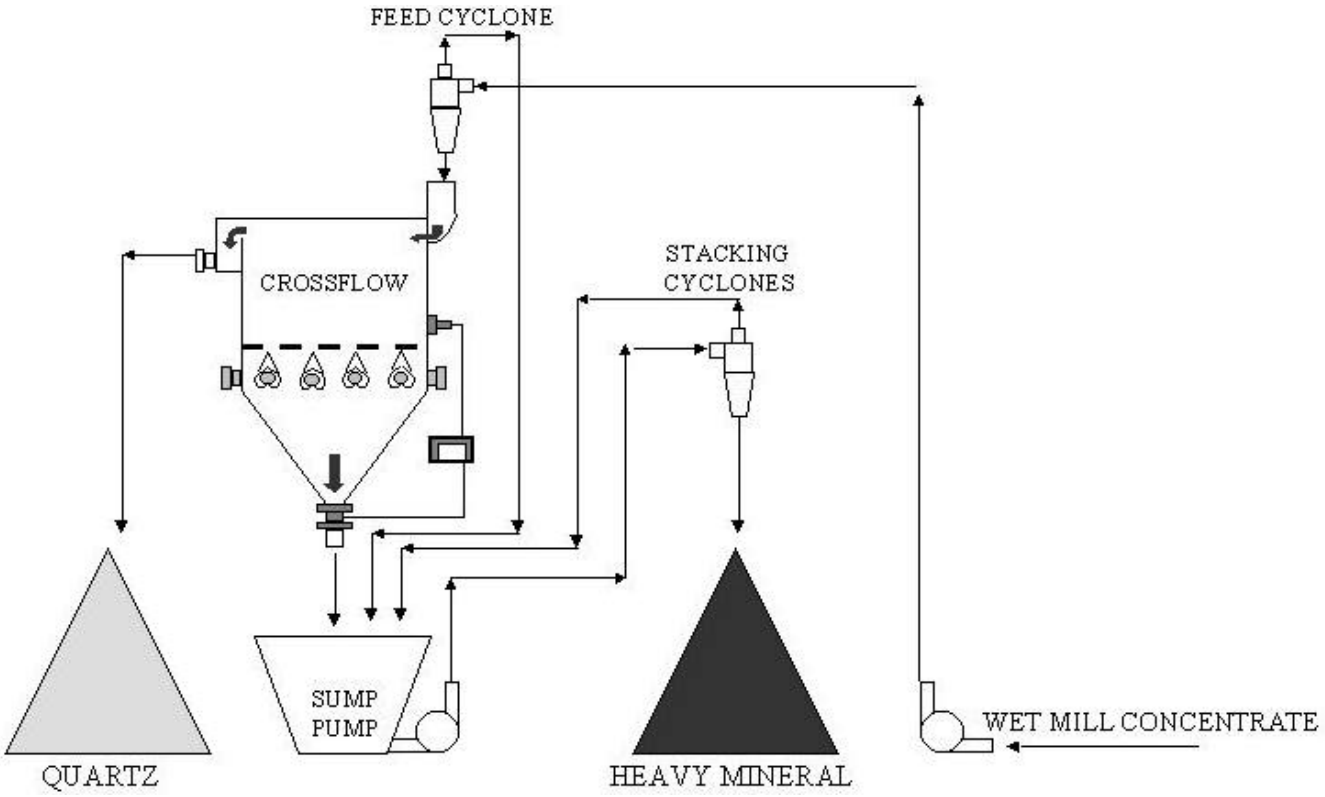

FIGURE 32: PILOT SCALE FLOWSHEET

4.1.2 Equipment Setup

Installation of the 2' x 2' CrossFlow posed several operational problems. Use of a larger, pilot-scale device required reconstruction of previous test stand facilities. New steelwork was constructed in an effort to safely withstand the added weight. An upper level was also constructed which could allow operators to safely inspect unit operation and make adjustments to unit feed equipment as necessary. The facility constructed for this phase of test work can be seen in Figure 33. Preliminary weight analysis of the test unit was performed in order to estimate the gages and extent of steel required to support the test unit. Weight of the empty, pre-operational unit was estimated at 1,500 lbs. Inner dimensions of the unit were used in order to calculate estimates on bulk heavy mineral weight present

during test work. Total material weight, for stand construction requirements, was estimated at 3,500 lbs. Another 500 lbs of capacity was added for personnel and miscellaneous equipment requirements. Thus, total operational weight was estimated at 5,500 lbs.

FIGURE 33: PILOT SCALE TESTING FACILITIES

Unit feed requirements were also drastically different than previous test work. Initial estimates on feed rate for this particular unit were 4–8 tph, or 1–2 tph/ft^2. The previous bypass feed sump would not handle both the required tonnages and percent solids for effective operation. Instead, two 4" Lynatex Hydrocyclones were installed in order to feed

the pilot-scale unit. The hydrocyclones would be fed directly from the bypass feed line installed prior to the full-scale stacker cyclone. As previously stated, pressure and percent solids of this bypass line were incorrect for unit feed conditions for laboratory scale testing. However, installation of the larger feed hydrocyclone would allow for effective operation under these high pressures and low percent solids present. The installed hydrocyclone had been previously tested in-line to determine its operational ability. Minimal loss of fines in the overflow stream was experienced with underflow percent solids reporting in the range of 40–70%.

The larger volume of elutriation water required for the pilot unit posed another installation problem. Required flowrates were initially estimated at 8–16 gpm, 2–4 gpm/ft^2. The 110 volt chemical pump previously used during lab-scale testing would prove to be inadequate. Instead, a ¾" by 1", 220 volt pump was installed. This particular pump was fixed speed and capable of supplying 35 gpm under the testing conditions.

Initial shakedown testing of the pilot-scale facilities included the use of a RCM Industries fixed aperture flowmeter. However, the fluctuations in flow readings experienced with this model flowmeter were much greater than desired and made precise flowrate changes difficult. Instead, a Cole-Parmer 5000 series variable area flowmeter was installed. This particular meter was a direct reading unit constructed from solid acrylic and was capable of reading flowrates from 0.1 to 20.0 gpm. Product specifications for this model showed an accuracy of 2% full scale, well within the required field. This type of meter makes use of a single calibrated stainless steel float, whose size and weight determines the relative flowrate present within the chamber. The inner chamber containing the float is bored at precise specifications from acrylic to allow for accurate flowrate readings. This particular unit was

well suited for field use due to its high pressure capacity, 100 psi, as well as its high temperature capacity, 150°F.

Underflow stacking of the high tonnages was also a new issue for the pilot-scale activities to address. Test stand facilities would need to be at least 20 ft in height in order to allow sufficient height for stacking. Instead, unit underflow was directed to a sump pump where it could be sent to stacking equipment. The underflow material, combined with added makeup water, would then be pumped directly to two stacker hydrocyclones. The hydrocyclones chosen for this task were 4" Lynatex models. The small apex diameter of this model would allow for higher underflow percent solids rates. In order to facilitate stacking, a percent solids greater than 65% would need to be created by the new hydrocyclones. Overflow from these units would be sent back to the underflow sump, and thus re-circulate the water. This system would also allow for re-circulation of any fine material that might become misplaced in the overflow streams. Re-circulating this material would increase its probability of reporting to the stacking underflow stream.

The sump pump chosen for transport of the unit underflow was a Warman 1.5" by 1" centrifugal pump. The impeller chosen for installation under these particular conditions was constructed of natural rubber in order to reduce capital cost. A 7.5 HP motor capable of reaching speeds of 2000 rpms was also chosen. This equipment setup would allow for ample capacity of the various underflow rates predicted. A variable speed drive unit was installed such that pump rpms could be changed quickly. This arrangement would allow important changes in pump discharge flowrate and pressure, vital to hydrocyclone performance under varying conditions.

The previous microprocessor based fuzzy logic controller operated during lab-scale testing was successfully adapted for use in the new system. However, some minor changes to the program logic were necessary to incorporate this equipment into the new setup. The most difficult aspect of this configuration was the setting of the response rate for the valve operation. As compared to the lab-scale unit, pressure changes in the pilot-scale unit were much slower and required careful programming of the process logic. If the valve response rate were too fast, steady state conditions would never predominate within the unit and successful separation would be quite difficult.

In addition to the tangential feed system used by the CrossFlow, a deflection plate was added. This plate forced solids downward into the separation bed. This addition appears to reduce the amount of fine heavy mineral lost to the unit overflow. These particles, having been introduced farther down into the cell, must be forced through significant amounts of material prior to overflow rejection. This development is believed to offer higher levels of TiO_2 recovery than the previous setup. Figure 34 shows the location of the deflection plate within the cell.

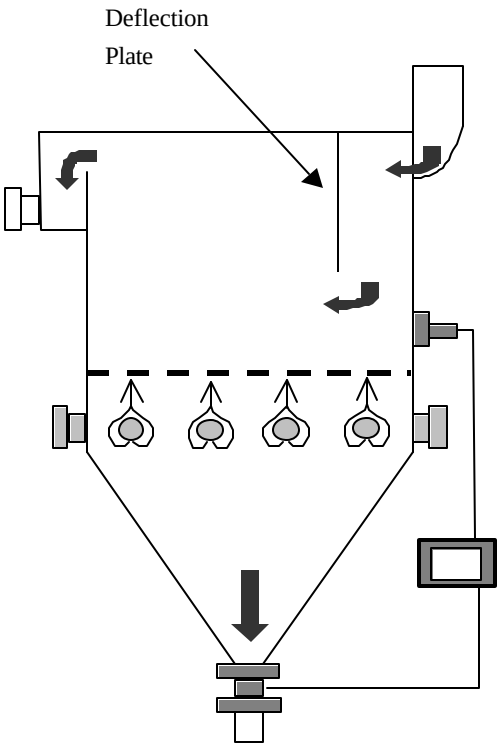

FIGURE 34: DEFLECTION PLATE LOCATION

4.1.3 Test Program

Initial unit operation began with preliminary testing aimed at identifying high and low operational conditions. The conditions examined were feed rate, elutriation flowrate, and bed level. Optical examination of the overflow amount generated and the heavy mineral content of this overflow was used for deciding the realistic range of operating conditions. Some preliminary operational set points displayed unacceptable combinations of both overflow mass yield and grade. Such operating points were removed and kept from further investigation. Table VII shows the relative high and low values determined for testing and modeling development. These values would be used in the new testing program in order to develop a statistical model of the unit's separation.

Table VII: High/Low Values for Pilot Operation

	Feed Rate (tph)	**Bed Level**	**Water Rate (gpm)**
High	8.0	96	16.0
Low	4.0	92	12.0

Instead of unit operation based on operator decision, a more thorough investigation for pilot-scale testing was constructed. Pilot testing would attempt to develop a model for unit operation based on several key factors. The factors determined for this process were:

- Feed Rate
- Bed Level
- Elutriation Water Rate
- Feed Percent Solids
- Feed TiO_2 Grade
- Feed Heavy Mineral Grade

Although feed rate, water rate, and bed level were relatively easy to control using the pilot-scale setup previously mentioned, the others were not. Variables that are not controllable through the developed testing facilities are often referred to as co-variants. These values are required for proper model development and must be identified and quantified during the testing program. Quantification for these particular variables was achieved through several previously discussed techniques.

4.2 Pilot-Scale Model Test Work Results

Test work using the pilot-scale setup was carried out based on the testing program previously described in Chapter 3. A total of 30 test runs were performed in order to extract sufficient information necessary to generate a statistical model for unit operation. Those aspects of the program which were controllable were changed between each test run, those variables not controllable were tracked and recorded. As previously stated, the key operational conditions under examination are feed rate, elutriation flow rate, and bed level. Although not specifically controllable, feed percent solids and feed grade were also tracked for model development. Table VIII shows the actual results experienced during this phase of testing. Sample 22 was removed due to error or mistakes in the sample laboratory analysis.

Mass balancing of the test data was performed using the program developed in Chapter 3. Unfortunately, there were excessive tonnage fluctuations experienced for both the overflow and underflow unit streams. Several test runs required relative changes of 50% or more to the overflow and underflow stream tonnage, much too high for the balancing software to make accurate predictions. Reaction rate of the pneumatic underflow valve was attributed as the primary source of these fluctuations. The reaction rate of the valve system forced periodic "purges" in order to maintain bed level at the specified level. Instead of mass balancing, the following common recovery and rejection equations were used for this stage of test work:

$$\text{Recovery} = \frac{Concentrate(Feed - Tailings)}{Feed(Concentrate - Tailings)}$$

$$\text{Rejection} = \frac{Tailings(Concentrate - Feed)}{Feed(Concentrate - Tailings)}$$

Table VIII: Test Design Results

RunOrder	Blocks	GPM	Bed Level	TPH	% Solids	Feed %TiO_2
1	1	16	94	3.59	57.20	27.20
2	1	14	92	5.03	77.51	29.47
3	1	14	94	7.38	67.84	30.01
4	1	14	94	5.31	68.22	29.37
5	1	14	92	7.50	60.57	29.51
6	1	14	94	6.85	57.61	29.29
7	1	14	96	6.82	58.95	25.64
8	1	12	92	3.28	46.00	29.88
9	1	12	96	7.31	63.28	27.33
10	1	16	92	6.72	63.77	26.64
11	1	12	94	3.97	61.69	29.53
12	1	12	94	8.28	63.07	24.67
13	1	16	94	7.27	59.23	24.15
14	1	16	96	5.94	71.46	27.27
15	1	14	96	3.54	56.89	27.74
16	2	16	94	2.71	49.80	29.05
17	2	14	92	2.76	47.28	30.29
18	2	14	94	6.53	60.31	22.65
19	2	14	94	5.73	52.71	23.40
20	2	14	92	5.99	54.32	21.08
21	2	14	94	6.66	57.60	27.47
~~22~~	~~2~~	~~14~~	~~96~~			
23	2	12	92	4.52	48.54	19.76
24	2	12	96	5.01	50.47	24.85
25	2	16	92	6.55	57.70	23.80
26	2	12	94	3.00	49.82	27.70
27	2	12	94	6.87	59.36	23.91
28	2	16	94	6.33	56.52	23.18
29	2	16	96	7.28	60.15	28.79
30	2	14	96	3.22	51.24	29.58

TiO_2 and Heavy Mineral Recoveries experienced during the testing program were significantly above expectations. The specific data generated for the testing plan can be seen in Appendix B. Based on the testing results, the pilot-scale unit appears to operate in a more

controllable and reproducible manner than the lower capacity laboratory units. It is believed that the larger cross-sectional area and deflection plate permits entry of unit feed in a more quiescent manner than previous lab-scale test work. Figure 35 compares the TiO_2 recovery and quartz rejection for both the pilot-scale testing and previous lab-scale testing. Although the pilot-scale modeling data represents both high and low operational settings, it generally performs a higher rejection of quartz at similar or higher recoveries of TiO_2. Once this data is used for model development, additional sampling at the optimum operational conditions can be performed. This data should allow for higher levels of both quartz separation and TiO_2 recovery.

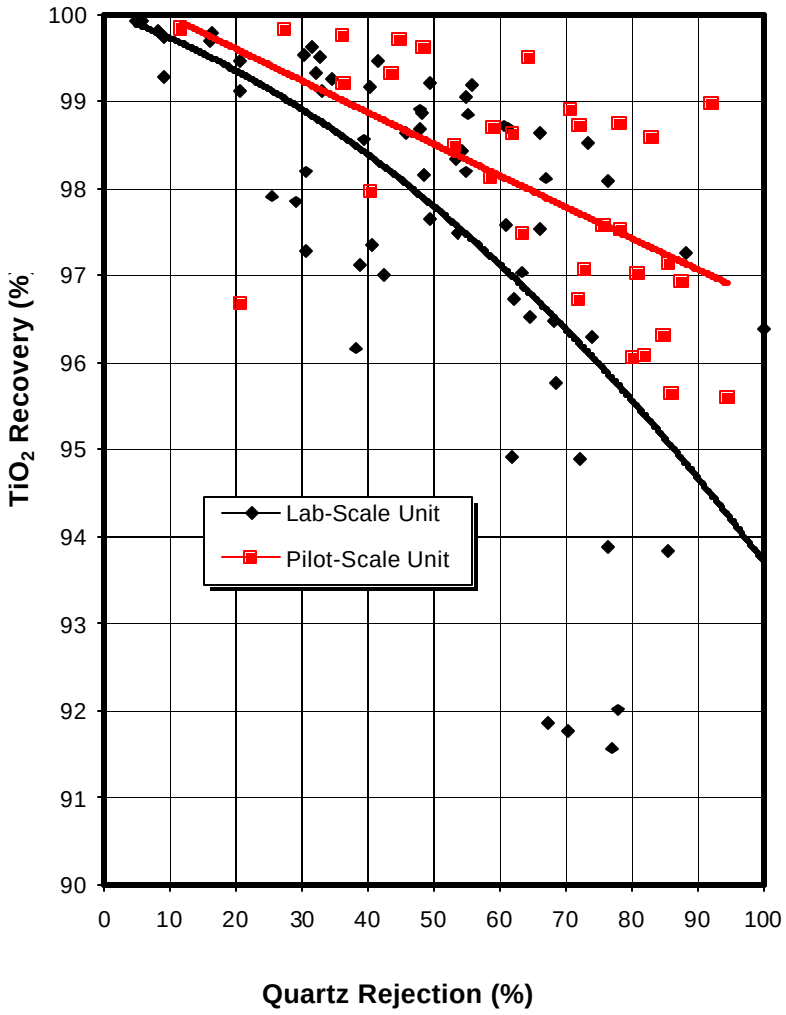

FIGURE 35: TiO_2 RECOVERY VS. QUARTZ REJECTION FOR PILOT-SCALE AND LAB-SCALE UNITS

In general, TiO_2 and Heavy Mineral recoveries experienced over the entire testing program averaged 97.87% and 98.42%, respectively. Table IX shows the average values for the model test work. The average feed TiO_2 grade experienced was 26.64% with a Heavy Mineral grade of 76.47%. These feed grades are within the plant operational output goals of 28-32% TiO_2 and 75-85% HM. These feed grades were less sporadic than those experienced during the previous lab-scale testing, allowing for significant improvements in overall unit

performance. The larger unit capacity and feed arrangement for the pilot unit are believed to have reduced these feed fluctuations quite drastically. Dramatic fluctuations in the feed material would have made test work extremely difficult since the pilot unit had a retention time of approximately 20 minutes, depending on feed rate.

Table IX: Average Pilot-Scale Model Testing Results

	Feed		Underflow		Overflow	
Test Runs	**Ave. TiO_2**	**Ave. HM**	**Ave. TiO_2**	**Ave. HM**	**Ave. TiO_2**	**Ave. HM**
30	26.64	76.47	32.63	91.28	2.55	5.87

Ave. Recovery	
TiO_2	**HM**
97.87	98.42

Ave. Rejection
Quartz
67.27

Quartz rejection was slightly lower than desired for the testing program. An average rejection of 67.27% was experienced for the entire test program. This phenomenon is explained by the high and low operational conditions used for testing. Certain test designs either had extremely low elutriation flowrates or low bed pressure levels, neither setting being optimal for quartz rejection. Model development from the test work should allow for significant improvement in rejection at similar TiO_2 and Heavy Mineral recoveries. Figures 36 and 37 depict the various recoveries as a function of both quartz rejection levels and feed rate. Although limited reduction in TiO_2 recovery occurs for higher feed rates, Heavy Mineral recovery is left completely unaffected. Feed tonnages above 2 tph/ft^2 are needed in order to assess the impacts on recovery and quartz rejection.

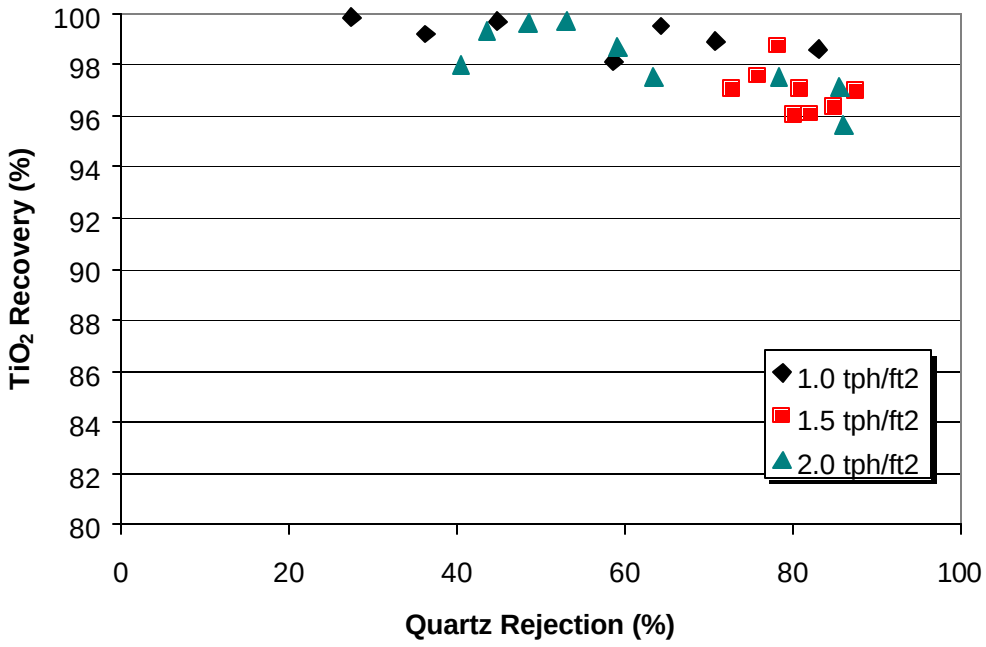

FIGURE 36: TiO_2 RECOVERY AS A FUNCTION OF QUARTZ REJECTION

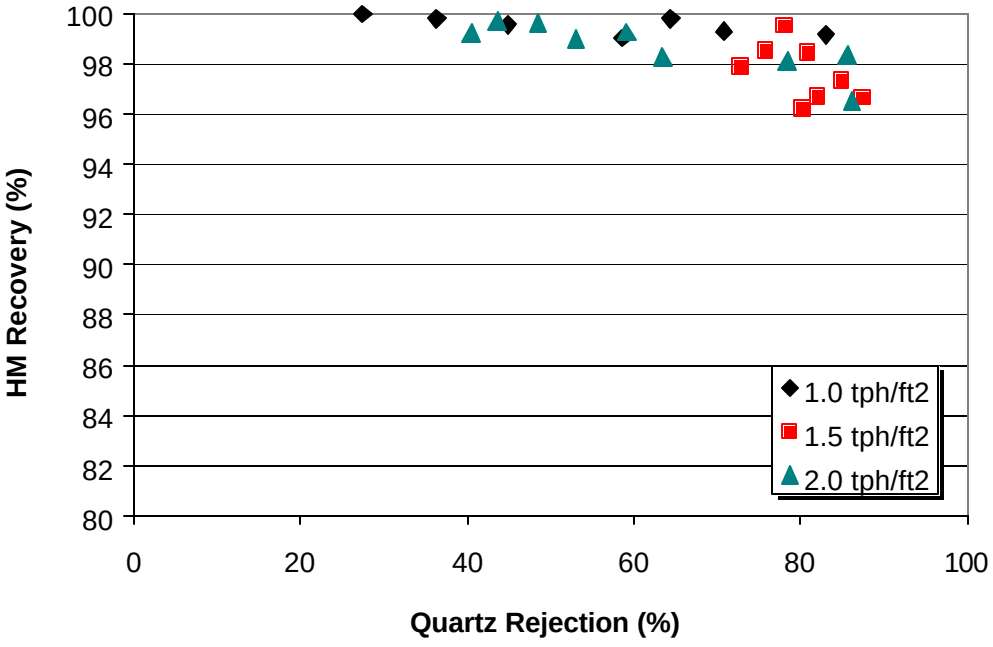

FIGURE 37: HM RECOVERY AS A FUNCTION OF QUARTZ REJECTION

Although the feed entering the system fluctuated quite drastically, unit underflow remained relatively constant for the entire testing program. Figure 38 shows descriptive statistics for the feed TiO_2 grade. Typical wet mill performance during this phase of testing gave a standard deviation for concentrate grade of 3.0%. Fluctuations in this plant performance are attributed to such things as tonnage shifts in dredging, mechanical issues and operational errors. Figure 39 shows that the CrossFlow pilot unit was successful in reducing these fluctuations by approximately 44%. Unit TiO_2 output grade averaged 32.63% with standard deviation of 1.68%. This drastic reduction in fluctuation would significantly improve subsequent dry mill processing. Constant output grades would allow dry mill operators to configure plant performance around relatively tight ranges of feed grade, improving overall dry mill recovery and performance.

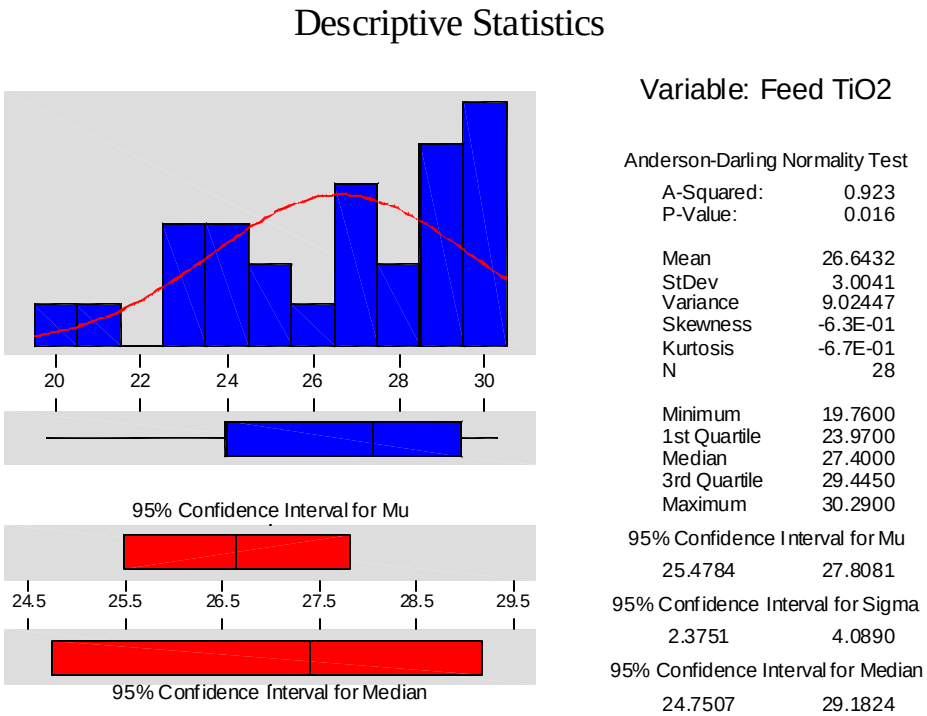

FIGURE 38: BASIC STATISTICS FOR UNIT FEED (%TiO_2)

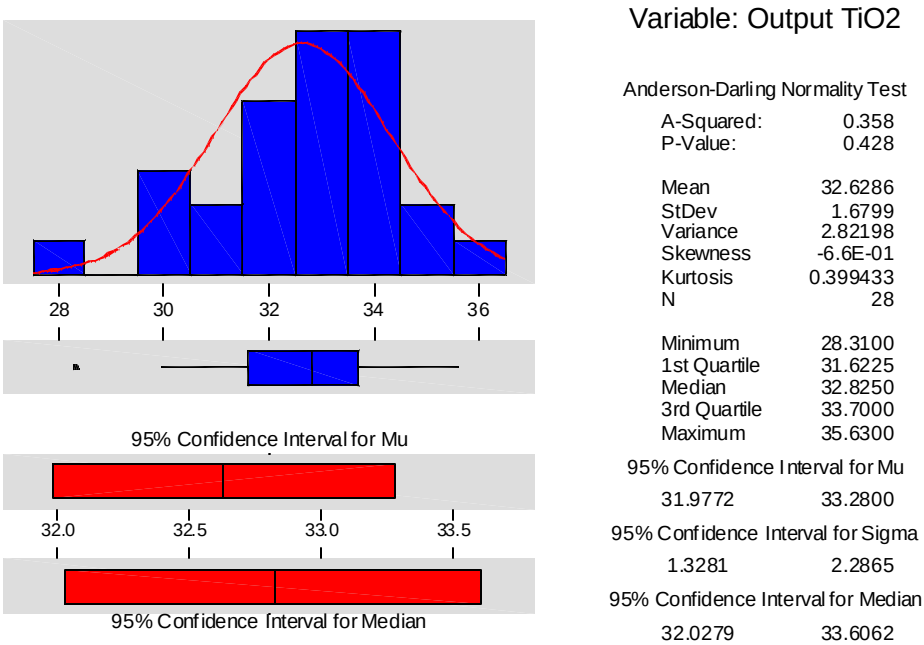

FIGURE 39: DESCRIPTIVE STATISTICS FOR UNIT OUTPUT (%TiO_2)

4.3 Statistical Model

4.3.1 Introduction

Data from the model test program was input into MiniTAB for statistical analysis. This software uses several different techniques to generate predictive models based on field test work. The user can pick the appropriate analysis tool based on information from the specific testing data. Although simple linear regression can quickly evaluate influences of the X variables, multiple regression using square and interaction terms is often necessary. The specific tool required for analysis depends entirely on the equipment being tested and data generated during test work.

Data from the test program can be analyzed through several techniques. However, for the investigation multiple linear regression is used. This technique allows for model development using the following terms:

- linear terms
- linear terms and all squared terms
- linear terms and all two-way interactions
- linear terms, all squared terms, and all two-way interactions (the default)
- a subset of linear terms, squared terms, and two-way interactions

The model fit chosen will determine the nature of the effects, linear or curvilinear, that can be detected from the experimental data.

4.3.2 Linear Regression Analysis for TiO_2 and HM

Based from data in Chapter 2, unit feed grade is known to contribute the vast majority of prediction for unit recovery. Simple linear and polynomial regression are used to determine the extent of feed grade on recovery. This procedure performs regression with linear and polynomial (second or third order) terms of a single predictor variable and plots a regression line through the data. Polynomial regression is one method for modeling curvature in the relationship between a response variable (Y) and a predictor variable (X) by extending the simple linear regression model to include X^2 and X^3 as predictors. The estimation methods used for this analysis is the least squares approach.

The quadratic model developed in Figure 40 appears to provide a good fit to the data for TiO_2 recovery. The R^2 indicates that feed grade accounts for 68.9% of the variation in TiO_2 recovery. A visual inspection of the plot reveals that the data are randomly spread

about the regression line, implying no systematic lack-of-fit. The lines labeled CI are the 95% confidence limits for the TiO_2 recovery. The lines labeled PI are the 95% prediction limits for new observations.

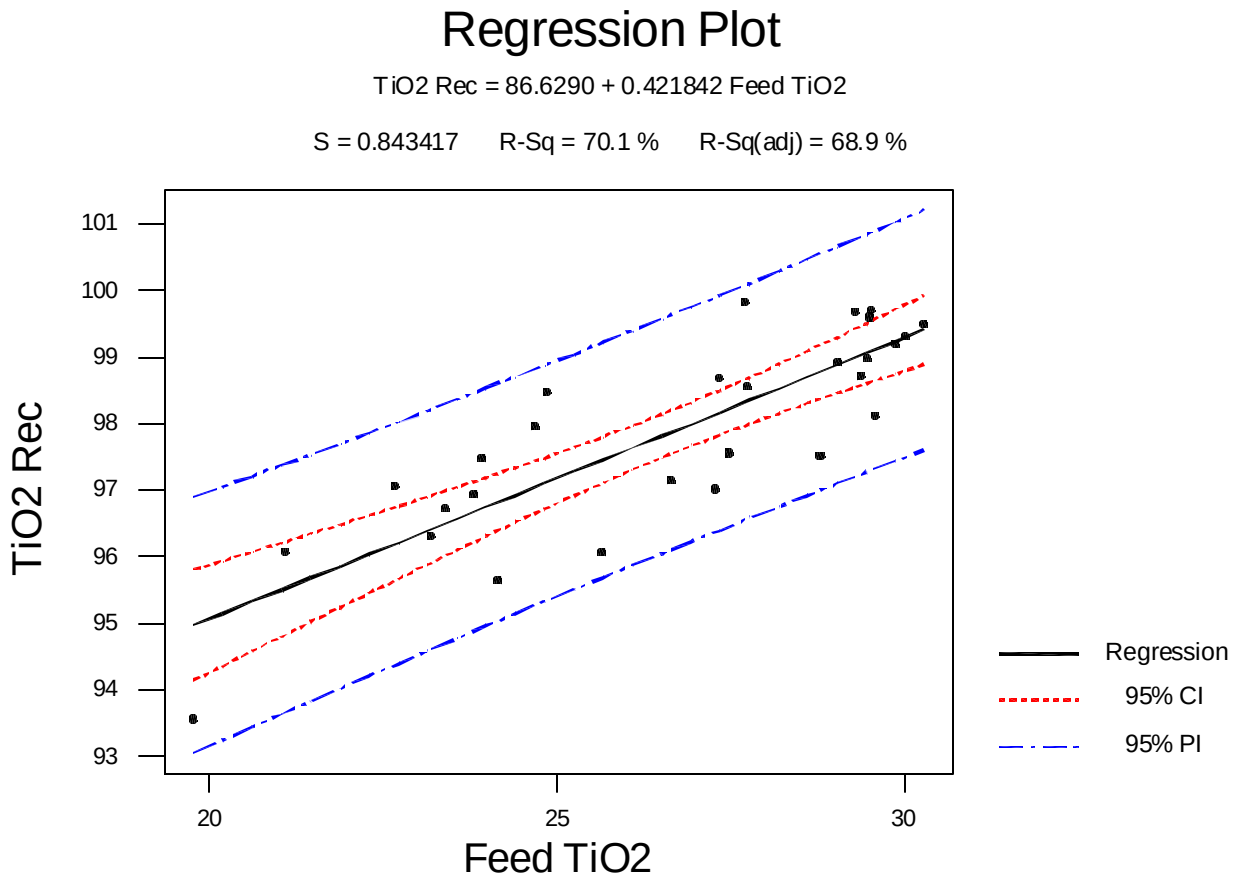

FIGURE 40: LINEAR REGRESSION OF TiO_2 RECOVERY BASED ON FEED GRADE

Similar analysis was carried out for heavy mineral recovery as a function of feed HM grade. The linear regression model developed in Figure 41 appears to provide even a better fit to the data for HM recovery. The R^2 indicates that feed grade accounts for 72.2% of the variation in HM recovery. A visual inspection of the plot reveals that the data are randomly

spread about the regression line, implying no systematic lack-of-fit. The lines labeled CI are the 95% confidence limits for the HM recovery and the lines labeled PI are the 95% prediction limits for new observations.

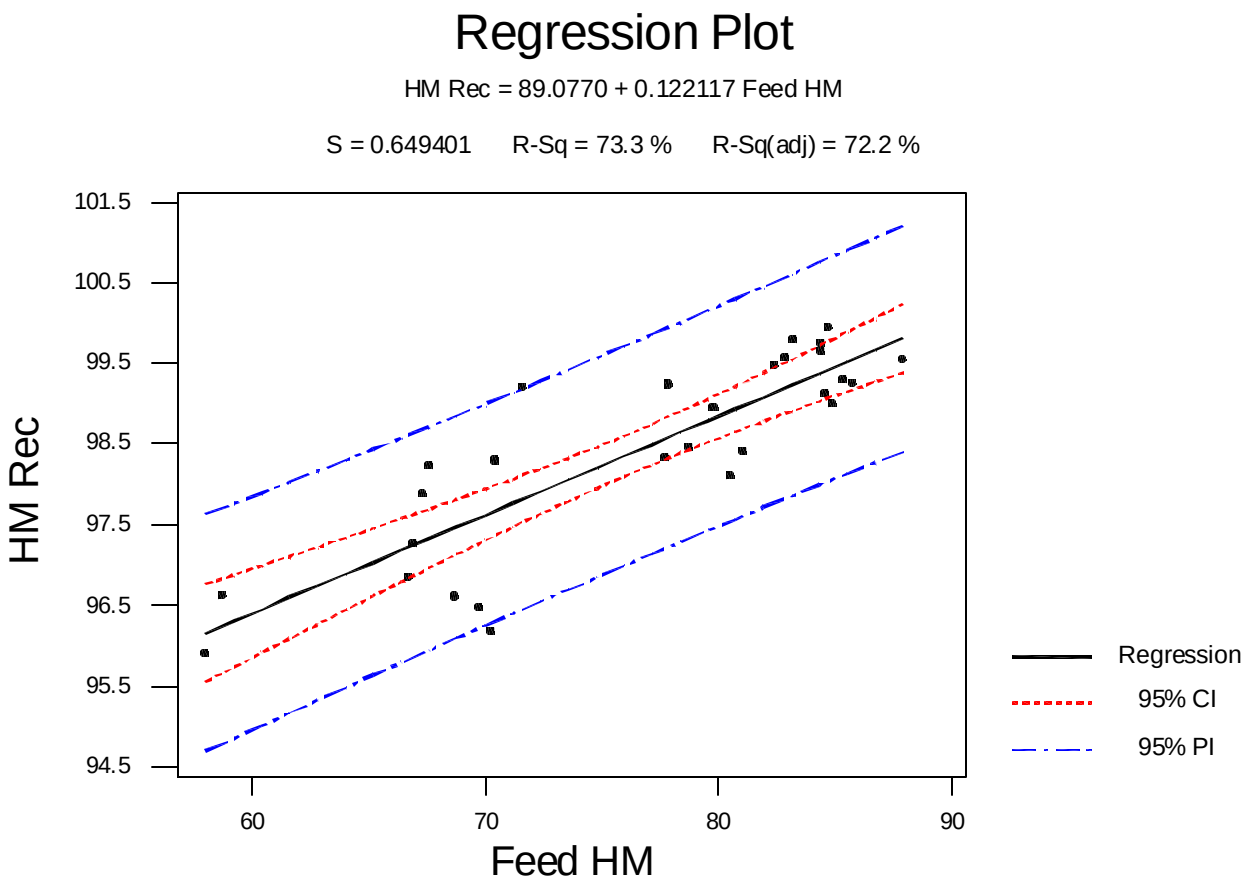

FIGURE 41: LINEAR REGRESSION OF HM RECOVERY BASED ON FEED GRADE

4.3.3 Multiple Regression Analysis for TiO_2

Although feed grade appears to account for the majority of unit performance, modeling that would include other terms such as feed tonnage, elutriation water rate and bed level was needed. The first step in multiple regression analysis is to determine the various

interactions present between X variables. MiniTAB provides a matrix plot option that quickly allows the interpretations of these interactions. Any interactions between terms can be seen by the plots through visible trends, either linear, logarithmic, or polynomial. Figure 42 shows the matrix plot developed from % Solids, TPH, GPM, Bed Level, and Feed TiO_2. In general, there appears no strong interactions involving GPM, Bed Level, and Feed TiO_2. However, TPH and % Solids does show a relatively strong interaction. This phenomenon is typical for a hydrocyclone feeding arrangement where an increase in tonnage corresponds to an associated increase in discharge percent solids. Using both TPH and % Solids in regression analysis is not advised given this occurrence. Further analysis is needed in order to assess which variable plays a more important role in model development.

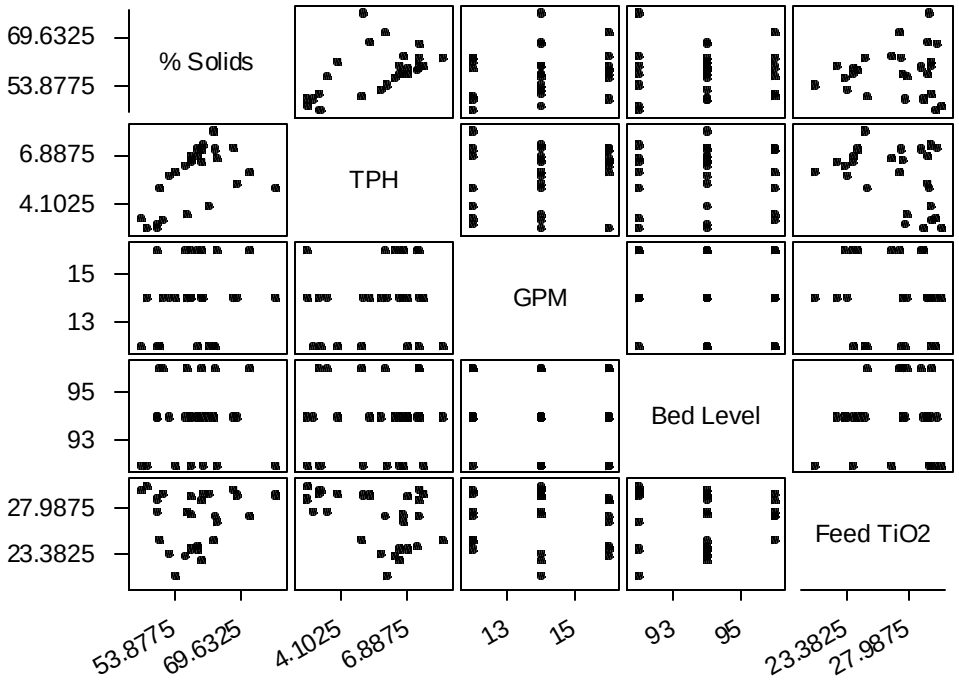

FIGURE 42: MATRIX PLOT ANALYSIS OF X INTERACTIONS FOR TiO_2

In order to assess the use of either % Solids or TPH, regression analysis using the best subset tool was used. The best subsets output from MiniTAB can be seen in Table X. Each line of the output represents a different model comprised of different variables or predictors. The predictors used in each model are indicated by use of an X in the table. From this data, it can be clearly seen that Feed TiO_2 accounts for as much as 62.4% of the predictive model. GPM also plays an important role with a R-sq(adj) value of 25.0. Since % Solids and TPH cannot both be used for model development, this table allows for understanding as to which factor plays a larger role in model development. If the model where to be developed using % Solids, GPM, Bed Level, and Feed TiO_2, the model fit would be 83.2% R-sq(adj). If TPH is added to the model and % Solids dropped, the fit remains 83.9%. For further modeling development, TPH will be used instead of % Solids. In the design of a full-scale unit, TPH plays a much larger role by determining the exact unit cross-sectional area needed for the intended feed tonnages. It is important to note that the TPH term used for analysis is not entirely independent and will consist of a TPH portion and an associated % Solids portion.

Table X: Best Subsets Regression for TiO_2 Recovery

Vars	R-Sq	R-Sq(adj)	C-p	S	% Solids	TPH	GPM	Bed Level	Feed TiO_2
1	64.0	62.4	30.1	0.74843					X
1	28.1	25.0	81.0	1.05740			X		
2	84.7	83.3	2.8	0.49960			X		X
2	66.3	63.3	28.8	0.73996		X			X
3	85.8	83.8	3.2	0.49213			X	X	X
3	85.5	83.5	3.5	0.49656		X	X		X
4	86.6	83.9	4.0	0.48956		X	X	X	X
4	86.0	83.2	4.8	0.49985	X		X	X	X
5	86.6	83.1	6.0	0.50212	X	X	X	X	X

Multiple regression analysis of TiO_2 recovery began by using a quadratic model that uses linear, square, and interaction terms. Each square or interaction term that displays a p-value greater than 0.05 is removed from the model. Although the linear term Feed TiO_2 exhibits a p-value greater than 0.05, it was left in the model based on its influence in the interaction term TPH x Feed TiO_2. It can be seen from Table XI that the R-sq(adj) value for the regression model developed is 83.3%. Based on the coefficients and terms used, equation [3] represents the best-fit model for the given pilot-scale test work. This equation will most likely display curvature for some settings due to the inclusion of the square term TPH^2 and the interaction term TPH x Feed TiO_2.

Table XI: Estimated Regression Coefficients for TiO_2 Recovery

Term	Coef	SE Coef	T	P
Constant	98.883	11.578	8.541	0.000
TPH	-0.079	0.0684	-1.161	0.260
GPM	-0.362	0.0679	-5.336	0.000
Bed Level	-0.104	0.0796	-1.310	0.206
Feed TiO_2	0.783	1.0196	0.768	0.452
Feed TiO_2^2	-0.009	0.0195	-0.461	0.650

S = 0.4995 **R-Sq = 86.8%** **R-Sq(adj) = 83.3%**

TiO_2 Recovery = 98.883 – 0.079(TPH) – 0.362(GPM) – 0.104(Bed Level)

$$+ 0.783(\text{Feed } TiO_2) - 0.009(\text{Feed } TiO_2)^2 \quad [3]$$

Regression analysis for the unit Output TiO_2 began through the same process. Full quadratic terms were first used for the model, then select terms were removed which possessed p-values less than 0.05. However, the use of several terms containing high p-values was necessary in order to create a model that showed an acceptable relative fit. Removal of these terms forced the overall fit, R-sq(adj), below the 84.2% value and also generated higher residual values. Leaving these terms in allows for a better fit of the model to the actual test data, however, will not accurately predict a model for a larger population of test work. This predictive equation displayed in Table XII can be used to predict the Output TiO_2 for the specific testing data observed, however, will not accurately predict a continued testing population. Equation [4] represents the predicted Output TiO_2 based on TPH, GPM, Bed Level, and Feed TiO_2. Running a 3rd replicate of the testing series would allow the model to base its fit off more substantial information and improve the overall population prediction.

Table XII: Estimated Regression Coefficients for TiO_2 Output

Term	Coef	SE Coef	T	P
Constant	-70.89	262.055	-0.271	0.792
TPH	12.30	9.068	1.356	0.205
GPM	-18.10	7.963	-2.273	0.046
Bed Level	-0.50	2.754	-0.183	0.859
Feed TiO_2	15.91	7.760	2.048	0.068
$Feed^2$	-0.05	0.039	-1.393	0.194
TPH x GPM	-0.14	0.083	-1.637	0.133
TPH x Bed Level	-0.07	0.091	-0.726	0.484
TPH x Feed TiO_2	-0.14	0.070	-1.952	0.079
GPM x Bed Level	0.25	0.089	2.824	0.018
GPM x Feed TiO_2	-0.16	0.060	-2.587	0.027
Bed Level x Feed TiO_2	-0.10	0.076	-1.342	0.209

S = 0.6870 **R-Sq = 91.6%** **R-Sq(adj) = 82.4%**

$$\textbf{TiO}_2\textbf{ Output} = -70.89 + 12.30(\text{TPH}) - 18.10(\text{GPM}) - 0.50(\text{Bed Level}) + 15.91(\text{Feed } TiO_2) - 0.05(\text{Feed } TiO_2)^2 - 0.14(\text{TPH x GPM}) - 0.07(\text{TPH x Bed Level}) - 0.14(\text{TPH x Feed } TiO_2) + 0.25(\text{GPM x Bed Level}) - 0.16(\text{GPM x Feed } TiO_2) - 0.10(\text{Bed Level x Feed } TiO_2) \quad [4]$$

In order to understand the TiO_2 recovery equation developed, graphical analysis is suggested. To examine more than two interactions a 3-D surface plot is used. Figure 43 shows a contour plot where Feed HM and GPM are used as the X and Y variables, while TiO_2 recovery is used as the Z value. For this particular instance, Bed Level is held at 94 and TPH is held at 6.0 tph, 1.5 tph/ft_2. It can be seen that GPM displays a linear relationship with TiO_2 recovery for this particular model range. If significantly lower and higher water rates are used, this model would most likely display curvature for TiO_2 recovery as a function of

GPM. However, the flowrates used in the model test work are relatively close which makes linear regression the most feasible solution. TiO_2 recovery as a function of feed grade is also a linear relationship for the given model range. It can be stated from interpretation of this graph that GPM plays a significant role in TiO_2 recovery for the entire range of feed grades experienced.

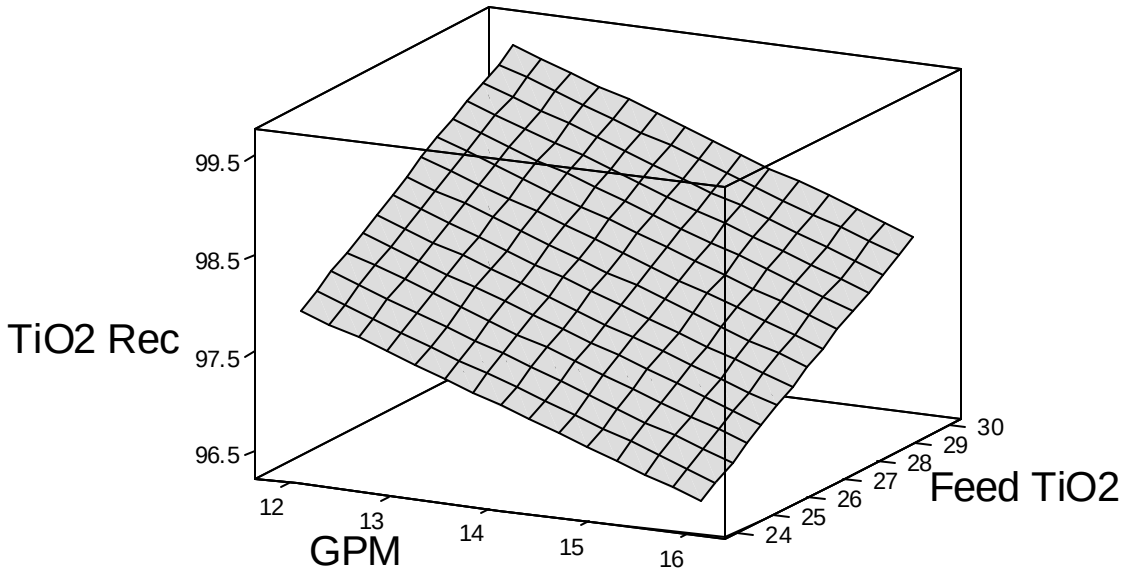

FIGURE 43: WIRE FRAME PLOT OF TiO_2 RECOVERY

Using both models developed for TiO_2 recovery and Output TiO_2, the ability to understand the ranges of unit operation is achieved. Both equations allow for the quick determination of unit performance under varying feed characteristics. The ideal tool for this analysis is an overlaid contour plot for both outputs. Figure 44 is one such contour plot for

these outputs given various inputs. Displayed are two overlaid contour plots on a single graph. The two factors, Feed TiO_2 and GPM, are used as the two axes in the plots and the third and fourth factors, TPH and Bed Level, have been held at levels 6.0 and 94 respectively. The white area inside each plot shows the range of Feed TiO_2 and GPM where the criteria for both response variables are satisfied. Responses used for this specific graph are a TiO_2 recovery above 98% and an Output TiO_2 above 33%. This plot, in combination with the predictive models, can be used to find the best operating conditions for maximizing recovery and output grade. To achieve these process outputs, feed grade entering the unit can drop to as low as 27%. The ideal GPM for this situation is 14 GPM, as displayed by the graph. This elutriation flowrate allows for the upgrading of the lower feed TiO_2 grades while outputting the proper responses previously described.

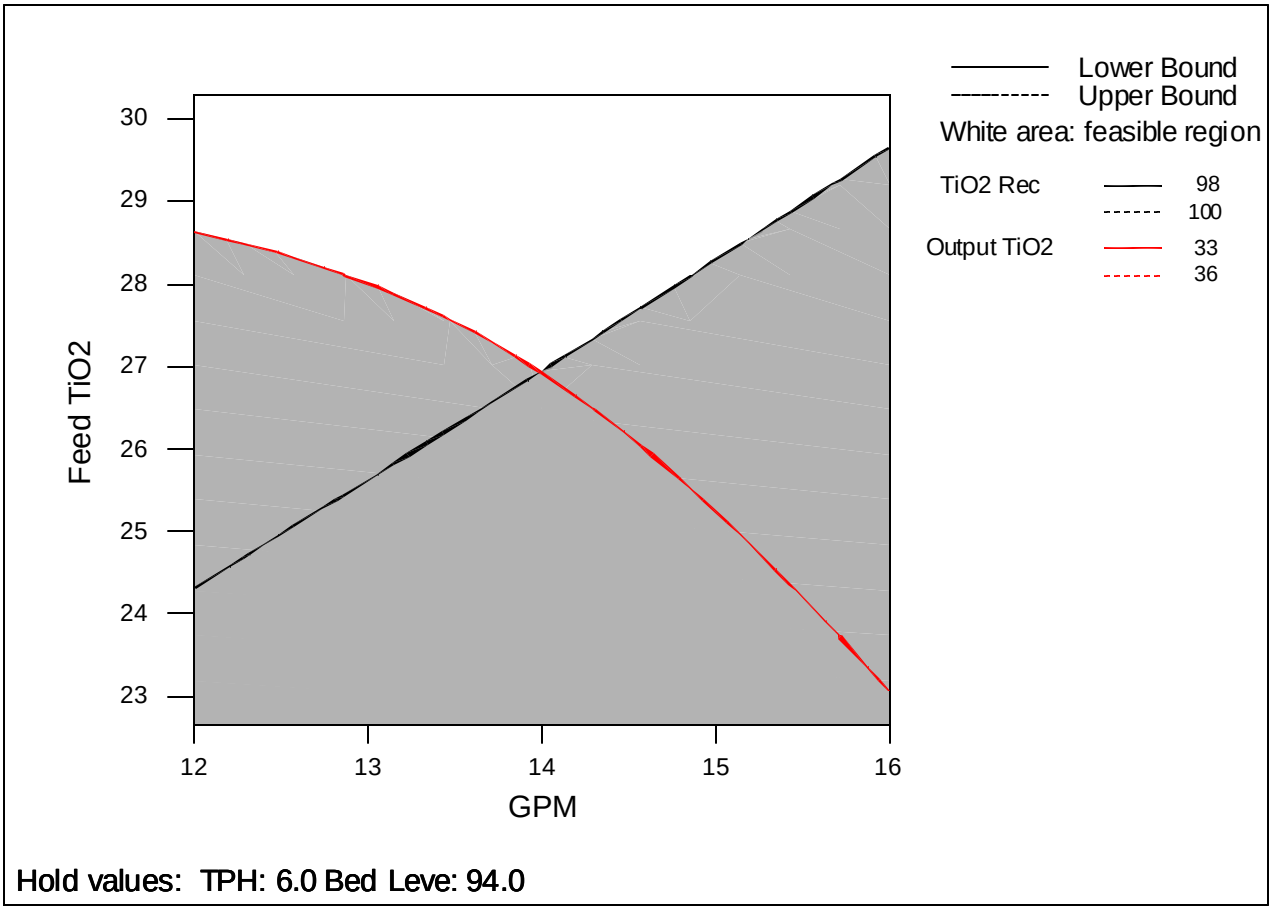

FIGURE 44: OVERLAID CONTOUR PLOT FOR TiO_2 RECOVERY AND OUTPUT TiO_2

Hold Values (Bed Level = 92 and Feed TiO_2 = 30%)

4.3.4 Multiple Regression Analysis for HM

The first step in multiple regression analysis for heavy mineral recovery and output grade is to determine the various interactions present between X variables. The same process as for TiO_2 is used, generation of a matrix plot through use of MiniTAB. This graph allows quick interpretations of these interactions for the variables selected. Figure 45 shows the matrix plot developed from % Solids, TPH, GPM, Bed Level, and Feed HM. In general, there appears no strong interactions involving GPM, Bed Level, and Feed HM. However, TPH and % Solids again show a relatively strong interaction. Thus, using both TPH and % Solids in the regression analysis for heavy mineral is not advised given this occurrence. Further analysis is needed in order to assess which variable plays a more important role in model development, TPH or % Solids.

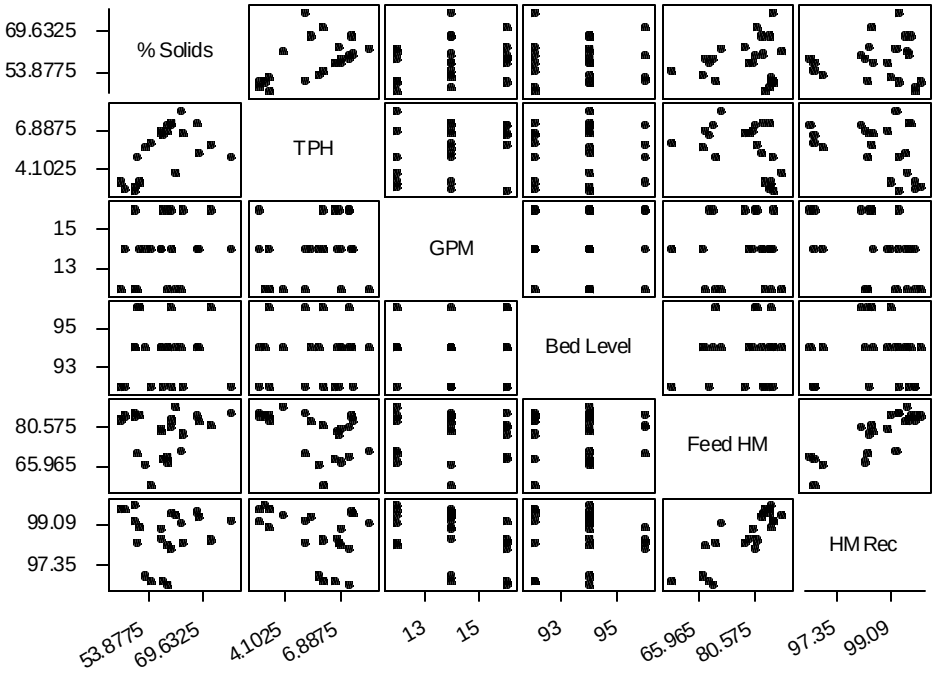

FIGURE 45: MATRIX PLOT ANALYSIS OF X INTERACTIONS FOR HM

In order to assess the use of either % Solids or TPH, regression analysis using the best subset tool was used. The best subsets output from MiniTAB can be seen in Table XIII. Each line of the output represents a different model comprised of different variables or predictors. The predictors used in each model are indicated by use of an X in the table. From this data, it can be clearly seen that Feed HM accounts for as much as 68.3% of the predictive model. GPM also plays an important role with a R-sq(adj) value of 15.6. Since % Solids and TPH cannot both be used for model development, this table allows for understanding as to which factor plays a larger role in model development. If the model where to be developed using TPH, GPM, Bed Level, and Feed HM, the model fit would be 87.3% R-sq(adj). If % Solids is added to the model and TPH dropped, the fit drops slightly to 86.6%. For further modeling development using heavy mineral analysis, TPH will be used instead of % Solids. However, initial observation using the best subsets regression information shows that GPM, Bed Level, and Feed HM account for a R-Sq(adj) value of 87.2. Based from this information, TPH does not appear to make a significant influence on the model, although further analysis is needed.

Table XIII: Best Subsets Regression for HM Recovery

Vars	R-Sq	R-Sq(adj)	C-p	S	% Solids	TPH	GPM	Bed Level	Feed HM
1	69.8	68.3	29.4	0.62575					X
1	19.6	15.6	108.3	1.02090			X		
2	88.3	87.1	2.4	0.39982			X		X
2	70.6	67.5	30.2	0.63376				X	X
3	89.1	87.2	3.2	0.39720			X	X	X
3	88.9	87.0	3.5	0.40029		X	X		X
4	89.7	87.3	4.1	0.39574		X	X	X	X
4	89.2	86.6	5.0	0.40684	X		X	X	X
5	89.8	86.6	6.0	0.40630	X	X	X	X	X

Multiple regression analysis of HM recovery began by using the same quadratic model as for TiO_2. This model uses linear, square, and interaction terms to develop a predictive model of unit operation. Each square or interaction term that displays a p-value greater than 0.05 is removed from the model. Through this process, the TPH linear, square, and interaction terms were determined to play no significant role in the overall model. Also, during this analysis, test runs #7, 18, 23, and 28 were removed for their excessive residuals based from the developed model. The error in these points is either the development of laboratory analysis error or field test work error. Removal of these data points both increase overall model fit and reduces the average residual value for the test work. It can be seen from Table XIV that the R-sq(adj) value for the regression model developed is 95.1%. Based on the coefficients and terms used, equation [5] represents the best-fit model for the given pilot-scale test work. This equation will most likely display curvature for some settings due

to the inclusion of the square term Feed HM and the interaction terms GPM x Feed HM and Bed Level x Feed HM.

Table XIV: Estimated Regression Coefficients for HM Recovery

Term	Coef	SE Coef	T	P
Constant	249.717	53.4195	4.675	0.000
GPM	-2.783	0.436	-6.384	0.000
Bed Level	-1.464	0.5906	-2.479	0.024
Feed HM	-1.436	0.6039	-2.377	0.029
Feed HM^2	-0.003	0.0012	-2.228	0.040
GPM x Feed HM	0.031	0.0055	5.634	0.000
Bed Level x Feed HM	0.016	0.0073	2.247	0.038

S = 0.2367 **R-Sq = 96.4%** **R-Sq(adj) = 95.1%**

HM Recovery = 249.717 – 2.783(GPM) – 1.464(Bed Level) – 1.436(Feed HM)

$$- 0.003(\text{Feed HM})^2 + 0.031(\text{GPM x Feed HM}) + 0.016(\text{Bed Level x Feed HM}) \quad [5]$$

Regression analysis for the unit Output HM began through the same process. Full quadratic terms were first used for the model, then select terms were removed which possessed p-values less than 0.05. All terms remaining contain extremely low p-values which represents a relatively high influence from each factor on the developed model. Besides linear terms, the square term Feed HM and the interaction term TPH x Feed HM were left in the model analysis. Unlike the HM recovery regression analysis, TPH and its square and interaction terms play significant roles in unit output HM grade. In addition to those test runs removed in the HM recovery analysis, test runs #9 and 15 were also removed for their high residual values relative to the developed model. Table XV shows the regression analysis information given the specific test runs and terms used in its

development. An R-sq(adj) value of 92.1% was achievable under the given circumstances. Equation [6] represents the predicted Output HM based on TPH, GPM, Bed Level, and Feed HM. Running a 3rd replicate of the testing series would allow the model to base its fit off more substantial information and improve the overall population prediction.

Table XV: Estimated Regression Coefficients for Output HM Grade

Term	**Coef**	**SE Coef**	**T**	**P**
Constant	-18.000	33.96	-0.530	0.604
TPH	24.060	5.1928	4.634	0.000
GPM	2.150	0.1922	11.165	0.000
Bed Level	-0.580	0.1993	-2.922	0.011
Feed HM	1.360	0.3003	4.528	0.000
TPH^2	-0.980	0.1562	-6.296	0.000
TPH x Feed HM	-0.170	0.0482	-3.525	0.003

S = 1.283 **R-Sq = 94.4%** **R-Sq(adj) = 92.1%**

HM Output = -18.000 + 24.060(TPH) + 2.150(GPM) – 0.580(Bed Level)

+ 1.360(Feed HM) – 0.980$(TPH)^2$ – 0.170(TPH x Feed HM) [6]

In order to understand the HM recovery equation developed, graphical analysis is needed. To examine more than two interactions a 3-D surface plot is used. Figure 46 shows one such contour plot where Feed HM and GPM are used as the X and Y variables, while HM recovery is used as the Z value. For this particular instance, Bed Level is held at 94 and TPH is not used. It can be seen that GPM displays a relatively linear relationship with HM recovery. If significantly lower and higher water rates are used, this model would most likely display curvature for HM recovery as a function of GPM. However, the flowrates used in the model test work are relatively close which makes linear regression the only

option. HM recovery as a function of feed grade shows slight curvature, similar to test work with the lab/pilot-scale unit previously tested. It can be stated from interrelation of this graph that GPM plays a significant role in HM recovery for lower feed grades, <75% HM, and plays minimal role for feed grades above 75% HM.

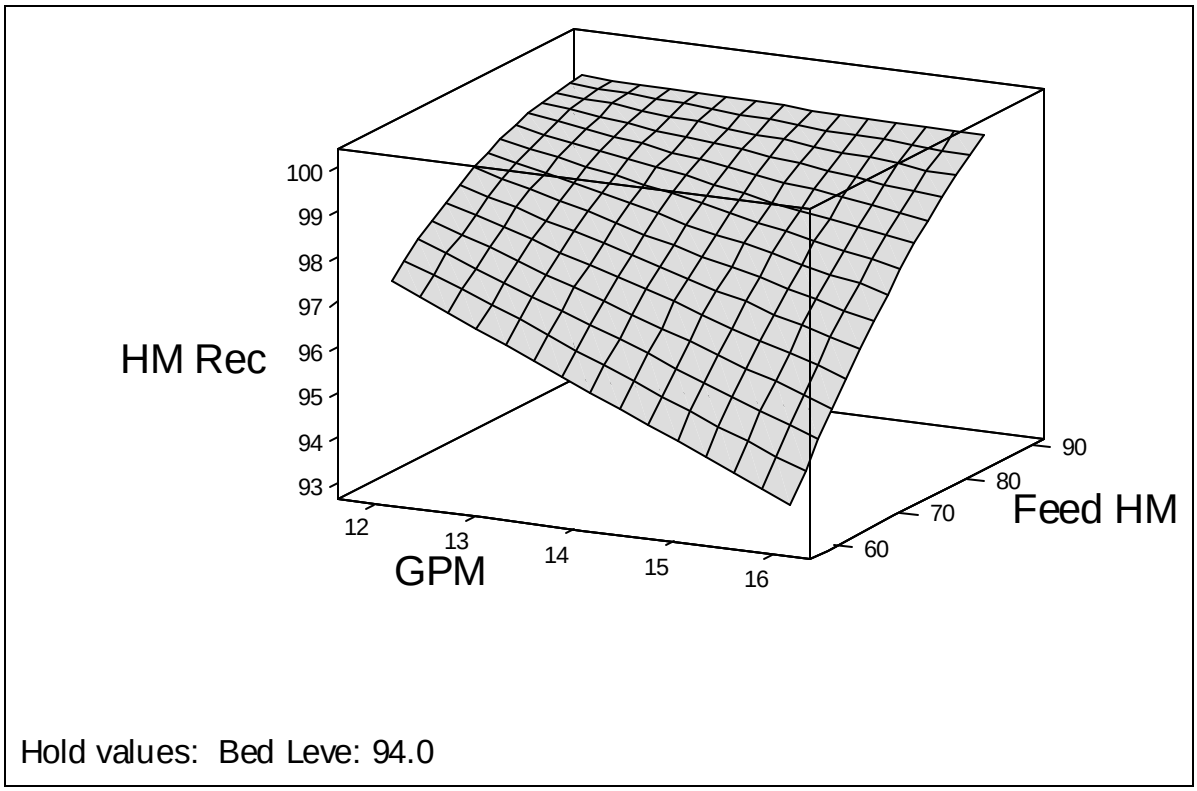

FIGURE 46: SURFACE PLOT FOR HM RECOVERY

Hold Values (Bed Level = 94 and TPH = 6.0)

Using the model developed for Output HM, it is important to develop an understanding of the ranges of Output HM possible under varying feed conditions. The associated HM recoveries for these particular unit operational conditions can also be quickly determined. The ideal tool for this analysis is an overlaid contour plot for both outputs.

Figure 47 is one such contour plot for these outputs given various inputs. Displayed are two overlaid contour plots on a single graph. The two factors, Feed HM and GPM, are used as the two axes in the plots and the third and fourth factors, TPH and Bed Level, has been held at levels 6.0 and 94 respectively. The white area inside each plot shows the range of Feed HM and GPM where the criteria for both response variables are satisfied. Responses used for this specific graph are a HM recovery above 98% and an Output HM above 90%. This plot, in combination with the predictive models, can be used to find the best operating conditions for maximizing recovery and HM output grade. To achieve these process outputs, feed grade entering the unit cannot drop below approximately 72% HM. The ideal GPM for this situation is 14 GPM, as displayed by the graph. This elutriation flowrate allows for the upgrading of the lower Feed HM grades while outputting the proper responses previously described.

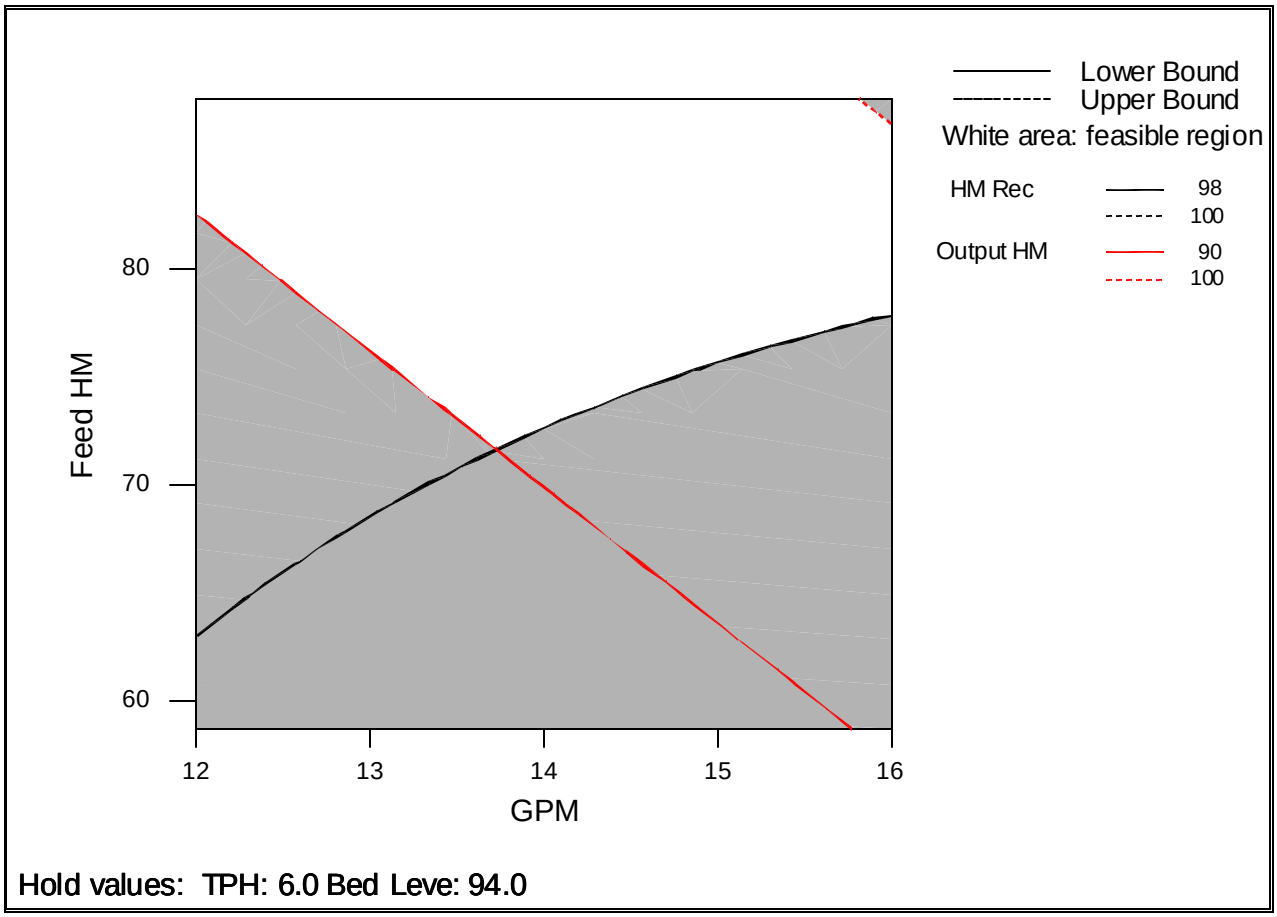

Figure 47: Overlaid Contour Plot for HM Recovery and Output HM

Hold Values (Bed Level = 94 and TPH = 6.0)

4.4 Full-Scale Installation

Full-scale installation of a CrossFlow has two different possibilities. The first installation option is located directly after the caustic scrub system. At this point in the process the feed material has been scrubbed and thus is relatively clean and free of clay and debris. The scrub system is also beneficial in that it acts as a surge suppressor that should reduce the large fluctuations in feed tonnage and feed grade. This location also allows the unit to act as a final rinse facility which should improve dry mill operation. Overflow

tailings material from this setup is directed towards a drainage area where solids can build up and be removed by heavy equipment periodically. Water from the overflow stream can run successfully through the existing water drainage and treatment system.

This particular installation option requires no ancillary equipment for unit operation. This particular setup makes use of existing sumps, pumps, and stacking cyclone. Figure 48 shows a schematic of the proposed system. This option offers the lowest capital cost and simplest operational requirements.

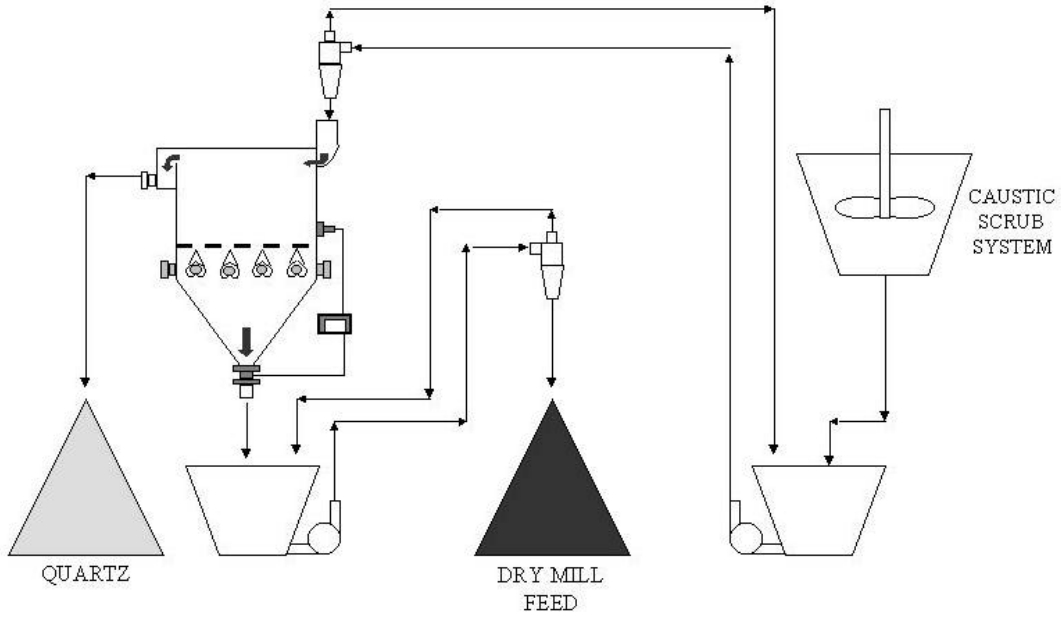

FIGURE 48: FULL SCALE INSTALLATION OPTION AFTER CAUSTIC SCRUB SYSTEM

The second installation option is directly before the caustic scrub system. In this setup, final wet mill concentrate is upgraded through the elutriator then sent through attrition scrubbing. Figure 49 depicts this installation option. This option allows for the reduction of material needing the caustic scrub phase. This allows for reduced variable cost through

lower chemical consumption rates. However, separation efficiency is expected to be lower in this option due to the large quantities of clay, humate, and wood debris present in the feed material.

This particular option requires installation of an additional sump and pump. This requirement makes capital cost for this option significantly higher. Feed fluctuations are also increased since there is no surge capacitance between the wet mill and the CrossFlow unit. The higher capital cost and reduced unit performance eliminates this particular installation option.

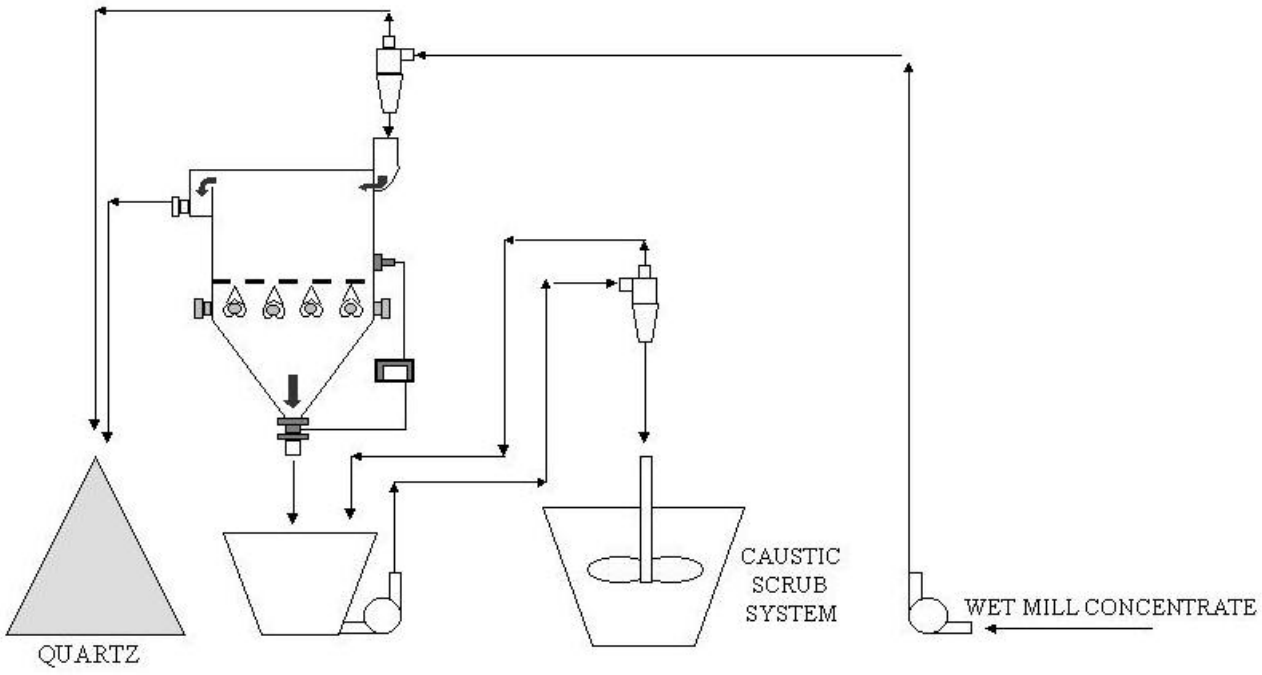

FIGURE 49: FULL SCALE INSTALLATION OPTION BEFORE CAUSTIC SCRUB SYSTEM

4.5 Economic Analysis

As previously stated, installation of a CrossFlow unit has several economic advantages. The largest financial incentive is the reduction of haulage requirements to the dry mill facilities. This material also carries an additional tailings haulage necessary for zircon retrieval. The cost of haulage to the dry mill facility and zircon wet mill facilities are estimated at $1.75 and $2.50 per ton of concentrate, respectfully. Given a yearly plant production of 355,000 tons of concentrate, a reduction in haulage of 10% would result in annual variable cost savings of $150,875.

This system also saves the cost of drying unnecessary material in the dry mill facilities. These costs are estimated at $1.50 per ton of feed material. A 10% reduction of material needing drying would thus result in annual variable cost savings of $53,250. This calculation does not take into account any maintenance costs associated with drying wet mill concentrate, only the cost of fuel consumption.

Installation costs of the proposed system is estimated at $200,000. This cost includes construction of the CrossFlow unit, necessary support structures, electrical services, water services, and engineering fees. Assuming no added variable cost for the proposed system, capital cost of $200,000 and yearly savings of $204,125 the Internal Rate of Return (IRR) of this project is estimated at 75% with a Net Present Value (NPV) of $372,897. Total economic calculations, including taxes, depreciation, and depletion, can be seen in Table XVI. This economic exercise used a tax rate of 38% with the typical graduated depreciation rates over 5 years.

Table XVI: Economic Analysis of CrossFlow Installation

Capital	$200,000

YEAR	2001	2002	2003	2004	2005	2006	
Revenue		$204,125	$204,125	$204,125	$204,125	$204,125	
Cash Costs							
Fixed		$0	$0	$0	$0	$0	$0
Variable		$0	$0	$0	$0	$0	$0
PTOI		$204,125	$204,125	$204,125	$204,125	$204,125	$0
Taxes							
Depreciation		20%	32%	19%	12%	12%	5%
		$40,000	$64,000	$38,000	$24,000	$24,000	###
Depletion		$44,908	$44,908	$44,908	$44,908	$44,908	###
Taxable Income		$119,218	$95,218	$121,218	$135,218	$135,218	###
Tax		$45,303	$36,183	$46,063	$51,383	$51,383	###
ATOI		$158,822	$167,942	$158,062	$152,742	$152,742	###

Cash Flow	-$200,000	$158,822	$167,942	$158,062	$152,742	$152,742	###

NPV	**$372,897**
IRR	**75%**

CHAPTER 5

Conclusions

Lab/pilot-scale testing was accomplished using a 4" x 16" CrossFlow unit in continuous field operation. The primary goal of this test work was to evaluate the feasibility of using elutriation technology for heavy mineral concentration. These tests were carried out for numerous feed grades and tonnages. Various operational parameters were also examined during these tests. As previously stated, the feed material used was from a mineral sands operation in northern Florida. The results achieved from this testing program are as follows:

- Quartz rejections greater than 80% were possible under certain operational conditions. TiO_2 recoveries at these rejection levels were above 95%.
- Elutriation flowrates were reduced to as low as 2 gpm/ft^2 under certain conditions. This reduction allows for significant savings of fresh water required for unit operation.
- Use of a deflection plate showed significant recovery/rejection improvement over the typical CrossFlow feed arrangement.
- Feed tonnages as high as 1.5 tph were successful in achieving the testing goals. This allows for reduced unit size and cost.

Pilot scale testing was accomplished using a 2' x 2' CrossFlow unit in continuous field operation. These tests were carried out for numerous feed grades, tonnages, elutriation flow rates and bed levels. The results achieved from this testing program are as follows:

- Quartz rejections greater than 80% were possible under many different operational conditions. TiO_2 recoveries at these rejection levels were approximately 98%.
- Elutriation flow rate was optimized to 14 gpm, 3.5 gpm/ft^2, for several operational conditions.
- Use of a deflection plate showed significant recovery/rejection improvement over the typical CrossFlow feed arrangement.
- Feed tonnages as high as 1.5 tph were successful in achieving the testing goals. This allows for reduced unit size and cost.
- Standard deviation for the wet mill concentrate TiO_2 grade was reduced from 3.0% to 1.68%

Along with experimental testing, both empirical and statistical models for unit operation were developed. Given a feed grade of 28% TiO_2 and a feed rate of 70 tph for full-scale operation, the statistical model was successful in determining the following:

- A minimum elutriation flow rate of 245 gpm (3.5 gpm/ft^2) would allow for successful quartz rejection.
- A feed rate of 1.5 tph/ft^2 could be used to achieve successful unit results. This tonnage requires the use of a 47 ft^2 CrossFlow unit. A typical 7' x 7' square configuration would achieve the proper cross-sectional feed rate.
- An overall quartz rejection of 80% with a TiO_2 recovery of 98% is possible for these particular unit operational conditions.

CHAPTER 6

Recommendations for Future Work

Improve Performance of Hindered-Bed Classifiers for Heavy Mineral Separations.

1. Laboratory testing focusing on optimal settings for the added baffle plate are needed in order to better understand this item's impact on unit performance. It is recommended that this baffle plate be set at various heights and distances from the feed presentation system to accomplish this task.
2. Full-scale installation of a CrossFlow unit in order to achieve the benefits previously mentioned within this report. Elaborate testing would be needed for this application to achieve the highest possible success. This testing should be used in order to generate model information that could be used by operators for precise field operation.

Improved Rejection of Fine TiO_2 from Zircon Wet Mill Concentrate.

1. Conducting testing to investigate the possible benefits of using elutriation technology in order to clean zircon wet mill concentrate. This particular concentration is comprised mainly of zircon, ilmenite, leucoxene, rutile, kyanite, sillmanite, and staurolite. This separation would be quite difficult given the near density of minerals such as ilmenite, 3.7, to the zircon product, 4.7.

2. Pilot-scale installation of a CrossFlow unit to achieve the desired TiO_2 rejection levels. Elaborate testing would need to develop a functioning model for unit operation.

REFERENCES

Drummond, R.B., Swanson, A.R., Nicols, S.K., and Newling, P.G., 1998, "Optimization studies on a 75 t/h teetered bed separator at Stratford coal preparation plant," Proceedings, XIII International Coal Preparation Congress, (A.C. Partridge and I.R. Partridge, eds.) Australian Coal Preparation Society, 215-224.

Dunn, P.L., Stewart, S.O., Kohmuench, J.N. and Cadena, C.A., 2000, "A Hydraulic Classifier Evaluation: Upgrading of Heavy Mineral Concentrates," Preprint No. 00-155, SME Annual Meeting, February 28-March 1, Salt Lake City, Utah.

Elder, J., Kow, W., Domenico, J. and Wyatt, D., 2001, "Gravity Concentration – A Better Way," Proceedings, International Heavy Minerals Conference, 115-118.

Grotjohann, P. and Snoby, R.J., 1998, "Allflux® Separator/A New Way to Process your Heavy Minerals," SME Annual Meeting, Orlando, Florida, March 9-11.

Heiskanen, K., 1993, Particle Classification, Powder Technology Series, Chapman and Hall, London, England.

Honaker, R.Q., Paul, B.C., Wang, D. and Ho, K., 1995, "Enhanced Gravity Separation: an Alternative to Floatation," High Efficiency Coal Preparation (ed. S.K. Kawatra,) Society for Mining, Metallurgy, and Exploration, Inc., Littleton, Colorado, Chapter 5, pp. 69-78.

Honaker, R.Q., 1996, "Hindered-bed Classifiers for Fine Coal Cleaning," Proceedings, 13th International Coal Preparation Conference, Lexington, Kentucky, pp. 59-70.

Honaker, R.Q., 1998, "High Capacity Fine Coal Cleaning using an Enhanced Gravity Concentrator," Minerals Engineering, Vol. 11, No. 12, pp. 159-170.

Honaker, R.Q., Ozsever, A.V. and Parekh, B.K., 2001, "Gravity Based Separation Using a Hydraulic Classifier for Fine Coal Cleaning," Preprint No. 01-186, SME Annual Meeting, February 26-28, Denver, Colorado.

Honaker, R.Q. and Mondal, K., 1999, "Dynamic Modeling of Fine Particle Separations in a Hindered Bed Classifier," SME Annual Meeting, Denver, Colorado, March 1-3.

Kohmuench, J.N., Luttrell, G.H. and Mankosa, M.J., 1998, "Testing of the Hydrofloat Cell for Recovery of Coarse Phosphate," Proceedings, Engineering Foundation Conference on Beneficiation of Phosphate, Palm Coast, Florida, December 6-11, 1998, pp. 1-6.

Kohmuench, J.N., Mankosa, M.J., Luttrell, G.H. and Adel, G.T., 2001, "A Process Engineering Evaluation of the Crossflow Separator," Preprint No. 01-80, SME Annual Meeting, February 26-28, Denver, Colorado.

Kohmuench, J.N., Luttrell, G.H. and Mankosa, M.J., 2000, "Coarse Particle Concentration Using the Hydrofloat Separator," SME Annual Meeting, February 28 – March 1, 2000, Salt Lake City, Utah.

Littler, A., 1986, "Automatic Hindered-Settling Classifier for Hydraulic Sizing and Mineral Beneficiation," Transactions, Institute of Mining and Metallurgy, Vol. 95, pp. 133-138

Luttrell, G.H., Kohmuench, J.N. and Mankosa and M.J., 2000, "Coarse Particle Concentration using the HydroFloat Separator," Preprint No. 00-100, SME Annual Meeting, February 28, Salt Lake City, Utah.

Luttrell, G.H., Kohmuench, J.N., Stanely, F.L. and Trump, G.D., 1999, "An Evaluation of Multi-Stage Spiral Circuits," Proceedings, 16th International Coal Preparation Conference, Lexington, Kentucky, April 27-29, pp. 79-88.

Mankosa, M.J., Kohmuench, J.N., Luttrell, G.H. and Eisenmann, M., 2000, "In-Plant Testing of the Hydrofloat Separator for Coarse Coal Recovery," Proceedings, 17th International Coal Preparation Conference, Lexington, Kentucky, May 4, pp. 333-340.

Mankosa, M.J., 1990, Scale-Up of Column Flotation, Dissertation, Virginia Polytechnic Institute and State University, Blacksburg, VA.

Mankosa, M.J. and Carver, R.M., 1995, "Processing of Chopped Wire Waste Material Using the Floatex Density Separator," Third International Symposium on Recycling of Metals and Engineered Materials, ed. P.B. Queneau and R.D. Peterson, The Minerals, Metals, and Materials Society, pp. 111-120.

Mankosa, M.J., Stanely, F.L., and Honaker, R.Q., 1995, "Combining Hydraulic Classification and Spiral Concentration for Improved Efficiency in Fine Coal Recovery Circuits," High Efficiency Coal Preparation, (S.K. Kawatra, ed.) SME, Littleton, Colorado, pp. 99-107.

Masliyah, J.H., 1979, "Hindered Settling in a Multi-Species Particle System," Chemical Engineering Science, Vol. 34, pp. 1166-1168.

McKnight, K., Stouffer, N., Domenico, J. and Mankosa, M.J., 1996, "Recovery of Zircon and Other Economic Minerals From Wet Gravity Tailings Using the Floatex Density Separator," SME Annual Meeting, Phoenix, Arizona, March 11-14.

Nicols, S.K. and Drummond, R.B., 1997, "A Review of Experience with Teetered Bed Separators," Preprints, Technology Review Seminar, Recent Developments in Gravity Separators, Australian Coal Preparation Society, May 21.

Rasul, M.G., Rudolph, V. and Wang, F.Y., 2000, "Particle Separation Using Fluidization Techniques," International Journal of Mineral Processing, Vol. 60, pp. 163-179.

Reed, S., Roger, R., Honaker, R.Q. and Mankosa, M.J., 1995, "In-Plant Testing of the Floatex Density Separator for Fine Coal Cleaning," Proceedings, 12th International Coal Preparation Conference, Lexington, Kentucky, pp.163-174.

Richardson, J. and Zaki, W., 1954, "Sedimentation and Fluidization: Part l, "Transactions of the Institute of Chemical Engineering, Vol. 39, pp. 35-53.

Swanson, S.F., 1999, "Settling Equation for Mineral Process Applications," Minerals and Metallurgical Processing, Vol. 16, No. 3, pp. 8-13.

Swanson, S.F., 1989, "Free and Hindered Settling," Minerals and Metallurgical Processing, Nov., pp. 190-196.

Yu, A.B. and Standish, N., 1993, "A Study of the Packing of Particles with a Mixture Size Distribution," Powder Technology, Vol. 76, pp. 113-124.

APPENDIX A

MASS BALANCE DATA FOR 4” X 16” CROSSFLOW

		Experimental Values							Adjusted Values						
		Tonnage	HM	SiO2	Al2O3	TiO2	Fe2O3	ZrO2	Tonnage	HM	SiO2	Al2O3	TiO2	Fe2O3	ZrO2
Sample 1	**Feed**	51.13	69.50	40.20	10.70	26.30	11.50	8.46	48.28	74.76	31.67	11.13	28.36	12.24	9.38
	Underflow	43.99	95.06	16.90	13.80	37.00	15.80	13.00	40.31	86.84	18.16	13.20	33.59	14.64	11.18
	Overflow	7.14	13.70	96.70	0.63	1.89	0.10	0.26	7.97	13.67	100.00	0.63	1.89	0.10	0.26

Relative Change							Relative Error						
Tonnage	HM	SiO2	Al2O3	TiO2	Fe2O3	ZrO2	Tonnage	HM	SiO2	Al2O3	TiO2	Fe2O3	ZrO2
-5.58	7.57	-21.23	4.01	7.84	6.42	10.89	1.00	1.00	1.00	1.00	1.00	1.00	1.00
-8.36	-8.65	7.45	-4.32	-9.21	-7.36	-13.97	1.00	1.00	1.00	1.00	1.00	1.00	1.00
11.59	-0.25	3.41	-0.04	-0.09	-0.01	-0.06	1.00	1.00	1.00	1.00	1.00	1.00	1.00

Weighted Sum-of-Squares							Total
Tonnage	HM	SiO2	Al2O3	TiO2	Fe2O3	ZrO2	WSSQ
0.00	0.01	0.05	0.00	0.01	0.00	0.01	0.08
0.01	0.01	0.01	0.00	0.01	0.01	0.02	0.06
0.01	0.00	0.00	0.00	0.00	0.00	0.00	0.01
							0.15

		Experimental Values							Adjusted Values						
		Tonnage	HM	SiO2	Al2O3	TiO2	Fe2O3	ZrO2	Tonnage	HM	SiO2	Al2O3	TiO2	Fe2O3	ZrO2
Sample 2	**Feed**	81.39	88.61	24.50	10.10	33.20	14.00	15.00	81.40	88.42	24.36	8.20	33.19	13.52	16.58
	Underflow	80.77	88.89	23.70	7.28	33.40	13.20	19.30	80.79	89.08	23.83	8.26	33.41	13.62	16.70
	Overflow	0.61	1.00	95.10	0.87	3.22	0.26	0.51	0.61	1.00	95.12	0.87	3.21	0.26	0.51

Relative Change							Relative Error						
Tonnage	HM	SiO2	Al2O3	TiO2	Fe2O3	ZrO2	Tonnage	HM	SiO2	Al2O3	TiO2	Fe2O3	ZrO2
0.02	-0.22	-0.56	-18.79	-0.04	-3.42	10.54	1.00	1.00	1.00	1.00	1.00	1.00	1.00
0.02	0.22	0.53	13.44	0.04	3.20	-13.46	1.00	1.00	1.00	1.00	1.00	1.00	1.00
-0.03	0.00	0.02	0.01	0.00	0.00	0.00	1.00	1.00	1.00	1.00	1.00	1.00	1.00

Weighted Sum-of-Squares							Total
Tonnage	HM	SiO2	Al2O3	TiO2	Fe2O3	ZrO2	WSSQ
0.00	0.00	0.00	0.04	0.00	0.00	0.01	0.05
0.00	0.00	0.00	0.02	0.00	0.00	0.02	0.04
0.00	0.00	0.00	0.00	0.00	0.00	0.00	0.00
							0.08

		Experimental Values							Adjusted Values						
		Tonnage	HM	SiO2	Al2O3	TiO2	Fe2O3	ZrO2	Tonnage	HM	SiO2	Al2O3	TiO2	Fe2O3	ZrO2
Sample 3	**Feed**	85.34	68.25	40.50	11.90	25.30	11.90	7.82	82.04	73.25	33.77	11.70	26.94	12.34	9.00
	Underflow	72.52	90.78	20.10	13.50	33.60	15.20	13.40	68.10	83.44	21.48	13.71	31.20	14.61	10.53
	Overflow	12.82	23.58	88.40	1.89	6.09	1.23	1.48	13.94	23.48	93.85	1.89	6.08	1.23	1.47

Relative Change							Relative Error						
Tonnage	HM	SiO2	Al2O3	TiO2	Fe2O3	ZrO2	Tonnage	HM	SiO2	Al2O3	TiO2	Fe2O3	ZrO2
-3.87	7.33	-16.62	-1.66	6.47	3.67	15.03	1.00	1.00	1.00	1.00	1.00	1.00	1.00
-6.09	-8.09	6.85	1.56	-7.13	-3.89	-21.38	1.00	1.00	1.00	1.00	1.00	1.00	1.00
8.68	-0.43	6.16	0.04	-0.26	-0.06	-0.48	1.00	1.00	1.00	1.00	1.00	1.00	1.00

Weighted Sum-of-Squares							Total
Tonnage	HM	SiO2	Al2O3	TiO2	Fe2O3	ZrO2	WSSQ
0.00	0.01	0.03	0.00	0.00	0.00	0.02	0.06
0.00	0.01	0.00	0.00	0.01	0.00	0.05	0.07
0.01	0.00	0.00	0.00	0.00	0.00	0.00	0.01
							0.14

		Experimental Values							Adjusted Values						
		Tonnage	HM	SiO2	Al2O3	TiO2	Fe2O3	ZrO2	Tonnage	HM	SiO2	Al2O3	TiO2	Fe2O3	ZrO2
Sample 4	**Feed**	72.17	78.21	33.30	11.30	29.10	13.20	10.20	72.30	79.63	33.97	11.55	28.46	12.80	10.41
	Underflow	61.71	91.35	23.70	13.70	32.30	14.50	12.40	61.89	89.69	23.41	13.38	32.98	14.92	12.14
	Overflow	10.46	19.89	97.60	0.69	1.58	0.20	0.15	10.41	19.88	96.77	0.69	1.58	0.20	0.15

Relative Change							Relative Error						
Tonnage	HM	SiO2	Al2O3	TiO2	Fe2O3	ZrO2	Tonnage	HM	SiO2	Al2O3	TiO2	Fe2O3	ZrO2
0.18	1.82	2.02	2.24	-2.21	-3.05	2.05	1.00	1.00	1.00	1.00	1.00	1.00	1.00
0.29	-1.82	-1.23	-2.33	2.10	2.87	-2.14	1.00	1.00	1.00	1.00	1.00	1.00	1.00
-0.48	-0.07	-0.85	-0.02	0.02	0.01	0.00	1.00	1.00	1.00	1.00	1.00	1.00	1.00

Weighted Sum-of-Squares							Total
Tonnage	HM	SiO2	Al2O3	TiO2	Fe2O3	ZrO2	WSSQ
0.00	0.00	0.00	0.00	0.00	0.00	0.00	0.00
0.00	0.00	0.00	0.00	0.00	0.00	0.00	0.00
0.00	0.00	0.00	0.00	0.00	0.00	0.00	0.00
							0.01

		Experimental Values							Adjusted Values						
		Tonnage	HM	SiO2	Al2O3	TiO2	Fe2O3	ZrO2	Tonnage	HM	SiO2	Al2O3	TiO2	Fe2O3	ZrO2
Sample 5	**Feed**	94.08	80.72	33.50	10.80	28.30	12.50	11.60	93.40	82.21	32.06	11.42	28.61	12.70	11.61
	Underflow	86.24	89.48	25.10	13.30	31.50	14.10	12.70	85.44	87.81	25.84	12.44	31.15	13.87	12.68
	Overflow	7.84	22.08	97.70	0.49	1.26	0.20	0.12	7.96	22.07	98.75	0.49	1.26	0.20	0.12

Relative Change							Relative Error						
Tonnage	HM	SiO2	Al2O3	TiO2	Fe2O3	ZrO2	Tonnage	HM	SiO2	Al2O3	TiO2	Fe2O3	ZrO2
-0.72	1.84	-4.31	5.75	1.08	1.61	0.12	1.00	1.00	1.00	1.00	1.00	1.00	1.00
-0.93	-1.87	2.95	-6.47	-1.10	-1.66	-0.12	1.00	1.00	1.00	1.00	1.00	1.00	1.00
1.61	-0.04	1.07	-0.02	0.00	0.00	0.00	1.00	1.00	1.00	1.00	1.00	1.00	1.00

Weighted Sum-of-Squares							Total
Tonnage	HM	SiO2	Al2O3	TiO2	Fe2O3	ZrO2	WSSQ
0.00	0.00	0.00	0.00	0.00	0.00	0.00	0.01
0.00	0.00	0.00	0.00	0.00	0.00	0.00	0.01
0.00	0.00	0.00	0.00	0.00	0.00	0.00	0.00
							0.01

		Experimental Values							Adjusted Values						
		Tonnage	HM	SiO2	Al2O3	TiO2	Fe2O3	ZrO2	Tonnage	HM	SiO2	Al2O3	TiO2	Fe2O3	ZrO2
Sample 6	**Feed**	105.93	75.05	35.50	11.20	26.90	12.10	10.40	104.75	78.19	31.38	11.12	28.20	12.35	11.67
	Underflow	100.67	85.54	25.70	11.60	31.30	13.30	14.70	99.37	81.67	27.75	11.68	29.63	13.01	12.29
	Overflow	5.25	14.02	97.00	0.61	1.70	0.19	0.24	5.38	14.01	98.58	0.61	1.70	0.19	0.24

Relative Change							Relative Error						
Tonnage	HM	SiO2	Al2O3	TiO2	Fe2O3	ZrO2	Tonnage	HM	SiO2	Al2O3	TiO2	Fe2O3	ZrO2
-1.11	4.19	-11.60	-0.74	4.83	2.09	12.23	1.00	1.00	1.00	1.00	1.00	1.00	1.00
-1.29	-4.53	7.97	0.73	-5.33	-2.18	-16.40	1.00	1.00	1.00	1.00	1.00	1.00	1.00
2.32	-0.04	1.63	0.00	-0.02	0.00	-0.01	1.00	1.00	1.00	1.00	1.00	1.00	1.00

Weighted Sum-of-Squares							Total
Tonnage	HM	SiO2	Al2O3	TiO2	Fe2O3	ZrO2	WSSQ
0.00	0.00	0.01	0.00	0.00	0.00	0.01	0.03
0.00	0.00	0.01	0.00	0.00	0.00	0.03	0.04
0.00	0.00	0.00	0.00	0.00	0.00	0.00	0.00
							0.07

		Experimental Values							Adjusted Values						
		Tonnage	HM	SiO2	Al2O3	TiO2	Fe2O3	ZrO2	Tonnage	HM	SiO2	Al2O3	TiO2	Fe2O3	ZrO2
Sample 7	**Feed**	74.97	61.75	50.10	10.20	20.70	9.51	5.75	70.16	68.99	32.66	11.33	23.61	10.61	6.93
	Underflow	68.16	90.21	21.60	14.60	32.40	13.90	13.90	62.52	76.44	24.49	12.53	26.05	11.81	7.77
	Overflow	6.81	8.03	93.00	1.53	3.61	0.83	-0.01	7.64	8.02	99.54	1.53	3.60	0.83	0.00

Relative Change							Relative Error						
Tonnage	HM	SiO2	Al2O3	TiO2	Fe2O3	ZrO2	Tonnage	HM	SiO2	Al2O3	TiO2	Fe2O3	ZrO2
-6.42	11.72	-34.81	11.11	14.05	11.57	20.46	1.00	1.00	1.00	1.00	1.00	1.00	1.00
-8.27	-15.26	13.37	-14.17	-19.59	-15.07	-44.08	1.00	1.00	1.00	1.00	1.00	1.00	1.00
12.12	-0.17	7.04	-0.18	-0.27	-0.11	-100.00	1.00	1.00	1.00	1.00	1.00	1.00	1.00

Weighted Sum-of-Squares							Total
Tonnage	HM	SiO2	Al2O3	TiO2	Fe2O3	ZrO2	WSSQ
0.00	0.01	0.12	0.01	0.02	0.01	0.04	0.23
0.01	0.02	0.02	0.02	0.04	0.02	0.19	0.32
0.01	0.00	0.00	0.00	0.00	0.00	1.00	1.02
							1.57

		Experimental Values							Adjusted Values						
		Tonnage	HM	SiO2	Al2O3	TiO2	Fe2O3	ZrO2	Tonnage	HM	SiO2	Al2O3	TiO2	Fe2O3	ZrO2
Sample 8	**Feed**	98.32	73.60	39.30	11.10	25.30	11.40	9.14	99.50	69.17	41.30	9.97	24.90	10.73	9.92
	Underflow	76.07	81.38	27.70	11.50	30.70	12.90	14.00	78.20	85.64	26.92	12.46	31.16	13.57	12.56
	Overflow	22.25	8.68	96.70	0.83	1.93	0.30	0.23	21.30	8.69	94.11	0.83	1.93	0.30	0.23

Relative Change							Relative Error						
Tonnage	HM	SiO2	Al2O3	TiO2	Fe2O3	ZrO2	Tonnage	HM	SiO2	Al2O3	TiO2	Fe2O3	ZrO2
1.20	-6.02	5.09	-10.20	-1.57	-5.86	8.54	1.00	1.00	1.00	1.00	1.00	1.00	1.00
2.80	5.23	-2.82	8.31	1.50	5.21	-10.28	1.00	1.00	1.00	1.00	1.00	1.00	1.00
-4.28	0.15	-2.68	0.16	0.03	0.03	-0.05	1.00	1.00	1.00	1.00	1.00	1.00	1.00

Weighted Sum-of-Squares							Total
Tonnage	HM	SiO2	Al2O3	TiO2	Fe2O3	ZrO2	WSSQ
0.00	0.00	0.00	0.01	0.00	0.00	0.01	0.03
0.00	0.00	0.00	0.01	0.00	0.00	0.01	0.02
0.00	0.00	0.00	0.00	0.00	0.00	0.00	0.00
							0.06

		Experimental Values							Adjusted Values						
		Tonnage	HM	SiO2	Al2O3	TiO2	Fe2O3	ZrO2	Tonnage	HM	SiO2	Al2O3	TiO2	Fe2O3	ZrO2
Sample 9	**Feed**	43.79	27.67	79.00	5.49	7.06	3.98	2.79	30.87	29.50	76.24	5.59	8.51	4.14	3.18
	Underflow	27.74	87.59	26.60	16.30	30.00	13.20	10.50	9.57	81.90	26.70	16.02	21.89	12.67	8.78
	Overflow	16.05	6.02	95.70	0.91	2.64	0.30	0.68	21.30	5.96	98.50	0.91	2.50	0.30	0.66

Relative Change							Relative Error						
Tonnage	HM	SiO2	Al2O3	TiO2	Fe2O3	ZrO2	Tonnage	HM	SiO2	Al2O3	TiO2	Fe2O3	ZrO2
-29.50	6.62	-3.50	1.87	20.52	3.90	14.02	1.00	1.00	1.00	1.00	1.00	1.00	1.00
-65.49	-6.50	0.37	-1.73	-27.03	-4.01	-16.36	1.00	1.00	1.00	1.00	1.00	1.00	1.00
32.70	-0.99	2.92	-0.21	-5.28	-0.20	-2.36	1.00	1.00	1.00	1.00	1.00	1.00	1.00

Weighted Sum-of-Squares							Total
Tonnage	HM	SiO2	Al2O3	TiO2	Fe2O3	ZrO2	WSSQ
0.09	0.00	0.00	0.00	0.04	0.00	0.02	0.16
0.43	0.00	0.00	0.00	0.07	0.00	0.03	0.53
0.11	0.00	0.00	0.00	0.00	0.00	0.00	0.11
							0.80

		Experimental Values							Adjusted Values						
		Tonnage	HM	SiO2	Al2O3	TiO2	Fe2O3	ZrO2	Tonnage	HM	SiO2	Al2O3	TiO2	Fe2O3	ZrO2
Sample 10	**Feed**	41.45	81.96	35.60	11.50	28.00	12.00	9.78	42.69	70.28	40.48	10.02	25.57	11.20	9.72
	Underflow	32.91	76.31	33.20	10.90	28.60	12.80	11.70	35.15	84.65	29.71	12.00	30.69	13.55	11.78
	Overflow	8.54	3.26	97.10	0.79	1.66	0.22	0.11	7.54	3.26	90.70	0.79	1.66	0.22	0.11

Relative Change							Relative Error						
Tonnage	HM	SiO2	Al2O3	TiO2	Fe2O3	ZrO2	Tonnage	HM	SiO2	Al2O3	TiO2	Fe2O3	ZrO2
2.99	-14.25	13.70	-12.89	-8.70	-6.69	-0.66	1.00	1.00	1.00	1.00	1.00	1.00	1.00
6.80	10.93	-10.52	10.06	7.31	5.87	0.65	1.00	1.00	1.00	1.00	1.00	1.00	1.00
-11.71	0.10	-6.60	0.16	0.09	0.02	0.00	1.00	1.00	1.00	1.00	1.00	1.00	1.00

Weighted Sum-of-Squares							Total
Tonnage	HM	SiO2	Al2O3	TiO2	Fe2O3	ZrO2	WSSQ
0.00	0.02	0.02	0.02	0.01	0.00	0.00	0.07
0.00	0.01	0.01	0.01	0.01	0.00	0.00	0.05
0.01	0.00	0.00	0.00	0.00	0.00	0.00	0.02
							0.13

		Experimental Values							Adjusted Values						
		Tonnage	HM	SiO2	Al2O3	TiO2	Fe2O3	ZrO2	Tonnage	HM	SiO2	Al2O3	TiO2	Fe2O3	ZrO2
Sample 11	**Feed**	50.25	51.24	57.20	9.80	19.30	8.65	2.54	50.38	54.03	58.74	7.91	17.99	7.54	3.08
	Underflow	35.94	66.24	46.00	8.98	22.70	9.38	9.28	36.24	62.89	45.28	10.12	24.01	10.32	4.14
	Overflow	14.30	31.61	94.40	2.20	2.56	0.44	0.35	14.14	31.31	93.22	2.23	2.57	0.44	0.35

Relative Change							Relative Error						
Tonnage	HM	SiO2	Al2O3	TiO2	Fe2O3	ZrO2	Tonnage	HM	SiO2	Al2O3	TiO2	Fe2O3	ZrO2
0.27	5.44	2.69	-19.32	-6.80	-12.79	21.08	1.00	1.00	1.00	1.00	1.00	1.00	1.00
0.83	-5.06	-1.56	12.73	5.75	9.97	-55.39	1.00	1.00	1.00	1.00	1.00	1.00	1.00
-1.13	-0.94	-1.25	1.22	0.25	0.18	-0.82	1.00	1.00	1.00	1.00	1.00	1.00	1.00

Weighted Sum-of-Squares							Total
Tonnage	HM	SiO2	Al2O3	TiO2	Fe2O3	ZrO2	WSSQ
0.00	0.00	0.00	0.04	0.00	0.02	0.04	0.11
0.00	0.00	0.00	0.02	0.00	0.01	0.31	0.34
0.00	0.00	0.00	0.00	0.00	0.00	0.00	0.00
							0.45

		Experimental Values							Adjusted Values						
		Tonnage	HM	SiO2	Al2O3	TiO2	Fe2O3	ZrO2	Tonnage	HM	SiO2	Al2O3	TiO2	Fe2O3	ZrO2
Sample 12	**Feed**	74.46	72.81	43.10	10.00	24.80	10.90	8.21	74.05	73.04	42.44	9.36	24.39	10.31	9.48
	Underflow	59.11	86.65	27.70	11.00	29.70	12.40	15.40	58.46	86.40	27.91	11.62	30.17	13.00	11.89
	Overflow	15.35	22.97	96.20	0.88	2.73	0.24	0.44	15.60	22.97	96.89	0.88	2.73	0.24	0.44

Relative Change							Relative Error						
Tonnage	HM	SiO2	Al2O3	TiO2	Fe2O3	ZrO2	Tonnage	HM	SiO2	Al2O3	TiO2	Fe2O3	ZrO2
-0.54	0.31	-1.53	-6.45	-1.66	-5.39	15.41	1.00	1.00	1.00	1.00	1.00	1.00	1.00
-1.10	-0.29	0.77	5.60	1.57	4.84	-22.82	1.00	1.00	1.00	1.00	1.00	1.00	1.00
1.61	-0.02	0.72	0.12	0.04	0.02	-0.17	1.00	1.00	1.00	1.00	1.00	1.00	1.00

Weighted Sum-of-Squares							Total
Tonnage	HM	SiO2	Al2O3	TiO2	Fe2O3	ZrO2	WSSQ
0.00	0.00	0.00	0.00	0.00	0.00	0.02	0.03
0.00	0.00	0.00	0.00	0.00	0.00	0.05	0.06
0.00	0.00	0.00	0.00	0.00	0.00	0.00	0.00
							0.09

		Experimental Values							Adjusted Values						
		Tonnage	HM	SiO2	Al2O3	TiO2	Fe2O3	ZrO2	Tonnage	HM	SiO2	Al2O3	TiO2	Fe2O3	ZrO2
Sample 13	**Feed**	114.41	80.13	32.10	10.80	30.60	13.20	10.40	113.05	83.13	25.79	11.05	31.96	13.50	11.75
	Underflow	110.67	89.53	20.70	11.70	34.70	14.30	14.80	109.22	85.91	23.23	11.41	33.01	13.96	12.16
	Overflow	3.74	3.76	96.80	0.77	2.06	0.13	0.23	3.83	3.76	98.74	0.77	2.06	0.13	0.23

Relative Change							Relative Error						
Tonnage	HM	SiO2	Al2O3	TiO2	Fe2O3	ZrO2	Tonnage	HM	SiO2	Al2O3	TiO2	Fe2O3	ZrO2
-1.19	3.74	-19.65	2.34	4.45	2.24	13.00	1.00	1.00	1.00	1.00	1.00	1.00	1.00
-1.31	-4.04	12.24	-2.45	-4.87	-2.35	-17.87	1.00	1.00	1.00	1.00	1.00	1.00	1.00
2.41	-0.01	2.01	-0.01	-0.01	0.00	-0.01	1.00	1.00	1.00	1.00	1.00	1.00	1.00

Weighted Sum-of-Squares							Total
Tonnage	HM	SiO2	Al2O3	TiO2	Fe2O3	ZrO2	WSSQ
0.00	0.00	0.04	0.00	0.00	0.00	0.02	0.06
0.00	0.00	0.01	0.00	0.00	0.00	0.03	0.05
0.00	0.00	0.00	0.00	0.00	0.00	0.00	0.00
							0.11

		Experimental Values							Adjusted Values						
		Tonnage	HM	SiO2	Al2O3	TiO2	Fe2O3	ZrO2	Tonnage	HM	SiO2	Al2O3	TiO2	Fe2O3	ZrO2
Sample 14	**Feed**	97.06	75.82	40.20	11.60	25.70	11.50	8.18	96.23	77.05	36.93	8.50	25.62	10.34	9.88
	Underflow	78.76	96.21	21.20	8.88	31.10	11.80	23.50	77.49	94.62	21.93	10.34	31.20	12.78	12.18
	Overflow	18.30	4.38	95.40	0.89	2.53	0.23	0.37	18.74	4.38	98.98	0.89	2.53	0.23	0.37

Relative Change							Relative Error						
Tonnage	HM	SiO2	Al2O3	TiO2	Fe2O3	ZrO2	Tonnage	HM	SiO2	Al2O3	TiO2	Fe2O3	ZrO2
-0.86	1.62	-8.12	-26.71	-0.33	-10.09	20.82	1.00	1.00	1.00	1.00	1.00	1.00	1.00
-1.61	-1.65	3.45	16.46	0.32	8.34	-48.16	1.00	1.00	1.00	1.00	1.00	1.00	1.00
2.37	-0.02	3.75	0.40	0.01	0.04	-0.18	1.00	1.00	1.00	1.00	1.00	1.00	1.00

Weighted Sum-of-Squares							Total
Tonnage	HM	SiO2	Al2O3	TiO2	Fe2O3	ZrO2	WSSQ
0.00	0.00	0.01	0.07	0.00	0.01	0.04	0.13
0.00	0.00	0.00	0.03	0.00	0.01	0.23	0.27
0.00	0.00	0.00	0.00	0.00	0.00	0.00	0.00
							0.40

		Experimental Values							Adjusted Values						
		Tonnage	HM	SiO2	Al2O3	TiO2	Fe2O3	ZrO2	Tonnage	HM	SiO2	Al2O3	TiO2	Fe2O3	ZrO2
Sample 15	**Feed**	99.01	69.76	42.30	10.80	26.10	10.90	7.80	98.86	70.69	41.56	10.85	26.10	10.97	8.07
	Underflow	95.01	74.38	38.80	11.30	27.00	11.50	8.70	94.85	73.36	39.40	11.25	27.00	11.42	8.37
	Overflow	4.00	7.51	92.40	1.46	4.63	0.45	1.03	4.01	7.51	92.54	1.46	4.63	0.45	1.03

Relative Change							Relative Error						
Tonnage	HM	SiO2	Al2O3	TiO2	Fe2O3	ZrO2	Tonnage	HM	SiO2	Al2O3	TiO2	Fe2O3	ZrO2
-0.15	1.34	-1.76	0.46	-0.02	0.69	3.52	1.00	1.00	1.00	1.00	1.00	1.00	1.00
-0.17	-1.37	1.55	-0.47	0.02	-0.70	-3.77	1.00	1.00	1.00	1.00	1.00	1.00	1.00
0.31	-0.01	0.16	0.00	0.00	0.00	-0.02	1.00	1.00	1.00	1.00	1.00	1.00	1.00

Weighted Sum-of-Squares							Total
Tonnage	HM	SiO2	Al2O3	TiO2	Fe2O3	ZrO2	WSSQ
0.00	0.00	0.00	0.00	0.00	0.00	0.00	0.00
0.00	0.00	0.00	0.00	0.00	0.00	0.00	0.00
0.00	0.00	0.00	0.00	0.00	0.00	0.00	0.00
							0.00

		Experimental Values							Adjusted Values						
		Tonnage	HM	SiO2	Al2O3	TiO2	Fe2O3	ZrO2	Tonnage	HM	SiO2	Al2O3	TiO2	Fe2O3	ZrO2
Sample 16	**Feed**	93.14	61.14	47.70	11.60	22.20	10.40	5.23	90.61	53.56	54.77	9.20	18.54	8.17	4.98
	Underflow	49.41	70.10	44.80	11.80	23.00	10.70	6.66	58.71	76.56	40.76	13.41	25.55	12.23	6.92
	Overflow	43.73	11.14	89.30	1.44	5.55	0.69	1.39	31.89	11.23	80.57	1.45	5.63	0.69	1.40

Relative Change							Relative Error						
Tonnage	HM	SiO2	Al2O3	TiO2	Fe2O3	ZrO2	Tonnage	HM	SiO2	Al2O3	TiO2	Fe2O3	ZrO2
-2.72	-12.40	14.83	-20.69	-16.50	-21.45	-4.81	1.00	1.00	1.00	1.00	1.00	1.00	1.00
18.84	9.21	-9.02	13.64	11.08	14.30	3.97	1.00	1.00	1.00	1.00	1.00	1.00	1.00
-27.07	0.80	-9.77	0.90	1.45	0.50	0.45	1.00	1.00	1.00	1.00	1.00	1.00	1.00

Weighted Sum-of-Squares							Total
Tonnage	HM	SiO2	Al2O3	TiO2	Fe2O3	ZrO2	WSSQ
0.00	0.02	0.02	0.04	0.03	0.05	0.00	0.16
0.04	0.01	0.01	0.02	0.01	0.02	0.00	0.11
0.07	0.00	0.01	0.00	0.00	0.00	0.00	0.08
							0.34

		Experimental Values							Adjusted Values						
		Tonnage	HM	SiO2	Al2O3	TiO2	Fe2O3	ZrO2	Tonnage	HM	SiO2	Al2O3	TiO2	Fe2O3	ZrO2
Sample 17	**Feed**	96.07	82.34	29.30	9.90	32.60	13.1	12.10	95.82	83.44	25.43	11.15	32.56	13.28	12.90
	Underflow	95.15	85.42	22.50	13.60	32.80	13.6	14.10	94.90	84.24	24.76	11.25	32.84	13.41	13.02
	Overflow	0.92	1.00	94.50	0.86	2.98	0.5	0.58	0.92	1.00	94.89	0.86	2.98	0.50	0.58

Relative Change							Relative Error						
Tonnage	HM	SiO2	Al2O3	TiO2	Fe2O3	ZrO2	Tonnage	HM	SiO2	Al2O3	TiO2	Fe2O3	ZrO2
-0.26	1.34	-13.20	12.67	-0.13	1.39	6.63	1.00	1.00	1.00	1.00	1.00	1.00	1.00
-0.26	-1.38	10.04	-17.24	0.13	-1.43	-7.65	1.00	1.00	1.00	1.00	1.00	1.00	1.00
0.52	0.00	0.41	-0.01	0.00	0.00	0.00	1.00	1.00	1.00	1.00	1.00	1.00	1.00

Weighted Sum-of-Squares							Total
Tonnage	HM	SiO2	Al2O3	TiO2	Fe2O3	ZrO2	WSSQ
0.00	0.00	0.02	0.02	0.00	0.00	0.00	0.04
0.00	0.00	0.01	0.03	0.00	0.00	0.01	0.05
0.00	0.00	0.00	0.00	0.00	0.00	0.00	0.00
							0.08

		Experimental Values							Adjusted Values						
		Tonnage	HM	SiO2	Al2O3	TiO2	Fe2O3	ZrO2	Tonnage	HM	SiO2	Al2O3	TiO2	Fe2O3	ZrO2
Sample 18	**Feed**	125.63	81.14	33.90	10.90	28.00	12.30	11.70	126.72	76.13	35.32	10.98	27.36	12.07	11.44
	Underflow	110.43	81.12	28.60	12.40	29.90	13.40	12.60	111.85	85.54	27.71	12.31	30.55	13.64	12.87
	Overflow	15.20	5.33	93.90	0.92	3.36	0.24	0.69	14.87	5.33	92.62	0.92	3.36	0.24	0.69

Relative Change							Relative Error						
Tonnage	HM	SiO2	Al2O3	TiO2	Fe2O3	ZrO2	Tonnage	HM	SiO2	Al2O3	TiO2	Fe2O3	ZrO2
0.86	-6.17	4.19	0.70	-2.29	-1.87	-2.23	1.00	1.00	1.00	1.00	1.00	1.00	1.00
1.29	5.45	-3.12	-0.70	2.16	1.80	2.12	1.00	1.00	1.00	1.00	1.00	1.00	1.00
-2.22	0.05	-1.36	-0.01	0.03	0.00	0.02	1.00	1.00	1.00	1.00	1.00	1.00	1.00

Weighted Sum-of-Squares							Total
Tonnage	HM	SiO2	Al2O3	TiO2	Fe2O3	ZrO2	WSSQ
0.00	0.00	0.00	0.00	0.00	0.00	0.00	0.01
0.00	0.00	0.00	0.00	0.00	0.00	0.00	0.01
0.00	0.00	0.00	0.00	0.00	0.00	0.00	0.00
							0.01

		Experimental Values							Adjusted Values						
		Tonnage	HM	SiO2	Al2O3	TiO2	Fe2O3	ZrO2	Tonnage	HM	SiO2	Al2O3	TiO2	Fe2O3	ZrO2
Sample 19	**Feed**	43.41	82.67	31.90	10.70	28.70	12.40	13.30	44.52	76.48	36.28	10.22	27.84	11.46	11.51
	Underflow	31.59	91.43	23.90	12.40	34.10	13.80	13.30	34.39	97.28	22.00	12.90	35.04	14.70	14.69
	Overflow	11.81	5.84	93.30	1.11	3.36	0.47	0.70	10.12	5.85	84.78	1.11	3.36	0.47	0.70

Relative Change							Relative Error						
Tonnage	HM	SiO2	Al2O3	TiO2	Fe2O3	ZrO2	Tonnage	HM	SiO2	Al2O3	TiO2	Fe2O3	ZrO2
2.55	-7.48	13.72	-4.50	-3.01	-7.56	-13.49	1.00	1.00	1.00	1.00	1.00	1.00	1.00
8.86	6.39	-7.94	4.03	2.76	6.50	10.42	1.00	1.00	1.00	1.00	1.00	1.00	1.00
-14.31	0.12	-9.13	0.11	0.08	0.07	0.16	1.00	1.00	1.00	1.00	1.00	1.00	1.00

Weighted Sum-of-Squares							Total
Tonnage	HM	SiO2	Al2O3	TiO2	Fe2O3	ZrO2	WSSQ
0.00	0.01	0.02	0.00	0.00	0.01	0.02	0.05
0.01	0.00	0.01	0.00	0.00	0.00	0.01	0.04
0.02	0.00	0.01	0.00	0.00	0.00	0.00	0.03
							0.12

		Experimental Values							Adjusted Values						
		Tonnage	HM	SiO2	Al2O3	TiO2	Fe2O3	ZrO2	Tonnage	HM	SiO2	Al2O3	TiO2	Fe2O3	ZrO2
Sample 20	**Feed**	86.38	79.23	38.50	12.10	25.50	11.80	8.51	85.70	75.10	37.29	10.50	26.43	11.66	9.86
	Underflow	64.29	98.19	15.90	12.60	36.00	15.60	17.30	63.04	100.00	16.05	13.88	34.64	15.78	13.19
	Overflow	22.09	5.85	94.40	1.08	3.61	0.23	0.61	22.67	5.86	96.33	1.08	3.61	0.23	0.61

Relative Change							Relative Error						
Tonnage	HM	SiO2	Al2O3	TiO2	Fe2O3	ZrO2	Tonnage	HM	SiO2	Al2O3	TiO2	Fe2O3	ZrO2
-0.78	-5.21	-3.15	-13.26	3.65	-1.16	15.89	1.00	1.00	1.00	1.00	1.00	1.00	1.00
-1.95	1.84	0.96	10.16	-3.78	1.12	-23.76	1.00	1.00	1.00	1.00	1.00	1.00	1.00
2.62	0.10	2.05	0.31	-0.14	0.01	-0.30	1.00	1.00	1.00	1.00	1.00	1.00	1.00

Weighted Sum-of-Squares							Total
Tonnage	HM	SiO2	Al2O3	TiO2	Fe2O3	ZrO2	WSSQ
0.00	0.00	0.00	0.02	0.00	0.00	0.03	0.05
0.00	0.00	0.00	0.01	0.00	0.00	0.06	0.07
0.00	0.00	0.00	0.00	0.00	0.00	0.00	0.00
							0.12

		Experimental Values							Adjusted Values						
		Tonnage	HM	SiO2	Al2O3	TiO2	Fe2O3	ZrO2	Tonnage	HM	SiO2	Al2O3	TiO2	Fe2O3	ZrO2
Sample 21	**Feed**	95.37	70.50	39.90	13.10	25.40	12.00	6.74	93.73	72.27	36.89	11.92	26.43	12.05	7.87
	Underflow	81.43	86.23	25.50	12.90	31.70	14.20	12.30	79.21	83.99	26.54	13.86	30.34	14.14	9.11
	Overflow	13.94	8.32	90.90	1.33	5.13	0.71	1.16	14.52	8.32	93.32	1.33	5.12	0.71	1.15

Relative Change							Relative Error						
Tonnage	HM	SiO2	Al2O3	TiO2	Fe2O3	ZrO2	Tonnage	HM	SiO2	Al2O3	TiO2	Fe2O3	ZrO2
-1.72	2.51	-7.55	-8.99	4.07	0.46	16.83	1.00	1.00	1.00	1.00	1.00	1.00	1.00
-2.73	-2.59	4.08	7.48	-4.29	-0.46	-25.96	1.00	1.00	1.00	1.00	1.00	1.00	1.00
4.17	-0.05	2.67	0.14	-0.13	0.00	-0.45	1.00	1.00	1.00	1.00	1.00	1.00	1.00

Weighted Sum-of-Squares							Total
Tonnage	HM	SiO2	Al2O3	TiO2	Fe2O3	ZrO2	WSSQ
0.00	0.00	0.01	0.01	0.00	0.00	0.03	0.04
0.00	0.00	0.00	0.01	0.00	0.00	0.07	0.08
0.00	0.00	0.00	0.00	0.00	0.00	0.00	0.00
							0.13

		Experimental Values							Adjusted Values						
		Tonnage	HM	SiO2	Al2O3	TiO2	Fe2O3	ZrO2	Tonnage	HM	SiO2	Al2O3	TiO2	Fe2O3	ZrO2
Sample 22	**Feed**	120.96	77.25	31.80	11.00	29.20	13.50	12.10	120.50	79.15	30.91	10.25	29.56	13.39	12.69
	Underflow	106.00	91.61	21.50	10.90	33.60	15.10	15.20	105.39	89.27	21.86	11.55	33.18	15.23	14.39
	Overflow	14.96	8.54	93.10	1.16	4.35	0.55	0.83	15.10	8.54	94.06	1.16	4.35	0.55	0.83

Relative Change							Relative Error						
Tonnage	HM	SiO2	Al2O3	TiO2	Fe2O3	ZrO2	Tonnage	HM	SiO2	Al2O3	TiO2	Fe2O3	ZrO2
-0.38	2.46	-2.81	-6.86	1.25	-0.85	4.86	1.00	1.00	1.00	1.00	1.00	1.00	1.00
-0.57	-2.55	1.66	5.94	-1.26	0.83	-5.34	1.00	1.00	1.00	1.00	1.00	1.00	1.00
0.94	-0.03	1.03	0.09	-0.02	0.00	-0.04	1.00	1.00	1.00	1.00	1.00	1.00	1.00

Weighted Sum-of-Squares							Total
Tonnage	HM	SiO2	Al2O3	TiO2	Fe2O3	ZrO2	WSSQ
0.00	0.00	0.00	0.00	0.00	0.00	0.00	0.01
0.00	0.00	0.00	0.00	0.00	0.00	0.00	0.01
0.00	0.00	0.00	0.00	0.00	0.00	0.00	0.00
							0.02

		Experimental Values							Adjusted Values						
		Tonnage	HM	SiO2	Al2O3	TiO2	Fe2O3	ZrO2	Tonnage	HM	SiO2	Al2O3	TiO2	Fe2O3	ZrO2
Sample 23	**Feed**	73.32	65.18	43.70	11.80	23.90	11.50	6.27	73.70	64.50	44.70	11.63	23.54	10.71	6.77
	Underflow	55.76	82.66	29.30	14.80	29.70	13.20	9.66	56.13	83.50	28.96	15.00	30.13	14.00	8.76
	Overflow	17.56	3.77	95.00	0.85	2.47	0.19	0.39	17.56	3.77	95.00	0.85	2.47	0.19	0.39

Relative Change							Relative Error						
Tonnage	HM	SiO2	Al2O3	TiO2	Fe2O3	ZrO2	Tonnage	HM	SiO2	Al2O3	TiO2	Fe2O3	ZrO2
0.51	-1.05	2.28	-1.44	-1.52	-6.90	7.92	1.00	1.00	1.00	1.00	1.00	1.00	1.00
0.68	1.01	-1.17	1.37	1.44	6.03	-9.30	1.00	1.00	1.00	1.00	1.00	1.00	1.00
0.00	0.00	0.00	0.00	0.00	0.00	0.00	1.00	1.00	1.00	1.00	1.00	1.00	1.00

Weighted Sum-of-Squares							Total
Tonnage	HM	SiO2	Al2O3	TiO2	Fe2O3	ZrO2	WSSQ
0.00	0.00	0.00	0.00	0.00	0.00	0.01	0.01
0.00	0.00	0.00	0.00	0.00	0.00	0.01	0.01
0.00	0.00	0.00	0.00	0.00	0.00	0.00	0.00
							0.03

		Experimental Values							Adjusted Values						
		Tonnage	HM	SiO2	Al2O3	TiO2	Fe2O3	ZrO2	Tonnage	HM	SiO2	Al2O3	TiO2	Fe2O3	ZrO2
Sample 24	**Feed**	112.72	74.46	34.30	11.40	28.50	13.10	8.85	112.63	75.12	34.79	11.08	28.33	12.60	9.67
	Underflow	97.00	87.33	25.40	12.40	32.30	14.10	12.60	96.87	86.54	25.17	12.72	32.49	14.60	11.17
	Overflow	15.72	4.90	94.50	0.98	2.78	0.33	0.48	15.75	4.90	93.98	0.98	2.78	0.33	0.48

Relative Change							Relative Error						
Tonnage	HM	SiO2	Al2O3	TiO2	Fe2O3	ZrO2	Tonnage	HM	SiO2	Al2O3	TiO2	Fe2O3	ZrO2
-0.08	0.89	1.44	-2.79	-0.59	-3.81	9.29	1.00	1.00	1.00	1.00	1.00	1.00	1.00
-0.13	-0.90	-0.91	2.61	0.58	3.52	-11.37	1.00	1.00	1.00	1.00	1.00	1.00	1.00
0.21	-0.01	-0.55	0.03	0.01	0.01	-0.07	1.00	1.00	1.00	1.00	1.00	1.00	1.00

Weighted Sum-of-Squares							Total
Tonnage	HM	SiO2	Al2O3	TiO2	Fe2O3	ZrO2	WSSQ
0.00	0.00	0.00	0.00	0.00	0.00	0.01	0.01
0.00	0.00	0.00	0.00	0.00	0.00	0.01	0.02
0.00	0.00	0.00	0.00	0.00	0.00	0.00	0.00
							0.03

		Experimental Values							Adjusted Values						
		Tonnage	HM	SiO2	Al2O3	TiO2	Fe2O3	ZrO2	Tonnage	HM	SiO2	Al2O3	TiO2	Fe2O3	ZrO2
Sample 25	**Feed**	90.35	76.60	39.10	10.60	27.30	12.10	7.62	86.84	81.91	25.07	11.26	30.05	12.96	9.03
	Underflow	85.11	95.04	17.30	12.90	36.60	15.10	14.30	81.21	87.39	19.87	11.99	31.98	13.85	9.64
	Overflow	5.24	2.84	97.00	0.68	2.14	0.13	0.28	5.63	2.84	100.00	0.68	2.14	0.13	0.28

Relative Change							Relative Error						
Tonnage	HM	SiO2	Al2O3	TiO2	Fe2O3	ZrO2	Tonnage	HM	SiO2	Al2O3	TiO2	Fe2O3	ZrO2
-3.88	6.93	-35.89	6.20	10.06	7.10	18.56	1.00	1.00	1.00	1.00	1.00	1.00	1.00
-4.58	-8.04	14.85	-7.05	-12.62	-8.29	-32.58	1.00	1.00	1.00	1.00	1.00	1.00	1.00
7.54	-0.02	3.09	-0.03	-0.05	0.00	-0.04	1.00	1.00	1.00	1.00	1.00	1.00	1.00

Weighted Sum-of-Squares							Total
Tonnage	HM	SiO2	Al2O3	TiO2	Fe2O3	ZrO2	WSSQ
0.00	0.00	0.13	0.00	0.01	0.01	0.03	0.19
0.00	0.01	0.02	0.00	0.02	0.01	0.11	0.16
0.01	0.00	0.00	0.00	0.00	0.00	0.00	0.01
							0.36

		Experimental Values							Adjusted Values						
		Tonnage	HM	SiO2	Al2O3	TiO2	Fe2O3	ZrO2	Tonnage	HM	SiO2	Al2O3	TiO2	Fe2O3	ZrO2
Sample 26	**Feed**	138.25	67.86	39.50	10.00	26.30	11.50	9.43	133.76	71.45	35.08	10.72	28.02	11.68	9.47
	Underflow	112.63	94.39	17.60	14.40	37.20	14.90	11.90	106.10	88.88	18.30	13.22	34.47	14.67	11.84
	Overflow	25.61	4.56	94.30	1.15	3.28	0.21	0.38	27.65	4.56	99.50	1.15	3.27	0.21	0.38

Relative Change							Relative Error						
Tonnage	HM	SiO2	Al2O3	TiO2	Fe2O3	ZrO2	Tonnage	HM	SiO2	Al2O3	TiO2	Fe2O3	ZrO2
-3.25	5.29	-11.18	7.20	6.54	1.53	0.47	1.00	1.00	1.00	1.00	1.00	1.00	1.00
-5.80	-5.83	3.95	-8.23	-7.34	-1.58	-0.47	1.00	1.00	1.00	1.00	1.00	1.00	1.00
7.97	-0.07	5.52	-0.17	-0.17	-0.01	0.00	1.00	1.00	1.00	1.00	1.00	1.00	1.00

Weighted Sum-of-Squares							Total
Tonnage	HM	SiO2	Al2O3	TiO2	Fe2O3	ZrO2	WSSQ
0.00	0.00	0.01	0.01	0.00	0.00	0.00	0.03
0.00	0.00	0.00	0.01	0.01	0.00	0.00	0.02
0.01	0.00	0.00	0.00	0.00	0.00	0.00	0.01
							0.06

		Experimental Values							Adjusted Values						
		Tonnage	HM	SiO2	Al2O3	TiO2	Fe2O3	ZrO2	Tonnage	HM	SiO2	Al2O3	TiO2	Fe2O3	ZrO2
Sample 27	**Feed**	77.75	60.79	53.30	9.65	21.20	9.58	4.13	77.92	58.53	52.20	7.62	20.76	8.36	5.00
	Underflow	45.83	90.93	22.70	10.50	31.90	12.50	19.00	46.72	93.96	22.82	11.94	32.49	13.74	7.99
	Overflow	31.92	5.47	94.80	1.13	3.19	0.31	0.53	31.20	5.48	96.20	1.14	3.20	0.31	0.52

Relative Change							Relative Error						
Tonnage	HM	SiO2	Al2O3	TiO2	Fe2O3	ZrO2	Tonnage	HM	SiO2	Al2O3	TiO2	Fe2O3	ZrO2
0.22	-3.71	-2.07	-21.06	-2.06	-12.69	21.02	1.00	1.00	1.00	1.00	1.00	1.00	1.00
1.94	3.33	0.53	13.74	1.86	9.93	-57.97	1.00	1.00	1.00	1.00	1.00	1.00	1.00
-2.25	0.13	1.47	0.99	0.12	0.16	-1.08	1.00	1.00	1.00	1.00	1.00	1.00	1.00

Weighted Sum-of-Squares							Total
Tonnage	HM	SiO2	Al2O3	TiO2	Fe2O3	ZrO2	WSSQ
0.00	0.00	0.00	0.04	0.00	0.02	0.04	0.11
0.00	0.00	0.00	0.02	0.00	0.01	0.34	0.37
0.00	0.00	0.00	0.00	0.00	0.00	0.00	0.00
							0.47

		Experimental Values							Adjusted Values						
		Tonnage	HM	SiO2	Al2O3	TiO2	Fe2O3	ZrO2	Tonnage	HM	SiO2	Al2O3	TiO2	Fe2O3	ZrO2
Sample 28	**Feed**	121.21	71.65	37.90	10.00	27.70	11.70	10.20	119.66	72.87	36.02	10.21	27.92	11.56	10.80
	Underflow	96.86	91.98	20.30	12.80	34.40	14.30	14.40	94.45	90.40	20.73	12.53	34.14	14.46	13.45
	Overflow	24.35	7.19	91.00	1.55	4.61	0.71	0.88	25.21	7.19	93.29	1.55	4.61	0.71	0.88

Relative Change							Relative Error						
Tonnage	HM	SiO2	Al2O3	TiO2	Fe2O3	ZrO2	Tonnage	HM	SiO2	Al2O3	TiO2	Fe2O3	ZrO2
-1.27	1.70	-4.97	2.12	0.78	-1.17	5.91	1.00	1.00	1.00	1.00	1.00	1.00	1.00
-2.49	-1.72	2.10	-2.15	-0.76	1.12	-6.58	1.00	1.00	1.00	1.00	1.00	1.00	1.00
3.56	-0.04	2.52	-0.07	-0.03	0.01	-0.11	1.00	1.00	1.00	1.00	1.00	1.00	1.00

Weighted Sum-of-Squares							Total
Tonnage	HM	SiO2	Al2O3	TiO2	Fe2O3	ZrO2	WSSQ
0.00	0.00	0.00	0.00	0.00	0.00	0.00	0.01
0.00	0.00	0.00	0.00	0.00	0.00	0.00	0.01
0.00	0.00	0.00	0.00	0.00	0.00	0.00	0.00
							0.02

		Experimental Values							Adjusted Values						
		Tonnage	HM	SiO2	Al2O3	TiO2	Fe2O3	ZrO2	Tonnage	HM	SiO2	Al2O3	TiO2	Fe2O3	ZrO2
Sample 29	**Feed**	95.72	69.91	38.00	9.97	26.70	12.10	9.50	95.79	69.94	38.34	10.13	26.65	12.13	9.34
	Underflow	83.55	79.92	30.30	11.70	30.20	13.90	10.50	83.63	79.88	30.11	11.51	30.25	13.86	10.67
	Overflow	12.17	1.51	95.30	0.67	1.85	0.25	0.19	12.15	1.51	95.02	0.67	1.85	0.25	0.19

Relative Change							Relative Error						
Tonnage	HM	SiO2	Al2O3	TiO2	Fe2O3	ZrO2	Tonnage	HM	SiO2	Al2O3	TiO2	Fe2O3	ZrO2
0.07	0.04	0.91	1.62	-0.18	0.28	-1.68	1.00	1.00	1.00	1.00	1.00	1.00	1.00
0.10	-0.04	-0.63	-1.66	0.18	-0.28	1.62	1.00	1.00	1.00	1.00	1.00	1.00	1.00
-0.17	0.00	-0.29	-0.01	0.00	0.00	0.00	1.00	1.00	1.00	1.00	1.00	1.00	1.00

Weighted Sum-of-Squares							Total
Tonnage	HM	SiO2	Al2O3	TiO2	Fe2O3	ZrO2	WSSQ
0.00	0.00	0.00	0.00	0.00	0.00	0.00	0.00
0.00	0.00	0.00	0.00	0.00	0.00	0.00	0.00
0.00	0.00	0.00	0.00	0.00	0.00	0.00	0.00
							0.00

		Experimental Values							Adjusted Values						
		Tonnage	HM	SiO2	Al2O3	TiO2	Fe2O3	ZrO2	Tonnage	HM	SiO2	Al2O3	TiO2	Fe2O3	ZrO2
Sample 30	**Feed**	85.21	72.59	36.20	11.50	27.80	12.10	9.36	84.87	75.03	35.14	11.18	28.79	11.99	9.71
	Underflow	79.11	83.15	29.70	11.70	32.10	12.80	10.90	78.71	80.18	30.36	12.00	30.87	12.91	10.45
	Overflow	6.10	9.12	95.70	0.69	2.14	0.21	0.24	6.15	9.12	96.24	0.69	2.14	0.21	0.24

Relative Change							Relative Error						
Tonnage	HM	SiO2	Al2O3	TiO2	Fe2O3	ZrO2	Tonnage	HM	SiO2	Al2O3	TiO2	Fe2O3	ZrO2
-0.40	3.36	-2.93	-2.75	3.57	-0.90	3.78	1.00	1.00	1.00	1.00	1.00	1.00	1.00
-0.50	-3.57	2.23	2.60	-3.82	0.88	-4.09	1.00	1.00	1.00	1.00	1.00	1.00	1.00
0.88	-0.03	0.56	0.01	-0.02	0.00	-0.01	1.00	1.00	1.00	1.00	1.00	1.00	1.00

Weighted Sum-of-Squares							Total
Tonnage	HM	SiO2	Al2O3	TiO2	Fe2O3	ZrO2	WSSQ
0.00	0.00	0.00	0.00	0.00	0.00	0.00	0.01
0.00	0.00	0.00	0.00	0.00	0.00	0.00	0.01
0.00	0.00	0.00	0.00	0.00	0.00	0.00	0.00
							0.01

		Experimental Values							Adjusted Values						
		Tonnage	HM	SiO2	Al2O3	TiO2	Fe2O3	ZrO2	Tonnage	HM	SiO2	Al2O3	TiO2	Fe2O3	ZrO2
Sample 31	**Feed**	85.91	73.48	37.70	10.90	27.70	11.50	9.68	85.73	74.15	36.37	11.07	28.21	11.61	9.96
	Underflow	83.25	77.22	33.50	11.60	29.60	12.10	10.60	83.06	76.50	34.51	11.41	29.04	11.98	10.27
	Overflow	2.66	1.00	93.90	0.69	2.44	0.27	0.33	2.67	1.00	94.16	0.69	2.44	0.27	0.33

Relative Change							Relative Error						
Tonnage	HM	SiO2	Al2O3	TiO2	Fe2O3	ZrO2	Tonnage	HM	SiO2	Al2O3	TiO2	Fe2O3	ZrO2
-0.20	0.91	-3.52	1.60	1.84	0.99	2.92	1.00	1.00	1.00	1.00	1.00	1.00	1.00
-0.22	-0.93	3.03	-1.65	-1.90	-1.01	-3.09	1.00	1.00	1.00	1.00	1.00	1.00	1.00
0.42	0.00	0.27	0.00	-0.01	0.00	0.00	1.00	1.00	1.00	1.00	1.00	1.00	1.00

Weighted Sum-of-Squares							Total
Tonnage	HM	SiO2	Al2O3	TiO2	Fe2O3	ZrO2	WSSQ
0.00	0.00	0.00	0.00	0.00	0.00	0.00	0.00
0.00	0.00	0.00	0.00	0.00	0.00	0.00	0.00
0.00	0.00	0.00	0.00	0.00	0.00	0.00	0.00
							0.01

		Experimental Values							Adjusted Values						
		Tonnage	HM	SiO2	Al2O3	TiO2	Fe2O3	ZrO2	Tonnage	HM	SiO2	Al2O3	TiO2	Fe2O3	ZrO2
Sample 32	**Feed**	94.39	75.49	35.20	12.60	28.10	12.90	8.51	94.11	75.68	34.43	12.24	28.43	12.69	8.97
	Underflow	84.92	83.70	26.90	13.20	31.80	13.90	10.60	84.57	83.49	27.30	13.55	31.42	14.11	9.96
	Overflow	9.47	6.37	97.10	0.61	1.89	0.11	0.24	9.54	6.37	97.69	0.61	1.89	0.11	0.24

Relative Change							Relative Error						
Tonnage	HM	SiO2	Al2O3	TiO2	Fe2O3	ZrO2	Tonnage	HM	SiO2	Al2O3	TiO2	Fe2O3	ZrO2
-0.30	0.25	-2.17	-2.84	1.17	-1.59	5.43	1.00	1.00	1.00	1.00	1.00	1.00	1.00
-0.41	-0.25	1.49	2.68	-1.19	1.54	-6.07	1.00	1.00	1.00	1.00	1.00	1.00	1.00
0.70	0.00	0.61	0.01	-0.01	0.00	-0.02	1.00	1.00	1.00	1.00	1.00	1.00	1.00

Weighted Sum-of-Squares							Total
Tonnage	HM	SiO2	Al2O3	TiO2	Fe2O3	ZrO2	WSSQ
0.00	0.00	0.00	0.00	0.00	0.00	0.00	0.00
0.00	0.00	0.00	0.00	0.00	0.00	0.00	0.01
0.00	0.00	0.00	0.00	0.00	0.00	0.00	0.00
							0.01

		Experimental Values							Adjusted Values						
		Tonnage	HM	SiO2	Al2O3	TiO2	Fe2O3	ZrO2	Tonnage	HM	SiO2	Al2O3	TiO2	Fe2O3	ZrO2
Sample 33	**Feed**	96.45	61.10	50.10	10.80	21.30	9.87	4.85	96.19	61.54	50.40	9.64	21.51	9.15	5.67
	Underflow	61.58	89.94	24.70	13.50	32.60	13.50	11.80	60.79	89.34	24.65	14.65	32.30	14.36	8.73
	Overflow	34.87	13.80	95.00	1.02	2.98	0.20	0.43	35.40	13.79	94.60	1.02	2.98	0.20	0.43

Relative Change							Relative Error						
Tonnage	HM	SiO2	Al2O3	TiO2	Fe2O3	ZrO2	Tonnage	HM	SiO2	Al2O3	TiO2	Fe2O3	ZrO2
-0.27	0.71	0.60	-10.79	0.97	-7.34	16.94	1.00	1.00	1.00	1.00	1.00	1.00	1.00
-1.29	-0.66	-0.19	8.52	-0.93	6.34	-26.05	1.00	1.00	1.00	1.00	1.00	1.00	1.00
1.53	-0.06	-0.42	0.37	-0.05	0.05	-0.55	1.00	1.00	1.00	1.00	1.00	1.00	1.00

Weighted Sum-of-Squares							Total
Tonnage	HM	SiO2	Al2O3	TiO2	Fe2O3	ZrO2	WSSQ
0.00	0.00	0.00	0.01	0.00	0.01	0.03	0.05
0.00	0.00	0.00	0.01	0.00	0.00	0.07	0.08
0.00	0.00	0.00	0.00	0.00	0.00	0.00	0.00
							0.13

		Estimated Values							Calculated Values						
		Tonnage	HM	SiO2	Al2O3	TiO2	Fe2O3	ZrO2	Tonnage	HM	SiO2	Al2O3	TiO2	Fe2O3	ZrO2
Sample 34	**Feed**	130.43	84.76	30.20	11.50	30.50	14.00	10.70	131.39	83.83	31.59	12.25	30.48	13.84	8.02
	Underflow	121.05	88.17	27.90	14.20	32.60	14.70	7.41	122.18	89.11	26.80	13.13	32.62	14.87	8.60
	Overflow	9.38	13.76	96.10	0.66	2.16	0.23	0.27	9.22	13.76	95.11	0.66	2.16	0.23	0.27

Relative Change							Relative Error						
Tonnage	HM	SiO2	Al2O3	TiO2	Fe2O3	ZrO2	Tonnage	HM	SiO2	Al2O3	TiO2	Fe2O3	ZrO2
0.74	-1.10	4.60	6.57	-0.06	-1.15	-25.04	1.00	1.00	1.00	1.00	1.00	1.00	1.00
0.93	1.07	-3.95	-7.54	0.06	1.12	16.13	1.00	1.00	1.00	1.00	1.00	1.00	1.00
-1.71	0.01	-1.03	-0.03	0.00	0.00	0.04	1.00	1.00	1.00	1.00	1.00	1.00	1.00

Weighted Sum-of-Squares							Total
Tonnage	HM	SiO2	Al2O3	TiO2	Fe2O3	ZrO2	WSSQ
0.00	0.00	0.00	0.00	0.00	0.00	0.06	0.07
0.00	0.00	0.00	0.01	0.00	0.00	0.03	0.03
0.00	0.00	0.00	0.00	0.00	0.00	0.00	0.00
							0.10

		Estimated Values							Calculated Values						
		Tonnage	HM	SiO2	Al2O3	TiO2	Fe2O3	ZrO2	Tonnage	HM	SiO2	Al2O3	TiO2	Fe2O3	ZrO2
Sample 35	**Feed**	133.63	77.13	35.80	11.80	28.20	12.40	8.95	133.00	77.58	33.98	11.50	29.37	12.50	9.41
	Underflow	125.47	82.71	28.90	11.90	32.50	13.40	10.60	124.75	82.22	30.01	12.19	31.04	13.29	9.99
	Overflow	8.16	7.45	93.30	1.12	4.20	0.58	0.70	8.25	7.45	94.07	1.12	4.20	0.58	0.70

Relative Change							Relative Error						
Tonnage	HM	SiO2	Al2O3	TiO2	Fe2O3	ZrO2	Tonnage	HM	SiO2	Al2O3	TiO2	Fe2O3	ZrO2
-0.48	0.59	-5.08	-2.54	4.16	0.82	5.18	1.00	1.00	1.00	1.00	1.00	1.00	1.00
-0.57	-0.59	3.84	2.41	-4.50	-0.83	-5.76	1.00	1.00	1.00	1.00	1.00	1.00	1.00
1.03	0.00	0.82	0.01	-0.04	0.00	-0.03	1.00	1.00	1.00	1.00	1.00	1.00	1.00

Weighted Sum-of-Squares							Total
Tonnage	HM	SiO2	Al2O3	TiO2	Fe2O3	ZrO2	WSSQ
0.00	0.00	0.00	0.00	0.00	0.00	0.00	0.01
0.00	0.00	0.00	0.00	0.00	0.00	0.00	0.01
0.00	0.00	0.00	0.00	0.00	0.00	0.00	0.00
							0.02

		Estimated Values							Calculated Values						
		Tonnage	HM	SiO2	Al2O3	TiO2	Fe2O3	ZrO2	Tonnage	HM	SiO2	Al2O3	TiO2	Fe2O3	ZrO2
Sample 36	**Feed**	102.47	74.90	36.10	12.50	27.80	13.20	7.91	102.90	73.90	36.74	12.55	27.55	12.75	7.66
	Underflow	92.42	79.53	31.50	13.80	29.60	13.60	8.16	92.95	80.54	31.06	13.74	29.86	14.03	8.40
	Overflow	10.05	11.87	90.20	1.49	5.95	0.81	0.83	9.95	11.87	89.81	1.49	5.95	0.81	0.83

Relative Change							Relative Error						
Tonnage	HM	SiO2	Al2O3	TiO2	Fe2O3	ZrO2	Tonnage	HM	SiO2	Al2O3	TiO2	Fe2O3	ZrO2
0.41	-1.33	1.77	0.44	-0.91	-3.40	-3.10	1.00	1.00	1.00	1.00	1.00	1.00	1.00
0.57	1.28	-1.40	-0.44	0.88	3.16	2.89	1.00	1.00	1.00	1.00	1.00	1.00	1.00
-1.00	0.02	-0.43	-0.01	0.02	0.02	0.03	1.00	1.00	1.00	1.00	1.00	1.00	1.00

Weighted Sum-of-Squares							Total
Tonnage	HM	SiO2	Al2O3	TiO2	Fe2O3	ZrO2	WSSQ
0.00	0.00	0.00	0.00	0.00	0.00	0.00	0.00
0.00	0.00	0.00	0.00	0.00	0.00	0.00	0.00
0.00	0.00	0.00	0.00	0.00	0.00	0.00	0.00
							0.01

		Estimated Values							Calculated Values						
		Tonnage	HM	SiO2	Al2O3	TiO2	Fe2O3	ZrO2	Tonnage	HM	SiO2	Al2O3	TiO2	Fe2O3	ZrO2
Sample 37	**Feed**	86.77	51.32	56.30	9.42	18.30	7.89	4.31	85.36	52.44	55.14	8.93	18.67	7.72	5.20
	Underflow	51.35	90.97	22.50	14.70	31.80	13.60	14.00	46.80	89.04	22.60	15.36	31.18	13.88	8.84
	Overflow	35.42	8.04	93.20	1.12	3.49	0.23	0.80	38.56	8.03	94.63	1.12	3.48	0.23	0.79

Relative Change							Relative Error						
Tonnage	HM	SiO2	Al2O3	TiO2	Fe2O3	ZrO2	Tonnage	HM	SiO2	Al2O3	TiO2	Fe2O3	ZrO2
-1.62	2.19	-2.06	-5.23	2.03	-2.21	20.69	1.00	1.00	1.00	1.00	1.00	1.00	1.00
-8.86	-2.13	0.45	4.47	-1.93	2.08	-36.86	1.00	1.00	1.00	1.00	1.00	1.00	1.00
8.88	-0.15	1.54	0.28	-0.17	0.03	-1.74	1.00	1.00	1.00	1.00	1.00	1.00	1.00

Weighted Sum-of-Squares							Total
Tonnage	HM	SiO2	Al2O3	TiO2	Fe2O3	ZrO2	WSSQ
0.00	0.00	0.00	0.00	0.00	0.00	0.04	0.05
0.01	0.00	0.00	0.00	0.00	0.00	0.14	0.15
0.01	0.00	0.00	0.00	0.00	0.00	0.00	0.01
							0.20

		Estimated Values							Calculated Values						
		Tonnage	HM	SiO2	Al2O3	TiO2	Fe2O3	ZrO2	Tonnage	HM	SiO2	Al2O3	TiO2	Fe2O3	ZrO2
Sample 38	**Feed**	96.07	72.83	38.70	10.90	26.70	11.10	9.21	93.75	75.69	33.18	10.42	27.71	11.37	10.80
	Underflow	86.80	87.80	23.60	11.10	32.00	13.00	16.70	84.00	84.08	25.44	11.55	30.70	12.67	12.03
	Overflow	9.27	3.46	96.30	0.65	1.96	0.21	0.19	9.75	3.46	99.86	0.65	1.95	0.21	0.19

Relative Change							Relative Error						
Tonnage	HM	SiO2	Al2O3	TiO2	Fe2O3	ZrO2	Tonnage	HM	SiO2	Al2O3	TiO2	Fe2O3	ZrO2
-2.42	3.93	-14.26	-4.44	3.78	2.44	17.22	1.00	1.00	1.00	1.00	1.00	1.00	1.00
-3.24	-4.24	7.79	4.05	-4.06	-2.56	-27.98	1.00	1.00	1.00	1.00	1.00	1.00	1.00
5.22	-0.02	3.69	0.03	-0.03	0.00	-0.04	1.00	1.00	1.00	1.00	1.00	1.00	1.00

Weighted Sum-of-Squares							Total
Tonnage	HM	SiO2	Al2O3	TiO2	Fe2O3	ZrO2	WSSQ
0.00	0.00	0.02	0.00	0.00	0.00	0.03	0.06
0.00	0.00	0.01	0.00	0.00	0.00	0.08	0.09
0.00	0.00	0.00	0.00	0.00	0.00	0.00	0.00
							0.15

		Estimated Values							Calculated Values						
		Tonnage	HM	SiO2	Al2O3	TiO2	Fe2O3	ZrO2	Tonnage	HM	SiO2	Al2O3	TiO2	Fe2O3	ZrO2
Sample 39	**Feed**	87.71	65.37	43.10	9.90	24.30	10.70	8.73	88.19	64.83	44.72	9.21	23.78	9.84	9.65
	Underflow	59.40	88.12	23.00	12.20	32.70	13.30	16.10	60.68	88.80	22.68	12.92	33.34	14.21	13.94
	Overflow	28.32	11.94	95.80	1.01	2.69	0.21	0.20	27.51	11.95	93.31	1.01	2.69	0.21	0.20

Relative Change							Relative Error						
Tonnage	HM	SiO2	Al2O3	TiO2	Fe2O3	ZrO2	Tonnage	HM	SiO2	Al2O3	TiO2	Fe2O3	ZrO2
0.55	-0.83	3.75	-6.99	-2.13	-8.01	10.58	1.00	1.00	1.00	1.00	1.00	1.00	1.00
2.16	0.77	-1.38	5.93	1.97	6.85	-13.42	1.00	1.00	1.00	1.00	1.00	1.00	1.00
-2.84	0.05	-2.60	0.22	0.07	0.05	-0.08	1.00	1.00	1.00	1.00	1.00	1.00	1.00

Weighted Sum-of-Squares							Total
Tonnage	HM	SiO2	Al2O3	TiO2	Fe2O3	ZrO2	WSSQ
0.00	0.00	0.00	0.00	0.00	0.01	0.01	0.02
0.00	0.00	0.00	0.00	0.00	0.00	0.02	0.03
0.00	0.00	0.00	0.00	0.00	0.00	0.00	0.00
							0.05

		Estimated Values							Calculated Values						
		Tonnage	HM	SiO2	Al2O3	TiO2	Fe2O3	ZrO2	Tonnage	HM	SiO2	Al2O3	TiO2	Fe2O3	ZrO2
Sample 40	**Feed**	143.89	78.46	33.20	10.40	28.10	12.70	2.92	145.07	76.65	34.24	10.09	27.93	12.35	2.65
	Underflow	117.20	90.32	22.30	11.80	33.20	14.60	2.46	119.05	92.29	21.91	12.12	33.39	14.98	2.62
	Overflow	26.69	5.06	92.10	0.81	2.93	0.31	2.77	26.02	5.06	90.66	0.81	2.93	0.31	2.81

Relative Change							Relative Error						
Tonnage	HM	SiO2	Al2O3	TiO2	Fe2O3	ZrO2	Tonnage	HM	SiO2	Al2O3	TiO2	Fe2O3	ZrO2
0.82	-2.31	3.15	-2.94	-0.61	-2.76	-9.19	1.00	1.00	1.00	1.00	1.00	1.00	1.00
1.58	2.19	-1.73	2.74	0.59	2.61	6.35	1.00	1.00	1.00	1.00	1.00	1.00	1.00
-2.50	0.03	-1.57	0.04	0.01	0.01	1.56	1.00	1.00	1.00	1.00	1.00	1.00	1.00

Weighted Sum-of-Squares							Total
Tonnage	HM	SiO2	Al2O3	TiO2	Fe2O3	ZrO2	WSSQ
0.00	0.00	0.00	0.00	0.00	0.00	0.01	0.01
0.00	0.00	0.00	0.00	0.00	0.00	0.00	0.01
0.00	0.00	0.00	0.00	0.00	0.00	0.00	0.00
							0.02

		Estimated Values							Calculated Values						
		Tonnage	HM	SiO2	Al2O3	TiO2	Fe2O3	ZrO2	Tonnage	HM	SiO2	Al2O3	TiO2	Fe2O3	ZrO2
Sample 41	**Feed**	87.71	75.78	35.20	10.90	28.90	12.60	1.54	87.46	79.09	30.99	10.68	29.86	12.51	1.84
	Underflow	85.78	84.86	27.10	10.70	31.60	12.70	2.77	85.52	80.80	29.54	10.90	30.48	12.79	1.84
	Overflow	1.93	4.13	94.30	0.98	2.46	0.41	1.85	1.94	4.13	94.97	0.98	2.46	0.41	1.84

Relative Change							Relative Error						
Tonnage	HM	SiO2	Al2O3	TiO2	Fe2O3	ZrO2	Tonnage	HM	SiO2	Al2O3	TiO2	Fe2O3	ZrO2
-0.29	4.37	-11.96	-1.99	3.31	-0.70	19.19	1.00	1.00	1.00	1.00	1.00	1.00	1.00
-0.31	-4.79	9.00	1.91	-3.54	0.69	-33.74	1.00	1.00	1.00	1.00	1.00	1.00	1.00
0.60	-0.01	0.71	0.00	-0.01	0.00	-0.51	1.00	1.00	1.00	1.00	1.00	1.00	1.00

Weighted Sum-of-Squares							Total
Tonnage	HM	SiO2	Al2O3	TiO2	Fe2O3	ZrO2	WSSQ
0.00	0.00	0.01	0.00	0.00	0.00	0.04	0.05
0.00	0.00	0.01	0.00	0.00	0.00	0.11	0.13
0.00	0.00	0.00	0.00	0.00	0.00	0.00	0.00
							0.18

		Estimated Values							Calculated Values						
		Tonnage	HM	SiO2	Al2O3	TiO2	Fe2O3	ZrO2	Tonnage	HM	SiO2	Al2O3	TiO2	Fe2O3	ZrO2
Sample 42	**Feed**	84.03	45.20	61.80	8.03	16.70	7.04	1.23	84.05	47.08	60.85	7.84	16.69	6.69	1.20
	Underflow	43.63	86.32	29.20	13.60	29.10	12.00	1.69	44.28	82.72	29.31	13.89	29.11	12.53	1.72
	Overflow	40.40	7.43	94.90	1.09	2.87	0.20	0.62	39.78	7.41	95.96	1.09	2.87	0.20	0.62

Relative Change							Relative Error						
Tonnage	HM	SiO2	Al2O3	TiO2	Fe2O3	ZrO2	Tonnage	HM	SiO2	Al2O3	TiO2	Fe2O3	ZrO2
0.02	4.15	-1.53	-2.42	-0.04	-4.91	-2.38	1.00	1.00	1.00	1.00	1.00	1.00	1.00
1.48	-4.18	0.38	2.16	0.03	4.41	1.73	1.00	1.00	1.00	1.00	1.00	1.00	1.00
-1.55	-0.32	1.12	0.16	0.00	0.07	0.57	1.00	1.00	1.00	1.00	1.00	1.00	1.00

Weighted Sum-of-Squares							Total
Tonnage	HM	SiO2	Al2O3	TiO2	Fe2O3	ZrO2	WSSQ
0.00	0.00	0.00	0.00	0.00	0.00	0.00	0.01
0.00	0.00	0.00	0.00	0.00	0.00	0.00	0.00
0.00	0.00	0.00	0.00	0.00	0.00	0.00	0.00
							0.01

		Estimated Values							Calculated Values						
		Tonnage	HM	SiO2	Al2O3	TiO2	Fe2O3	ZrO2	Tonnage	HM	SiO2	Al2O3	TiO2	Fe2O3	ZrO2
Sample 43	**Feed**	69.66	49.85	58.30	8.73	18.30	8.24	0.77	67.96	53.35	53.75	7.97	19.55	8.07	0.92
	Underflow	43.72	93.31	20.60	12.10	33.40	13.40	1.85	39.34	86.22	20.93	12.94	30.99	13.66	1.36
	Overflow	25.94	8.19	93.90	1.14	3.84	0.38	0.31	28.62	8.15	98.87	1.15	3.82	0.38	0.30

Relative Change							Relative Error						
Tonnage	HM	SiO2	Al2O3	TiO2	Fe2O3	ZrO2	Tonnage	HM	SiO2	Al2O3	TiO2	Fe2O3	ZrO2
-2.44	7.01	-7.80	-8.66	6.83	-2.08	18.91	1.00	1.00	1.00	1.00	1.00	1.00	1.00
-10.01	-7.60	1.60	6.95	-7.21	1.95	-26.30	1.00	1.00	1.00	1.00	1.00	1.00	1.00
10.32	-0.49	5.29	0.48	-0.60	0.04	-3.21	1.00	1.00	1.00	1.00	1.00	1.00	1.00

Weighted Sum-of-Squares							Total
Tonnage	HM	SiO2	Al2O3	TiO2	Fe2O3	ZrO2	WSSQ
0.00	0.00	0.01	0.01	0.00	0.00	0.04	0.06
0.01	0.01	0.00	0.00	0.01	0.00	0.07	0.10
0.01	0.00	0.00	0.00	0.00	0.00	0.00	0.01
							0.17

		Estimated Values							Calculated Values						
		Tonnage	HM	SiO2	Al2O3	TiO2	Fe2O3	ZrO2	Tonnage	HM	SiO2	Al2O3	TiO2	Fe2O3	ZrO2
Sample 44	**Feed**	55.61	53.34	55.80	11.20	19.00	9.13	2.44	55.59	55.12	54.76	8.77	19.40	8.24	2.91
	Underflow	31.95	92.55	23.50	12.80	32.50	13.20	15.30	31.80	89.48	23.61	14.62	31.83	14.27	4.69
	Overflow	23.67	9.23	95.10	0.94	2.78	0.17	0.54	23.79	9.21	96.40	0.95	2.77	0.17	0.53

Relative Change							Relative Error						
Tonnage	HM	SiO2	Al2O3	TiO2	Fe2O3	ZrO2	Tonnage	HM	SiO2	Al2O3	TiO2	Fe2O3	ZrO2
-0.05	3.35	-1.87	-21.72	2.09	-9.80	19.33	1.00	1.00	1.00	1.00	1.00	1.00	1.00
-0.47	-3.32	0.45	14.20	-2.05	8.10	-69.33	1.00	1.00	1.00	1.00	1.00	1.00	1.00
0.51	-0.25	1.36	0.78	-0.13	0.08	-1.83	1.00	1.00	1.00	1.00	1.00	1.00	1.00

Weighted Sum-of-Squares							Total
Tonnage	HM	SiO2	Al2O3	TiO2	Fe2O3	ZrO2	WSSQ
0.00	0.00	0.00	0.05	0.00	0.01	0.04	0.10
0.00	0.00	0.00	0.02	0.00	0.01	0.48	0.51
0.00	0.00	0.00	0.00	0.00	0.00	0.00	0.00
							0.61

		Estimated Values							Calculated Values						
		Tonnage	HM	SiO2	Al2O3	TiO2	Fe2O3	ZrO2	Tonnage	HM	SiO2	Al2O3	TiO2	Fe2O3	ZrO2
Sample 45	**Feed**	62.34	35.98	71.60	8.45	11.80	5.95	0.13	62.23	39.02	66.83	7.18	13.58	6.08	0.16
	Underflow	25.15	91.70	20.80	14.40	34.40	14.60	12.80	25.48	83.62	20.96	15.91	28.21	14.29	0.00
	Overflow	37.19	8.18	93.80	1.12	3.52	0.38	0.66	36.75	8.09	98.64	1.13	3.43	0.38	0.26

Relative Change							Relative Error						
Tonnage	HM	SiO2	Al2O3	TiO2	Fe2O3	ZrO2	Tonnage	HM	SiO2	Al2O3	TiO2	Fe2O3	ZrO2
-0.17	8.44	-6.66	-14.99	15.07	2.12	20.00	1.00	1.00	1.00	1.00	1.00	1.00	1.00
1.34	-8.81	0.79	10.46	-17.99	-2.13	-100.00	1.00	1.00	1.00	1.00	1.00	1.00	1.00
-1.20	-1.13	5.15	1.17	-2.66	-0.08	-59.97	1.00	1.00	1.00	1.00	1.00	1.00	1.00

Weighted Sum-of-Squares							Total
Tonnage	HM	SiO2	Al2O3	TiO2	Fe2O3	ZrO2	WSSQ
0.00	0.01	0.00	0.02	0.02	0.00	0.04	0.10
0.00	0.01	0.00	0.01	0.03	0.00	1.00	1.05
0.00	0.00	0.00	0.00	0.00	0.00	0.36	0.36
							1.51

		Estimated Values							Calculated Values						
		Tonnage	HM	SiO2	Al2O3	TiO2	Fe2O3	ZrO2	Tonnage	HM	SiO2	Al2O3	TiO2	Fe2O3	ZrO2
Sample 46	**Feed**	60.11	64.98	47.90	11.60	23.90	12.00	2.62	61.22	59.52	53.19	10.40	20.46	9.84	3.06
	Underflow	44.61	67.36	44.90	12.30	23.60	11.30	5.34	46.97	71.86	41.33	13.34	26.18	12.77	3.94
	Overflow	15.51	18.73	97.40	0.70	1.59	0.17	0.14	14.25	18.84	92.31	0.70	1.59	0.17	0.14

Relative Change							Relative Error						
Tonnage	HM	SiO2	Al2O3	TiO2	Fe2O3	ZrO2	Tonnage	HM	SiO2	Al2O3	TiO2	Fe2O3	ZrO2
1.84	-8.40	11.05	-10.37	-14.41	-18.01	16.72	1.00	1.00	1.00	1.00	1.00	1.00	1.00
5.31	6.68	-7.95	8.44	10.92	13.01	-26.16	1.00	1.00	1.00	1.00	1.00	1.00	1.00
-8.13	0.56	-5.23	0.15	0.22	0.06	-0.21	1.00	1.00	1.00	1.00	1.00	1.00	1.00

Weighted Sum-of-Squares							Total
Tonnage	HM	SiO2	Al2O3	TiO2	Fe2O3	ZrO2	WSSQ
0.00	0.01	0.01	0.01	0.02	0.03	0.03	0.11
0.00	0.00	0.01	0.01	0.01	0.02	0.07	0.12
0.01	0.00	0.00	0.00	0.00	0.00	0.00	0.01
							0.24

		Estimated Values							Calculated Values						
		Tonnage	HM	SiO2	Al2O3	TiO2	Fe2O3	ZrO2	Tonnage	HM	SiO2	Al2O3	TiO2	Fe2O3	ZrO2
Sample 47	**Feed**	135.23	66.09	48.30	11.10	22.40	11.00	4.78	128.78	73.49	32.41	12.48	25.42	12.17	5.57
	Underflow	125.08	92.66	22.80	16.30	33.90	15.40	8.13	117.69	79.36	26.04	13.58	27.58	13.30	6.05
	Overflow	10.16	11.24	95.10	0.88	2.53	0.28	0.41	11.10	11.22	100.00	0.88	2.52	0.28	0.41

Relative Change							Relative Error						
Tonnage	HM	SiO2	Al2O3	TiO2	Fe2O3	ZrO2	Tonnage	HM	SiO2	Al2O3	TiO2	Fe2O3	ZrO2
-4.77	11.20	-32.90	12.45	13.48	10.68	16.44	1.00	1.00	1.00	1.00	1.00	1.00	1.00
-5.91	-14.35	14.19	-16.71	-18.65	-13.66	-25.56	1.00	1.00	1.00	1.00	1.00	1.00	1.00
9.24	-0.16	5.15	-0.09	-0.13	-0.02	-0.12	1.00	1.00	1.00	1.00	1.00	1.00	1.00

Weighted Sum-of-Squares							Total
Tonnage	HM	SiO2	Al2O3	TiO2	Fe2O3	ZrO2	WSSQ
0.00	0.01	0.11	0.02	0.02	0.01	0.03	0.20
0.00	0.02	0.02	0.03	0.03	0.02	0.07	0.19
0.01	0.00	0.00	0.00	0.00	0.00	0.00	0.01
							0.40

		Estimated Values							Calculated Values						
		Tonnage	HM	SiO2	Al2O3	TiO2	Fe2O3	ZrO2	Tonnage	HM	SiO2	Al2O3	TiO2	Fe2O3	ZrO2
Sample 48	**Feed**	54.12	52.87	62.80	9.77	16.40	8.15	1.01	51.75	55.83	55.08	9.86	17.83	8.56	1.16
	Underflow	37.61	88.44	28.70	15.10	29.40	14.00	8.74	33.08	83.14	29.73	14.96	26.47	13.22	1.49
	Overflow	16.51	7.48	95.10	0.82	2.53	0.30	0.59	18.67	7.46	100.00	0.82	2.51	0.30	0.57

Relative Change							Relative Error						
Tonnage	HM	SiO2	Al2O3	TiO2	Fe2O3	ZrO2	Tonnage	HM	SiO2	Al2O3	TiO2	Fe2O3	ZrO2
-4.38	5.61	-12.29	0.92	8.70	5.05	14.99	1.00	1.00	1.00	1.00	1.00	1.00	1.00
-12.04	-5.99	3.59	-0.91	-9.97	-5.54	-82.90	1.00	1.00	1.00	1.00	1.00	1.00	1.00
13.07	-0.29	5.15	-0.03	-0.48	-0.07	-3.16	1.00	1.00	1.00	1.00	1.00	1.00	1.00

Weighted Sum-of-Squares							Total
Tonnage	HM	SiO2	Al2O3	TiO2	Fe2O3	ZrO2	WSSQ
0.00	0.00	0.02	0.00	0.01	0.00	0.02	0.05
0.01	0.00	0.00	0.00	0.01	0.00	0.69	0.72
0.02	0.00	0.00	0.00	0.00	0.00	0.00	0.02
							0.79

		Estimated Values							Calculated Values						
		Tonnage	HM	SiO2	Al2O3	TiO2	Fe2O3	ZrO2	Tonnage	HM	SiO2	Al2O3	TiO2	Fe2O3	ZrO2
Sample 49	**Feed**	91.07	71.85	42.40	11.90	23.40	11.20	6.39	90.23	71.14	41.92	11.42	24.11	11.23	7.06
	Underflow	66.94	91.71	22.00	14.80	33.10	15.40	11.00	65.34	92.54	22.09	15.34	32.07	15.36	9.55
	Overflow	24.13	14.97	93.30	1.12	3.25	0.40	0.53	24.89	14.98	93.95	1.12	3.24	0.40	0.53

Relative Change							Relative Error						
Tonnage	HM	SiO2	Al2O3	TiO2	Fe2O3	ZrO2	Tonnage	HM	SiO2	Al2O3	TiO2	Fe2O3	ZrO2
-0.93	-0.98	-1.14	-4.05	3.05	0.28	10.55	1.00	1.00	1.00	1.00	1.00	1.00	1.00
-2.40	0.91	0.43	3.65	-3.12	-0.28	-13.15	1.00	1.00	1.00	1.00	1.00	1.00	1.00
3.16	0.06	0.69	0.11	-0.12	0.00	-0.24	1.00	1.00	1.00	1.00	1.00	1.00	1.00

Weighted Sum-of-Squares							Total
Tonnage	HM	SiO2	Al2O3	TiO2	Fe2O3	ZrO2	WSSQ
0.00	0.00	0.00	0.00	0.00	0.00	0.01	0.01
0.00	0.00	0.00	0.00	0.00	0.00	0.02	0.02
0.00	0.00	0.00	0.00	0.00	0.00	0.00	0.00
							0.04

		Estimated Values							Calculated Values						
		Tonnage	HM	SiO2	Al2O3	TiO2	Fe2O3	ZrO2	Tonnage	HM	SiO2	Al2O3	TiO2	Fe2O3	ZrO2
Sample 50	**Feed**	72.53	60.95	50.00	11.30	21.10	10.70	4.42	70.69	62.60	47.46	11.35	21.51	10.39	5.18
	Underflow	53.47	88.83	26.20	15.70	30.00	14.10	9.83	50.15	86.35	26.69	15.63	29.42	14.48	7.17
	Overflow	19.07	4.59	95.50	0.90	2.19	0.40	0.33	20.53	4.59	98.19	0.90	2.19	0.40	0.33

Relative Change							Relative Error						
Tonnage	HM	SiO2	Al2O3	TiO2	Fe2O3	ZrO2	Tonnage	HM	SiO2	Al2O3	TiO2	Fe2O3	ZrO2
-2.54	2.70	-5.07	0.45	1.93	-2.89	17.18	1.00	1.00	1.00	1.00	1.00	1.00	1.00
-6.20	-2.79	1.89	-0.45	-1.95	2.70	-27.11	1.00	1.00	1.00	1.00	1.00	1.00	1.00
7.70	-0.06	2.82	-0.01	-0.06	0.03	-0.37	1.00	1.00	1.00	1.00	1.00	1.00	1.00

Weighted Sum-of-Squares							Total
Tonnage	HM	SiO2	Al2O3	TiO2	Fe2O3	ZrO2	WSSQ
0.00	0.00	0.00	0.00	0.00	0.00	0.03	0.03
0.00	0.00	0.00	0.00	0.00	0.00	0.07	0.08
0.01	0.00	0.00	0.00	0.00	0.00	0.00	0.01
							0.12

		Estimated Values							Calculated Values						
		Tonnage	HM	SiO2	Al2O3	TiO2	Fe2O3	ZrO2	Tonnage	HM	SiO2	Al2O3	TiO2	Fe2O3	ZrO2
Sample 51	**Feed**	128.27	83.15	31.70	15.00	28.10	13.90	8.35	128.53	82.62	31.95	14.49	28.26	13.76	8.46
	Underflow	113.98	91.75	24.10	15.70	31.70	15.30	9.63	114.32	92.32	23.97	16.19	31.52	15.45	9.49
	Overflow	14.29	4.64	96.30	0.85	2.08	0.23	0.18	14.22	4.64	96.05	0.85	2.08	0.23	0.18

Relative Change							Relative Error						
Tonnage	HM	SiO2	Al2O3	TiO2	Fe2O3	ZrO2	Tonnage	HM	SiO2	Al2O3	TiO2	Fe2O3	ZrO2
0.20	-0.63	0.78	-3.37	0.57	-0.98	1.37	1.00	1.00	1.00	1.00	1.00	1.00	1.00
0.29	0.62	-0.53	3.13	-0.57	0.96	-1.40	1.00	1.00	1.00	1.00	1.00	1.00	1.00
-0.50	0.00	-0.26	0.02	0.00	0.00	0.00	1.00	1.00	1.00	1.00	1.00	1.00	1.00

Weighted Sum-of-Squares							Total
Tonnage	HM	SiO2	Al2O3	TiO2	Fe2O3	ZrO2	WSSQ
0.00	0.00	0.00	0.00	0.00	0.00	0.00	0.00
0.00	0.00	0.00	0.00	0.00	0.00	0.00	0.00
0.00	0.00	0.00	0.00	0.00	0.00	0.00	0.00
							0.00

		Estimated Values							Calculated Values						
		Tonnage	HM	SiO2	Al2O3	TiO2	Fe2O3	ZrO2	Tonnage	HM	SiO2	Al2O3	TiO2	Fe2O3	ZrO2
Sample 52	**Feed**	109.36	77.33	35.30	13.20	27.50	13.10	8.20	108.81	76.89	34.53	12.68	27.63	12.96	8.90
	Underflow	93.50	89.13	23.40	14.20	32.20	15.00	11.60	92.75	89.63	23.69	14.71	32.05	15.16	10.40
	Overflow	15.86	3.34	96.30	0.92	2.15	0.28	0.27	16.06	3.34	97.14	0.92	2.15	0.28	0.27

Relative Change							Relative Error						
Tonnage	HM	SiO2	Al2O3	TiO2	Fe2O3	ZrO2	Tonnage	HM	SiO2	Al2O3	TiO2	Fe2O3	ZrO2
-0.50	-0.57	-2.18	-3.95	0.48	-1.07	8.58	1.00	1.00	1.00	1.00	1.00	1.00	1.00
-0.80	0.56	1.23	3.62	-0.48	1.04	-10.35	1.00	1.00	1.00	1.00	1.00	1.00	1.00
1.28	0.00	0.88	0.04	-0.01	0.00	-0.04	1.00	1.00	1.00	1.00	1.00	1.00	1.00

Weighted Sum-of-Squares							Total
Tonnage	HM	SiO2	Al2O3	TiO2	Fe2O3	ZrO2	WSSQ
0.00	0.00	0.00	0.00	0.00	0.00	0.01	0.01
0.00	0.00	0.00	0.00	0.00	0.00	0.01	0.01
0.00	0.00	0.00	0.00	0.00	0.00	0.00	0.00
							0.02

		Estimated Values							Calculated Values						
		Tonnage	HM	SiO2	Al2O3	TiO2	Fe2O3	ZrO2	Tonnage	HM	SiO2	Al2O3	TiO2	Fe2O3	ZrO2
Sample 53	**Feed**	106.79	67.48	43.00	14.40	22.90	11.90	4.95	104.24	69.83	40.32	12.75	24.09	11.75	5.88
	Underflow	83.65	93.22	21.90	15.00	32.60	15.10	11.30	79.59	89.80	22.43	16.37	30.76	15.28	7.59
	Overflow	23.14	5.32	95.00	1.06	2.52	0.37	0.39	24.64	5.32	98.09	1.06	2.52	0.37	0.39

Relative Change							Relative Error						
Tonnage	HM	SiO2	Al2O3	TiO2	Fe2O3	ZrO2	Tonnage	HM	SiO2	Al2O3	TiO2	Fe2O3	ZrO2
-2.39	3.48	-6.23	-11.46	5.18	-1.22	18.86	1.00	1.00	1.00	1.00	1.00	1.00	1.00
-4.85	-3.67	2.42	9.12	-5.63	1.19	-32.88	1.00	1.00	1.00	1.00	1.00	1.00	1.00
6.52	-0.06	3.26	0.20	-0.13	0.01	-0.35	1.00	1.00	1.00	1.00	1.00	1.00	1.00

Weighted Sum-of-Squares							Total
Tonnage	HM	SiO2	Al2O3	TiO2	Fe2O3	ZrO2	WSSQ
0.00	0.00	0.00	0.01	0.00	0.00	0.04	0.06
0.00	0.00	0.00	0.01	0.00	0.00	0.11	0.12
0.00	0.00	0.00	0.00	0.00	0.00	0.00	0.01
							0.19

		Estimated Values							Calculated Values						
		Tonnage	HM	SiO2	Al2O3	TiO2	Fe2O3	ZrO2	Tonnage	HM	SiO2	Al2O3	TiO2	Fe2O3	ZrO2
Sample 54	**Feed**	96.71	67.81	42.60	11.80	24.40	11.20	6.93	96.13	68.93	42.64	11.07	23.83	10.81	8.03
	Underflow	68.55	91.64	20.60	14.50	31.90	14.80	14.50	67.31	90.21	20.59	15.27	32.59	15.27	11.14
	Overflow	28.16	19.24	94.20	1.25	3.37	0.39	0.75	28.82	19.21	94.14	1.25	3.37	0.39	0.75

Relative Change							Relative Error						
Tonnage	HM	SiO2	Al2O3	TiO2	Fe2O3	ZrO2	Tonnage	HM	SiO2	Al2O3	TiO2	Fe2O3	ZrO2
-0.61	1.65	0.10	-6.19	-2.35	-3.46	15.81	1.00	1.00	1.00	1.00	1.00	1.00	1.00
-1.81	-1.56	-0.03	5.33	2.15	3.21	-23.16	1.00	1.00	1.00	1.00	1.00	1.00	1.00
2.33	-0.14	-0.07	0.20	0.10	0.04	-0.51	1.00	1.00	1.00	1.00	1.00	1.00	1.00

Weighted Sum-of-Squares							Total
Tonnage	HM	SiO2	Al2O3	TiO2	Fe2O3	ZrO2	WSSQ
0.00	0.00	0.00	0.00	0.00	0.00	0.02	0.03
0.00	0.00	0.00	0.00	0.00	0.00	0.05	0.06
0.00	0.00	0.00	0.00	0.00	0.00	0.00	0.00
							0.09

		Estimated Values							Calculated Values						
		Tonnage	HM	SiO2	Al2O3	TiO2	Fe2O3	ZrO2	Tonnage	HM	SiO2	Al2O3	TiO2	Fe2O3	ZrO2
Sample 55	**Feed**	82.03	55.00	55.70	10.70	18.70	9.28	3.42	81.62	53.74	55.69	10.23	18.65	8.72	4.10
	Underflow	47.83	87.92	25.50	16.50	30.30	14.40	10.00	46.13	89.74	25.50	17.13	30.37	15.16	6.73
	Overflow	34.20	6.93	94.90	1.26	3.43	0.35	0.69	35.49	6.94	94.92	1.26	3.43	0.35	0.68

Relative Change							Relative Error						
Tonnage	HM	SiO2	Al2O3	TiO2	Fe2O3	ZrO2	Tonnage	HM	SiO2	Al2O3	TiO2	Fe2O3	ZrO2
-0.50	-2.30	-0.02	-4.39	-0.25	-6.03	19.80	1.00	1.00	1.00	1.00	1.00	1.00	1.00
-3.56	2.08	0.01	3.82	0.23	5.29	-32.72	1.00	1.00	1.00	1.00	1.00	1.00	1.00
3.79	0.13	0.02	0.22	0.02	0.10	-1.74	1.00	1.00	1.00	1.00	1.00	1.00	1.00

Weighted Sum-of-Squares							Total
Tonnage	HM	SiO2	Al2O3	TiO2	Fe2O3	ZrO2	WSSQ
0.00	0.00	0.00	0.00	0.00	0.00	0.04	0.05
0.00	0.00	0.00	0.00	0.00	0.00	0.11	0.11
0.00	0.00	0.00	0.00	0.00	0.00	0.00	0.00
							0.16

		Estimated Values							Calculated Values						
		Tonnage	HM	SiO2	Al2O3	TiO2	Fe2O3	ZrO2	Tonnage	HM	SiO2	Al2O3	TiO2	Fe2O3	ZrO2
Sample 56	**Feed**	124.33	73.68	34.10	12.90	29.50	13.90	6.97	124.94	74.63	35.52	13.56	27.85	13.04	7.24
	Underflow	103.03	89.59	24.40	17.00	31.40	14.80	9.01	103.93	88.43	23.80	16.05	32.95	15.62	8.63
	Overflow	21.30	6.35	95.40	1.20	2.61	0.27	0.35	21.01	6.35	93.53	1.20	2.61	0.27	0.35

Relative Change							Relative Error						
Tonnage	HM	SiO2	Al2O3	TiO2	Fe2O3	ZrO2	Tonnage	HM	SiO2	Al2O3	TiO2	Fe2O3	ZrO2
0.49	1.28	4.16	5.08	-5.59	-6.22	3.89	1.00	1.00	1.00	1.00	1.00	1.00	1.00
0.88	-1.30	-2.48	-5.57	4.95	5.51	-4.18	1.00	1.00	1.00	1.00	1.00	1.00	1.00
-1.39	-0.02	-1.96	-0.08	0.08	0.02	-0.03	1.00	1.00	1.00	1.00	1.00	1.00	1.00

Weighted Sum-of-Squares							Total
Tonnage	HM	SiO2	Al2O3	TiO2	Fe2O3	ZrO2	WSSQ
0.00	0.00	0.00	0.00	0.00	0.00	0.00	0.01
0.00	0.00	0.00	0.00	0.00	0.00	0.00	0.01
0.00	0.00	0.00	0.00	0.00	0.00	0.00	0.00
							0.02

		Estimated Values							Calculated Values						
		Tonnage	HM	SiO2	Al2O3	TiO2	Fe2O3	ZrO2	Tonnage	HM	SiO2	Al2O3	TiO2	Fe2O3	ZrO2
Sample 57	**Feed**	102.21	77.14	40.30	11.70	24.80	11.90	8.33	100.79	77.67	38.17	11.75	25.52	12.09	8.84
	Underflow	84.88	88.92	24.40	14.20	31.60	14.90	11.50	82.84	88.34	25.04	14.14	30.64	14.66	10.70
	Overflow	17.33	28.42	96.60	0.76	1.90	0.21	0.29	17.95	28.41	98.78	0.76	1.89	0.21	0.29

Relative Change							Relative Error						
Tonnage	HM	SiO2	Al2O3	TiO2	Fe2O3	ZrO2	Tonnage	HM	SiO2	Al2O3	TiO2	Fe2O3	ZrO2
-1.39	0.69	-5.28	0.46	2.90	1.57	6.16	1.00	1.00	1.00	1.00	1.00	1.00	1.00
-2.40	-0.65	2.63	-0.46	-3.04	-1.61	-6.99	1.00	1.00	1.00	1.00	1.00	1.00	1.00
3.58	-0.05	2.25	-0.01	-0.04	0.00	-0.04	1.00	1.00	1.00	1.00	1.00	1.00	1.00

Weighted Sum-of-Squares							Total
Tonnage	HM	SiO2	Al2O3	TiO2	Fe2O3	ZrO2	WSSQ
0.00	0.00	0.00	0.00	0.00	0.00	0.00	0.01
0.00	0.00	0.00	0.00	0.00	0.00	0.00	0.01
0.00	0.00	0.00	0.00	0.00	0.00	0.00	0.00
							0.02

		Estimated Values							Calculated Values						
		Tonnage	HM	SiO2	Al2O3	TiO2	Fe2O3	ZrO2	Tonnage	HM	SiO2	Al2O3	TiO2	Fe2O3	ZrO2
Sample 58	**Feed**	91.47	70.35	42.70	12.00	23.70	11.80	6.32	91.27	62.57	42.45	11.13	23.93	11.35	7.29
	Underflow	66.53	71.28	22.20	14.10	32.40	15.00	12.80	66.12	77.07	22.25	14.97	32.08	15.53	9.93
	Overflow	24.95	24.21	95.20	1.05	2.50	0.35	0.34	25.15	24.46	95.55	1.05	2.50	0.35	0.34

Relative Change							Relative Error						
Tonnage	HM	SiO2	Al2O3	TiO2	Fe2O3	ZrO2	Tonnage	HM	SiO2	Al2O3	TiO2	Fe2O3	ZrO2
-0.22	-11.06	-0.59	-7.23	0.98	-3.84	15.29	1.00	1.00	1.00	1.00	1.00	1.00	1.00
-0.61	8.12	0.22	6.15	-0.97	3.54	-22.43	1.00	1.00	1.00	1.00	1.00	1.00	1.00
0.82	1.05	0.36	0.17	-0.03	0.03	-0.23	1.00	1.00	1.00	1.00	1.00	1.00	1.00

Weighted Sum-of-Squares							Total
Tonnage	HM	SiO2	Al2O3	TiO2	Fe2O3	ZrO2	WSSQ
0.00	0.01	0.00	0.01	0.00	0.00	0.02	0.04
0.00	0.01	0.00	0.00	0.00	0.00	0.05	0.06
0.00	0.00	0.00	0.00	0.00	0.00	0.00	0.00
							0.10

		Estimated Values							Calculated Values						
		Tonnage	HM	SiO2	Al2O3	TiO2	Fe2O3	ZrO2	Tonnage	HM	SiO2	Al2O3	TiO2	Fe2O3	ZrO2
Sample 59	**Feed**	90.43	80.12	51.30	9.85	18.30	9.74	6.24	89.68	55.47	49.32	10.59	19.33	9.93	6.54
	Underflow	67.88	57.87	32.00	15.20	27.10	13.40	9.32	66.51	67.41	32.57	13.90	25.43	13.13	8.82
	Overflow	22.56	20.79	95.60	1.10	1.81	0.73	-0.01	23.17	21.22	97.38	1.10	1.80	0.73	0.00

Relative Change							Relative Error						
Tonnage	HM	SiO2	Al2O3	TiO2	Fe2O3	ZrO2	Tonnage	HM	SiO2	Al2O3	TiO2	Fe2O3	ZrO2
-0.83	-30.76	-3.87	7.50	5.61	1.94	4.84	1.00	1.00	1.00	1.00	1.00	1.00	1.00
-2.01	16.48	1.79	-8.58	-6.16	-1.98	-5.36	1.00	1.00	1.00	1.00	1.00	1.00	1.00
2.72	2.06	1.86	-0.22	-0.14	-0.04	-100.00	1.00	1.00	1.00	1.00	1.00	1.00	1.00

Weighted Sum-of-Squares							Total
Tonnage	HM	SiO2	Al2O3	TiO2	Fe2O3	ZrO2	WSSQ
0.00	0.09	0.00	0.01	0.00	0.00	0.00	0.11
0.00	0.03	0.00	0.01	0.00	0.00	0.00	0.04
0.00	0.00	0.00	0.00	0.00	0.00	1.00	1.00
							1.15

		Estimated Values							Calculated Values						
		Tonnage	HM	SiO2	Al2O3	TiO2	Fe2O3	ZrO2	Tonnage	HM	SiO2	Al2O3	TiO2	Fe2O3	ZrO2
Sample 60	**Feed**	98.04	61.03	44.40	12.90	22.20	11.60	5.42	96.86	59.43	43.70	12.64	22.55	11.39	6.22
	Underflow	75.64	69.59	26.90	16.00	29.50	14.60	10.30	73.65	71.17	27.10	16.30	29.02	14.86	8.10
	Overflow	22.40	22.12	95.60	1.05	2.03	0.38	0.27	23.21	22.17	96.38	1.05	2.03	0.38	0.27

Relative Change							Relative Error						
Tonnage	HM	SiO2	Al2O3	TiO2	Fe2O3	ZrO2	Tonnage	HM	SiO2	Al2O3	TiO2	Fe2O3	ZrO2
-1.20	-2.62	-1.58	-1.98	1.60	-1.84	14.79	1.00	1.00	1.00	1.00	1.00	1.00	1.00
-2.63	2.27	0.73	1.87	-1.61	1.76	-21.38	1.00	1.00	1.00	1.00	1.00	1.00	1.00
3.62	0.23	0.81	0.04	-0.03	0.01	-0.18	1.00	1.00	1.00	1.00	1.00	1.00	1.00

Weighted Sum-of-Squares							Total
Tonnage	HM	SiO2	Al2O3	TiO2	Fe2O3	ZrO2	WSSQ
0.00	0.00	0.00	0.00	0.00	0.00	0.02	0.02
0.00	0.00	0.00	0.00	0.00	0.00	0.05	0.05
0.00	0.00	0.00	0.00	0.00	0.00	0.00	0.00
							0.07

		Estimated Values							Calculated Values						
		Tonnage	HM	SiO2	Al2O3	TiO2	Fe2O3	ZrO2	Tonnage	HM	SiO2	Al2O3	TiO2	Fe2O3	ZrO2
Sample 61	**Feed**	124.21	77.50	38.10	13.00	25.20	12.20	0.00	124.39	77.06	37.33	12.36	25.88	12.00	0.00
	Underflow	100.97	93.71	22.90	14.50	32.00	14.60	0.00	100.89	93.92	23.52	15.01	31.44	14.74	0.00
	Overflow	23.23	4.61	96.50	0.87	2.16	0.18	0.00	23.49	4.66	96.64	0.99	2.03	0.21	0.00

Relative Change							Relative Error						
Tonnage	HM	SiO2	Al2O3	TiO2	Fe2O3	ZrO2	Tonnage	HM	SiO2	Al2O3	TiO2	Fe2O3	ZrO2
0.15	-0.56	-2.01	-4.90	2.71	-1.66	0.00	1.00	1.00	1.00	1.00	1.00	1.00	1.00
-0.08	0.23	2.72	3.53	-1.75	0.97	0.00	1.00	1.00	1.00	1.00	1.00	1.00	1.00
1.12	1.06	0.15	13.53	-5.99	18.09	0.00	1.00	1.00	1.00	1.00	1.00	1.00	1.00

Weighted Sum-of-Squares							Total
Tonnage	HM	SiO2	Al2O3	TiO2	Fe2O3	ZrO2	WSSQ
0.00	0.00	0.00	0.00	0.00	0.00	0.00	0.00
0.00	0.00	0.00	0.00	0.00	0.00	0.00	0.00
0.00	0.00	0.00	0.02	0.00	0.03	0.00	0.05
							0.06

		Estimated Values							Calculated Values						
		Tonnage	HM	SiO2	Al2O3	TiO2	Fe2O3	ZrO2	Tonnage	HM	SiO2	Al2O3	TiO2	Fe2O3	ZrO2
Sample 62	**Feed**	126.93	82.79	32.00	13.70	28.80	13.70	0.00	126.12	82.83	33.45	13.12	28.35	13.38	0.00
	Underflow	116.42	87.86	30.70	13.40	29.40	13.90	0.00	116.46	88.08	29.36	13.96	29.87	14.23	0.00
	Overflow	10.51	19.43	82.90	2.92	10.00	3.14	0.00	9.66	19.45	82.78	2.97	10.04	3.17	0.00

Relative Change							Relative Error						
Tonnage	HM	SiO2	Al2O3	TiO2	Fe2O3	ZrO2	Tonnage	HM	SiO2	Al2O3	TiO2	Fe2O3	ZrO2
-0.64	0.05	4.54	-4.25	-1.57	-2.33	0.00	1.00	1.00	1.00	1.00	1.00	1.00	1.00
0.03	0.25	-4.36	4.18	1.59	2.36	0.00	1.00	1.00	1.00	1.00	1.00	1.00	1.00
-8.14	0.10	-0.14	1.69	0.41	0.94	0.00	1.00	1.00	1.00	1.00	1.00	1.00	1.00

Weighted Sum-of-Squares							Total
Tonnage	HM	SiO2	Al2O3	TiO2	Fe2O3	ZrO2	WSSQ
0.00	0.00	0.00	0.00	0.00	0.00	0.00	0.00
0.00	0.00	0.00	0.00	0.00	0.00	0.00	0.00
0.01	0.00	0.00	0.00	0.00	0.00	0.00	0.01
							0.02

		Estimated Values							Calculated Values						
		Tonnage	HM	SiO2	Al2O3	TiO2	Fe2O3	ZrO2	Tonnage	HM	SiO2	Al2O3	TiO2	Fe2O3	ZrO2
Sample 63	**Feed**	129.68	77.13	40.00	12.90	24.90	12.10	0.00	129.41	76.32	39.51	12.61	25.07	11.78	0.00
	Underflow	107.72	90.15	27.80	14.70	29.80	13.80	0.00	107.78	90.82	28.12	14.96	29.71	14.08	0.00
	Overflow	21.96	3.93	96.20	0.88	1.98	0.26	0.00	21.63	4.07	96.26	0.93	1.96	0.32	0.00

Relative Change							Relative Error						
Tonnage	HM	SiO2	Al2O3	TiO2	Fe2O3	ZrO2	Tonnage	HM	SiO2	Al2O3	TiO2	Fe2O3	ZrO2
-0.21	-1.05	-1.23	-2.22	0.68	-2.63	0.00	1.00	1.00	1.00	1.00	1.00	1.00	1.00
0.05	0.75	1.15	1.75	-0.31	2.05	0.00	1.00	1.00	1.00	1.00	1.00	1.00	1.00
-1.49	3.48	0.07	5.96	-0.96	22.15	0.00	1.00	1.00	1.00	1.00	1.00	1.00	1.00

Weighted Sum-of-Squares							Total
Tonnage	HM	SiO2	Al2O3	TiO2	Fe2O3	ZrO2	WSSQ
0.00	0.00	0.00	0.00	0.00	0.00	0.00	0.00
0.00	0.00	0.00	0.00	0.00	0.00	0.00	0.00
0.00	0.00	0.00	0.00	0.00	0.05	0.00	0.05
							0.06

		Estimated Values							Calculated Values						
		Tonnage	HM	SiO2	Al2O3	TiO2	Fe2O3	ZrO2	Tonnage	HM	SiO2	Al2O3	TiO2	Fe2O3	ZrO2
Sample 64	**Feed**	72.79	63.93	46.90	10.10	21.30	9.89	0.00	66.56	61.48	51.97	10.23	20.51	9.54	0.00
	Underflow	56.52	68.11	49.00	11.30	22.10	10.30	0.00	57.07	70.84	44.84	11.77	23.46	11.07	0.00
	Overflow	16.27	4.54	95.70	0.84	2.40	0.13	0.00	9.49	5.19	94.79	0.97	2.76	0.34	0.00

Relative Change							Relative Error						
Tonnage	HM	SiO2	Al2O3	TiO2	Fe2O3	ZrO2	Tonnage	HM	SiO2	Al2O3	TiO2	Fe2O3	ZrO2
-8.56	-3.83	10.80	1.28	-3.72	-3.51	0.00	1.00	1.00	1.00	1.00	1.00	1.00	1.00
0.98	4.01	-8.48	4.14	6.15	7.50	0.00	1.00	1.00	1.00	1.00	1.00	1.00	1.00
-41.69	14.39	-0.95	16.03	15.02	165.25	0.00	1.00	1.00	1.00	1.00	1.00	1.00	1.00

Weighted Sum-of-Squares							Total
Tonnage	HM	SiO2	Al2O3	TiO2	Fe2O3	ZrO2	WSSQ
0.01	0.00	0.01	0.00	0.00	0.00	0.00	0.02
0.00	0.00	0.01	0.00	0.00	0.01	0.00	0.02
0.17	0.02	0.00	0.03	0.02	2.73	0.00	2.97
							3.02

		Estimated Values							Calculated Values						
		Tonnage	HM	SiO2	Al2O3	TiO2	Fe2O3	ZrO2	Tonnage	HM	SiO2	Al2O3	TiO2	Fe2O3	ZrO2
Sample 65	**Feed**	180.77	87.06	27.80	13.10	29.40	14.20	0.00	180.42	86.63	28.32	13.58	29.51	14.09	0.00
	Underflow	168.90	91.76	24.20	14.90	31.40	14.90	0.00	168.92	92.17	23.71	14.45	31.35	15.02	0.00
	Overflow	11.86	5.16	96.00	0.88	2.51	0.31	0.00	11.50	5.19	95.97	0.85	2.51	0.32	0.00

Relative Change							Relative Error						
Tonnage	HM	SiO2	Al2O3	TiO2	Fe2O3	ZrO2	Tonnage	HM	SiO2	Al2O3	TiO2	Fe2O3	ZrO2
-0.19	-0.49	1.87	3.69	0.36	-0.80	0.00	1.00	1.00	1.00	1.00	1.00	1.00	1.00
0.01	0.45	-2.01	-3.02	-0.17	0.83	0.00	1.00	1.00	1.00	1.00	1.00	1.00	1.00
-3.07	0.56	-0.04	-3.56	-0.15	2.81	0.00	1.00	1.00	1.00	1.00	1.00	1.00	1.00

Weighted Sum-of-Squares							Total
Tonnage	HM	SiO2	Al2O3	TiO2	Fe2O3	ZrO2	WSSQ
0.00	0.00	0.00	0.00	0.00	0.00	0.00	0.00
0.00	0.00	0.00	0.00	0.00	0.00	0.00	0.00
0.00	0.00	0.00	0.00	0.00	0.00	0.00	0.00
							0.01

		Estimated Values							Calculated Values						
		Tonnage	HM	SiO2	Al2O3	TiO2	Fe2O3	ZrO2	Tonnage	HM	SiO2	Al2O3	TiO2	Fe2O3	ZrO2
Sample 66	**Feed**	149.27	85.06	31.70	12.60	28.90	13.70	0.00	146.44	83.23	35.04	11.83	27.27	13.04	0.00
	Underflow	130.95	90.56	31.00	12.30	28.60	13.80	0.00	131.13	92.42	28.04	13.09	30.16	14.53	0.00
	Overflow	18.31	4.19	95.40	0.90	2.29	0.21	0.00	15.31	4.44	95.02	1.01	2.50	0.31	0.00

Relative Change							Relative Error						
Tonnage	HM	SiO2	Al2O3	TiO2	Fe2O3	ZrO2	Tonnage	HM	SiO2	Al2O3	TiO2	Fe2O3	ZrO2
-1.90	-2.16	10.54	-6.11	-5.64	-4.82	0.00	1.00	1.00	1.00	1.00	1.00	1.00	1.00
0.13	2.06	-9.55	6.45	5.46	5.26	0.00	1.00	1.00	1.00	1.00	1.00	1.00	1.00
-16.40	5.91	-0.40	12.27	9.18	48.30	0.00	1.00	1.00	1.00	1.00	1.00	1.00	1.00

Weighted Sum-of-Squares							Total
Tonnage	HM	SiO2	Al2O3	TiO2	Fe2O3	ZrO2	WSSQ
0.00	0.00	0.01	0.00	0.00	0.00	0.00	0.02
0.00	0.00	0.01	0.00	0.00	0.00	0.00	0.02
0.03	0.00	0.00	0.02	0.01	0.23	0.00	0.29
							0.33

		Estimated Values							Calculated Values						
		Tonnage	HM	SiO2	Al2O3	TiO2	Fe2O3	ZrO2	Tonnage	HM	SiO2	Al2O3	TiO2	Fe2O3	ZrO2
Sample 67	**Feed**	159.87	83.39	31.40	13.70	29.10	13.80	0.00	159.27	82.26	31.03	13.13	28.77	13.45	0.00
	Underflow	145.75	88.39	25.00	13.70	30.80	14.30	0.00	145.79	89.42	25.12	14.24	31.16	14.65	0.00
	Overflow	14.12	4.72	95.00	1.01	2.83	0.36	0.00	13.47	4.82	95.01	1.06	2.86	0.39	0.00

Relative Change							Relative Error						
Tonnage	HM	SiO2	Al2O3	TiO2	Fe2O3	ZrO2	Tonnage	HM	SiO2	Al2O3	TiO2	Fe2O3	ZrO2
-0.38	-1.35	-1.17	-4.19	-1.15	-2.57	0.00	1.00	1.00	1.00	1.00	1.00	1.00	1.00
0.03	1.16	0.48	3.95	1.17	2.46	0.00	1.00	1.00	1.00	1.00	1.00	1.00	1.00
-4.56	2.08	0.01	5.15	1.23	9.44	0.00	1.00	1.00	1.00	1.00	1.00	1.00	1.00

Weighted Sum-of-Squares							Total
Tonnage	HM	SiO2	Al2O3	TiO2	Fe2O3	ZrO2	WSSQ
0.00	0.00	0.00	0.00	0.00	0.00	0.00	0.00
0.00	0.00	0.00	0.00	0.00	0.00	0.00	0.00
0.00	0.00	0.00	0.00	0.00	0.01	0.00	0.01
							0.02

		Estimated Values							Calculated Values						
		Tonnage	HM	SiO2	Al2O3	TiO2	Fe2O3	ZrO2	Tonnage	HM	SiO2	Al2O3	TiO2	Fe2O3	ZrO2
Sample 68	**Feed**	122.30	64.17	46.00	11.40	21.30	10.30	0.00	123.32	66.45	44.94	11.35	21.68	10.17	0.00
	Underflow	92.16	89.01	26.60	15.00	28.70	13.60	0.00	91.49	87.31	27.56	14.93	28.27	13.58	0.00
	Overflow	30.14	7.04	94.60	1.09	2.89	0.37	0.00	31.82	6.47	94.92	1.07	2.75	0.36	0.00

Relative Change							Relative Error						
Tonnage	HM	SiO2	Al2O3	TiO2	Fe2O3	ZrO2	Tonnage	HM	SiO2	Al2O3	TiO2	Fe2O3	ZrO2
0.83	3.55	-2.30	-0.45	1.80	-1.25	0.00	1.00	1.00	1.00	1.00	1.00	1.00	1.00
-0.73	-1.91	3.61	-0.50	-1.51	-0.13	0.00	1.00	1.00	1.00	1.00	1.00	1.00	1.00
5.59	-8.13	0.34	-2.24	-4.91	-1.53	0.00	1.00	1.00	1.00	1.00	1.00	1.00	1.00

Weighted Sum-of-Squares							Total
Tonnage	HM	SiO2	Al2O3	TiO2	Fe2O3	ZrO2	WSSQ
0.00	0.00	0.00	0.00	0.00	0.00	0.00	0.00
0.00	0.00	0.00	0.00	0.00	0.00	0.00	0.00
0.00	0.01	0.00	0.00	0.00	0.00	0.00	0.01
							0.02

		Estimated Values							Calculated Values						
		Tonnage	HM	SiO2	Al2O3	TiO2	Fe2O3	ZrO2	Tonnage	HM	SiO2	Al2O3	TiO2	Fe2O3	ZrO2
Sample 69	**Feed**	161.19	87.33	32.60	13.70	28.80	13.40	0.00	159.67	84.59	32.23	14.12	27.74	12.94	0.00
	Underflow	141.08	92.38	24.30	16.10	29.90	14.10	0.00	141.21	94.79	24.13	15.83	30.94	14.58	0.00
	Overflow	20.11	6.20	94.20	1.14	3.14	0.35	0.00	18.46	6.53	94.18	1.10	3.29	0.42	0.00

Relative Change							Relative Error						
Tonnage	HM	SiO2	Al2O3	TiO2	Fe2O3	ZrO2	Tonnage	HM	SiO2	Al2O3	TiO2	Fe2O3	ZrO2
-0.94	-3.14	-1.13	3.10	-3.68	-3.40	0.00	1.00	1.00	1.00	1.00	1.00	1.00	1.00
0.10	2.61	-0.69	-1.70	3.46	3.42	0.00	1.00	1.00	1.00	1.00	1.00	1.00	1.00
-8.20	5.37	-0.03	-3.40	4.62	19.46	0.00	1.00	1.00	1.00	1.00	1.00	1.00	1.00

Weighted Sum-of-Squares							Total
Tonnage	HM	SiO2	Al2O3	TiO2	Fe2O3	ZrO2	WSSQ
0.00	0.00	0.00	0.00	0.00	0.00	0.00	0.00
0.00	0.00	0.00	0.00	0.00	0.00	0.00	0.00
0.01	0.00	0.00	0.00	0.00	0.04	0.00	0.05
							0.06

		Estimated Values							Calculated Values						
		Tonnage	HM	SiO2	Al2O3	TiO2	Fe2O3	ZrO2	Tonnage	HM	SiO2	Al2O3	TiO2	Fe2O3	ZrO2
Sample 70	**Feed**	67.80	66.80	45.00	10.80	22.30	10.60	0.00	67.60	66.15	44.38	10.35	22.41	10.48	0.00
	Underflow	54.85	79.39	32.40	12.10	26.90	12.70	0.00	54.89	79.92	32.86	12.47	26.87	12.82	0.00
	Overflow	12.95	6.56	94.00	1.12	3.16	0.36	0.00	12.71	6.68	94.11	1.21	3.15	0.39	0.00

Relative Change							Relative Error						
Tonnage	HM	SiO2	Al2O3	TiO2	Fe2O3	ZrO2	Tonnage	HM	SiO2	Al2O3	TiO2	Fe2O3	ZrO2
-0.30	-0.97	-1.39	-4.13	0.49	-1.12	0.00	1.00	1.00	1.00	1.00	1.00	1.00	1.00
0.06	0.66	1.42	3.07	-0.12	0.93	0.00	1.00	1.00	1.00	1.00	1.00	1.00	1.00
-1.84	1.89	0.12	7.80	-0.25	7.77	0.00	1.00	1.00	1.00	1.00	1.00	1.00	1.00

Weighted Sum-of-Squares							Total
Tonnage	HM	SiO2	Al2O3	TiO2	Fe2O3	ZrO2	WSSQ
0.00	0.00	0.00	0.00	0.00	0.00	0.00	0.00
0.00	0.00	0.00	0.00	0.00	0.00	0.00	0.00
0.00	0.00	0.00	0.01	0.00	0.01	0.00	0.01
							0.02

		Estimated Values							Calculated Values						
		Tonnage	HM	SiO2	Al2O3	TiO2	Fe2O3	ZrO2	Tonnage	HM	SiO2	Al2O3	TiO2	Fe2O3	ZrO2
Sample 71	**Feed**	136.26	81.20	34.80	13.00	28.10	12.80	0.00	134.52	78.24	34.43	12.71	27.61	12.15	0.00
	Underflow	114.79	87.69	24.60	14.30	31.10	13.50	0.00	115.01	90.20	24.33	14.65	31.70	14.13	0.00
	Overflow	21.47	7.28	94.00	1.20	3.34	0.38	0.00	19.51	7.73	93.95	1.27	3.45	0.50	0.00

Relative Change							Relative Error						
Tonnage	HM	SiO2	Al2O3	TiO2	Fe2O3	ZrO2	Tonnage	HM	SiO2	Al2O3	TiO2	Fe2O3	ZrO2
-1.27	-3.65	-1.06	-2.24	-1.76	-5.04	0.00	1.00	1.00	1.00	1.00	1.00	1.00	1.00
0.20	2.86	-1.09	2.45	1.94	4.69	0.00	1.00	1.00	1.00	1.00	1.00	1.00	1.00
-9.14	6.22	-0.05	5.44	3.33	30.70	0.00	1.00	1.00	1.00	1.00	1.00	1.00	1.00

Weighted Sum-of-Squares							Total
Tonnage	HM	SiO2	Al2O3	TiO2	Fe2O3	ZrO2	WSSQ
0.00	0.00	0.00	0.00	0.00	0.00	0.00	0.00
0.00	0.00	0.00	0.00	0.00	0.00	0.00	0.00
0.01	0.00	0.00	0.00	0.00	0.09	0.00	0.11
							0.12

		Estimated Values							Calculated Values						
		Tonnage	HM	SiO2	Al2O3	TiO2	Fe2O3	ZrO2	Tonnage	HM	SiO2	Al2O3	TiO2	Fe2O3	ZrO2
Sample 72	**Feed**	171.21	83.02	30.30	12.60	28.50	13.30	0.00	171.00	82.47	30.12	12.30	28.65	12.96	0.00
	Underflow	150.16	92.61	21.10	13.60	32.30	14.40	0.00	150.19	93.09	21.18	13.87	32.20	14.70	0.00
	Overflow	21.05	5.79	94.60	1.00	3.03	0.37	0.00	20.81	5.86	94.61	1.04	3.02	0.41	0.00

Relative Change							Relative Error						
Tonnage	HM	SiO2	Al2O3	TiO2	Fe2O3	ZrO2	Tonnage	HM	SiO2	Al2O3	TiO2	Fe2O3	ZrO2
-0.12	-0.66	-0.60	-2.35	0.52	-2.54	0.00	1.00	1.00	1.00	1.00	1.00	1.00	1.00
0.02	0.52	0.38	1.95	-0.31	2.10	0.00	1.00	1.00	1.00	1.00	1.00	1.00	1.00
-1.14	1.16	0.01	3.73	-0.46	11.43	0.00	1.00	1.00	1.00	1.00	1.00	1.00	1.00

Weighted Sum-of-Squares							Total
Tonnage	HM	SiO2	Al2O3	TiO2	Fe2O3	ZrO2	WSSQ
0.00	0.00	0.00	0.00	0.00	0.00	0.00	0.00
0.00	0.00	0.00	0.00	0.00	0.00	0.00	0.00
0.00	0.00	0.00	0.00	0.00	0.01	0.00	0.01
							0.02

APPENDIX B

FIELD DATA FOR 2’ X 2’ CROSSFLOW

Sample ID		Time (s)	Wet Weight (lb)	Decant Weight (lb)	Dry Weight (g)	Actual TPH	GPM	Bed Level	Goal TPH	Actual TPH	Actual % Solids	Overflow Yield	% HM	% Quartz	% TiO2
1	**Feed**	3.00	11.705	7.645	3038.1	3.59	16.0	94	4.0	3.59	57.22	14.13	83.68	16.32	27.20
	Overflow	16.65		6.48	2382.1	0.51							7.63	92.37	xxx
	Underflow	3.30		9.88	3841.7	4.12							98.22	1.78	34.22
2	**Feed**	3.00	12.125	8.45	4262.8	5.03	14.0	92	4.0	5.03	77.51	13.63	85.29	14.71	29.47
	Overflow	15.53		8.24	3007.4	0.69							4.23	95.77	2.04
	Underflow	3.34		10.875	3346.5	3.55							98.65	1.35	34.25
3	**Feed**	4.00	27.073	21.38	8330.4	7.38	14.0	94	6.0	7.38	67.84	9.58	84.41	15.59	30.01
	Overflow	13.94		7.72	2780.8	0.71							4.03	95.97	1.97
	Underflow	2.87		14.95	5887.9	7.27							90.54	9.46	33.26
4	**Feed**	4.00	19.357	15.04	5989.5	5.31	14.0	94	6.0	5.31	68.22	14.12	82.35	17.65	29.37
	Overflow	13.68		8.20	2892	0.75							3.00	97.00	2.00
	Underflow	3.88		14.07	5634.8	5.15							95.52	4.48	35.63
5	**Feed**	3.00	23.100	16.20	6346.3	7.50	14.0	92	8.0	7.50	60.57	1.62	82.84	17.16	29.51
	Overflow	12.87		1.40	442	0.12							4.00	96.00	1.22
	Underflow	2.25		12.40	4799.9	7.56							90.33	9.67	32.47
6	**Feed**	4.00	29.600	19.90	7735.3	6.85	14.0	94	6.0	6.85	57.61	8.61	79.74	20.26	29.29
	Overflow	10.08		4.80	1679.3	0.59							7.14	92.86	3.71
	Underflow	4.05		13.00	4985.9	4.36							89.25	10.75	29.96
7	**Feed**	3.00	21.600	15.00	5775.8	6.82	14.0	96	8.0	6.82	58.95	22.20	70.23	29.77	25.64
	Overflow	7.11		8.40	3039.5	1.51							10.07	89.93	3.81
	Underflow	3.55		14.10		0.00							92.01	7.99	33.54
8	**Feed**	4.00	17.725	9.57	3698.1	3.28	12.0	92	6.0	3.28	46.00	1.78	83.17	16.83	29.88
	Overflow	10.75		0.53	177.2	0.06							2.70	97.30	1.79
	Underflow	4.41		8.86	3412.1	2.74							88.57	11.43	34.19
9	**Feed**	4.00	28.748	21.21	8251.7	7.31	12.0	96	6.0	7.31	63.28	10.26	77.82	22.18	27.33
	Overflow	8.41		4.89	1779.3	0.75							4.30	95.70	2.32
	Underflow	2.84		11.55	4501.4	5.62							89.50	10.50	31.88
10	**Feed**	4.00	26.235	19.31	7588.9	6.72	16.0	92	6.0	6.72	63.77	19.33	77.69	22.31	26.64
	Overflow	6.94		6.92	2545.2	1.30							6.32	93.68	3.30
	Underflow	2.53		9.39	3714.7	5.20							95.98	4.02	33.66

Sample ID		Time (s)	Wet Weight (lb)	Decant Weight (lb)	Dry Weight (g)	Actual TPH	GPM	Bed Level	Goal TPH	Actual TPH	Actual % Solids	Overflow Yield	% HM	% Quartz	% TiO2
11	**Feed**	3.00	12.020	8.47	3363.3	3.97	12.0	94	4.0	3.97	61.69	8.44	87.88	12.12	29.53
	Overflow	18.37		4.77	1738.3	0.34							6.75	93.25	1.04
	Underflow	3.09		5.96	2329.1	2.67							92.91	7.09	32.21
12	**Feed**	3.00	24.500	18.00	7008.6	8.28	12.0	94	8.0	8.28	63.07	10.99	71.58	28.42	24.67
	Overflow	9.65		9.60	2477.4	0.91							4.67	95.33	1.93
	Underflow	3.64		15.40		0.00							80.78	19.22	32.69
13	**Feed**	3.00	22.900	15.80	6152.4	7.27	16.0	94	8.0	7.27	59.23	21.42	69.72	30.28	24.15
	Overflow	7.52		9.10	3303.1	1.56							8.60	91.40	3.35
	Underflow	3.52		13.50		0.00							94.13	5.87	33.67
14	**Feed**	4.00	20.679	16.89	6703	5.94	16.0	96	6.0	5.94	71.46	13.75	81.02	18.98	27.27
	Overflow	12.78		8.02	2945.2	0.82							7.71	92.29	3.35
	Underflow	3.79		13.36	5230.2	4.89							95.66	4.34	34.92
15	**Feed**	3.00	11.600	7.565	2993.2	3.54	14.0	96	4.0	3.54	56.89	10.20	84.54	15.46	27.74
	Overflow	19.87		5.595	2021.8	0.36							5.46	94.54	2.25
	Underflow	3.00		10.425	4091.9	4.83							96.97	3.03	33.18
16	**Feed**	4.00	13.536	7.89	3057.8	2.71	16.0	94	4.0	2.71	49.80	20.29	85.71	14.29	29.05
	Overflow	15.00		6.61	2326.8	0.55							5.81	94.19	2.35
	Underflow	5.65		10.80	4200.8	2.63							95.33	4.67	33.22
17	**Feed**	4.00	14.506	8.07	3111.2	2.76	14.0	92	4.0	2.76	47.28	7.20	84.38	15.62	30.29
	Overflow	15.00		4.67	840	0.20							1.86	98.14	1.15
	Underflow	4.25		2.65	1796.3	1.50							93.80	6.20	34.71
18	**Feed**	3.00	20.200	14.10	5525.8	6.53	14.0	94	6.0	6.53	60.31	13.51	67.26	32.74	22.65
	Overflow	10.46		7.40	2602.9	0.88							5.63	94.37	2.19
	Underflow	3.37		8.90		0.00							88.11	11.89	31.61
19	**Feed**	3.00	20.300	12.50	4854.0	5.73	14.0	94	6.0	5.73	52.71	30.90	66.65	33.35	23.40
	Overflow	6.48		8.90	3239.9	1.77							8.04	91.96	2.75
	Underflow	3.39		14.40		0.00							87.34	12.66	31.41
20	**Feed**	3.00	20.600	13.20	5075.6	5.99	14.0	92	8.0	5.99	54.32	20.56	58.66	41.34	21.08
	Overflow	8.23		7.70	2862.3	1.23							5.51	94.49	2.30
	Underflow	3.36		11.30		0.00							88.45	11.55	31.66

Sample ID		Time (s)	Wet Weight (lb)	Decant Weight (lb)	Dry Weight (g)	Actual TPH	GPM	Bed Level	Goal TPH	Actual TPH	Actual % Solids	Overflow Yield	% HM	% Quartz	% TiO2
21	**Feed**	3.00	21.600	14.50	5643.1	6.66	14.0	94	6.0	6.66	57.60	15.41	78.72	21.28	27.47
	Overflow	6.34		5.20	1838	1.03							6.89	93.11	3.27
	Underflow	2.52		10.50	3442.5	4.84							93.78	6.22	33.71
23	**Feed**	4.00	23.200	13.40	5108	4.52	12.0	92	6.0	4.52	48.54	36.70	57.99	42.01	19.76
	Overflow	7.64		10.10	3580.1	1.66							6.66	93.34	3.12
	Underflow	4.55		7.80	2969.8	2.31							86.33	13.67	31.28
24	**Feed**	4.00	24.700	14.60	5654.7	5.01	12.0	96	6.0	5.01	50.47	19.80	70.39	29.61	24.85
	Overflow	11.05		8.60	3093.5	0.99							7.03	92.97	2.78
	Underflow	4.39		10.80	4346.5	3.51							83.35	16.65	28.31
25	**Feed**	3.00	21.200	14.30	5548.1	6.55	16.0	92	6.0	6.55	57.70	24.34	68.66	31.34	23.80
	Overflow	7.93		10.00	3569.9	1.60							7.81	92.19	2.51
	Underflow	3.45		13.00		0.00							94.46	5.54	32.54
26	**Feed**	4.00	14.991	8.64	3388	3.00	12.0	94	4.0	3.00	49.82	1.54	84.70	15.30	27.70
	Overflow	15.00		0.57	195.4	0.05							0.89	99.11	0.58
	Underflow	5.37		11.55	4465.2	2.95							88.41	11.59	30.11
27	**Feed**	3.00	21.600	14.80	5816.2	6.87	12.0	94	8.0	6.87	59.36	22.08	67.56	32.44	23.91
	Overflow	8.27		9.90	3540.3	1.52							5.49	94.51	2.72
	Underflow	3.80		11.60		0.00							84.85	15.15	29.93
28	**Feed**	3.00	20.900	13.70	5358.3	6.33	16.0	94	8.0	6.33	56.52	20.37	66.85	33.15	23.18
	Overflow	7.40		7.60	2692.7	1.29							6.09	93.91	2.70
	Underflow	3.30		13.40		0.00							92.88	7.12	32.68
29	**Feed**	3.00	22.600	15.70	6166.3	7.28	16.0	96	6.0	7.28	60.15	10.52	80.45	19.55	28.79
	Overflow	7.59		4.60	1641.7	0.77							9.04	90.96	4.12
	Underflow	2.95		10.00	3927	4.72							94.92	5.08	33.96
30	**Feed**	4.00	15.653	9.44	3638.1	3.22	14.0	96	4.0	3.22	51.24	9.35	84.84	15.16	29.58
	Overflow	15.00		3.59	1275.8	0.30							8.66	91.34	4.65
	Underflow	5.84		8.91	3406.6	2.07							93.06	6.94	32.96

VITA

Matthew Donnel Eisenmann was born on September 21, 1977 in Rochester, Minnesota. He graduated from John Jay Senior High School located in Fishkill, N.Y. in 1995. From there he enrolled at Virginia Polytechnic and State University and received his Bachelor of Science degree in Mining and Minerals Engineering. Following completion of his degree, he passed the EIT and is currently working to fulfill requirements for his PE license.

After graduation in May 1999, he was admitted into the Graduate School at Virginia Tech were he continued his studies in Mining and Minerals Engineering. His research focused mainly around mineral separation technology for the phosphate, coal and mineral sands industries. He married to Colleen Kelly Sproull from Pittsburgh, Pennsylvania on August 14. They currently reside in Orange Park, Florida where Matt works as a Process Engineer for DuPont White Pigments and Mineral Products.